Oil & Natural Gas Technology

DOE Award No.: DE-FC26-03NT15413

Final Report

Mineral-Surfactant Interactions for Minimum Reagents Precipitation and Adsorption for Improved Oil Recovery

Submitted by:
Columbia University
2960 Broadway
New York, NY

Prepared for:
United States Department of Energy
National Energy Technology Laboratory

September 30, 2008

Office of Fossil Energy

MINERAL-SURFACTANT INTERACTIONS FOR MINIMUM REAGENTS PRECIPITATION AND ADSORPTION FOR IMPROVED OIL RECOVERY

TECHNICAL PROGRESS REPORT

Reporting Period Start Date:	09/30/2003
Reporting Period End Date:	09/30/2008
Principal Author:	Prof. P. Somasundaran
Date Report Issued:	Sep. 30, 2008
DOE Award Number:	DE-FC26-03NT15413
Principal Investigator	Prof. P. Somasundaran
Submitting Organization	Office of Projects and Grants Columbia University in the City of New York 1210 Amsterdam Avenue, Mail Code 2205 Room 254 Engineering Terrace New York, NY 10027
Contracting Officer's Representative	Chandra Nautiyal U.S. Department of Energy, National Petroleum Technology Office One West Third Street, Suit 1400 Tulsa, Oklahoma 74101-3519

DISCLAIMER

ABSTRACT

Chemical EOR can be an effective method for increasing oil recovery and reducing the amount of produced water; however, reservoir fluids are chemically complex and may react adversely to the polymers and surfactants injected into the reservoir. While a major goal is to alter rock wettability and interfacial tension between oil and water, rock-fluid and fluid-fluid interactions must be understood and controlled to minimize reagent loss, maximize recovery and mitigate costly failures.

The overall objective of this project was to elucidate the mechanisms of interactions between polymers/surfactants and the mineral surfaces responsible for determining the chemical loss due to adsorption and precipitation in EOR processes. The role of dissolved inorganic species that are dependent on the mineralogy is investigated with respect to their effects on adsorption. Adsorption, wettability and interfacial tension are studied with the aim to control chemical losses, the ultimate goal being to devise schemes to develop guidelines for surfactant and polymer selection in EOR.

The adsorption behavior of mixed polymer/surfactant and surfactant/surfactant systems on typical reservoir minerals (quartz, alumina, calcite, dolomite, kaolinite, gypsum, pyrite, etc.) was correlated to their molecular structures, intermolecular interactions and the solution conditions such as pH and/or salinity. Predictive models as well as general guidelines for the use of polymer/surfactant surfactant/surfactant system in EOR have been developed

The following tasks have been completed under the scope of the project:

- Mineral characterization, in terms of SEM, BET, size, surface charge, and point zero charge.
- Study of the interactions among typical reservoir minerals (quartz, alumina, calcite, dolomite, kaolinite, gypsum, pyrite, etc.) and surfactants and/or polymers in terms of adsorption

properties that include both macroscopic (adsorption density, wettability) and microscopic (orientation/conformation of the adsorbed layers), as well as precipitation/abstraction characteristics.

- Investigation of the role of dissolved species, especially multivalent ions, on interactions between reservoir minerals and surfactants and/or polymers leading to surfactant precipitation or activated adsorption.
- Solution behavior tests—surface tension, interaction, ultra filtration, and other tests
- Surfactant-mineral interactions relative to adsorption, wettability, and electrophoresis
- Work on the effects of multivalent ions, pH, temperature, salinity, and mixing ratio on the adsorption. Developments of adsorption models to explain interactions between surfactants/polymers/minerals.
- General guidelines for the use of certain surfactants, polymers and their mixtures in micelle flooding processes.

TABLE OF CONTENTS

LIST OF GRAPHICAL MATERIALS

EXECUTIVE SUMMARY

In this project we characterized typical reservoir mineral materials and studied the interactions among surfactants, polymers and minerals with the aim of minimizing the loss of the chemicals due to adsorption and precipitation.

Solid substrates selected for the study were alumina, silica, kaolinite, sandstone, limestone, gypsum and pyrite. Specific surface area and isoelectric points have been measured using BET and zeta potential methods. Morphology of the selected minerals is very different from those of each other. Kaolinite has the highest specific surface area of 23.12 m^2/g suggesting porous structure and thus a high potential for adsorption. Alumina and silica have a medium specific surface area of around 10~13m^2/g. The others have a relatively low specific surface area suggesting crystal-like surfaces and thus a low capability for adsorption. Isoelectric points of the minerals vary from 2 to 9 suggesting a dramatic difference in the nature of surface species that will have to be modified to control adsorption.

The studies completed show three major interactions between surfactants and the minerals: hydrophobic chain-chain interactions, electrostatic forces and hydrogen bonding. An interplay and balance among these three interactions determines the adsorption behavior of surfactant and polymer molecules. Solution conditions (salinity, pH, temperature and hardness) affect the magnitude of the three major interactions and thus affect the adsorption behavior.

Typical anionic surfactant sodium dodecyl sulfonate has been evaluated in this work under different solution conditions. A novel cationic surfactant of the Gemini type has also been synthesized and evaluated in the study. Results show that the major interaction between the anionic as well as the Gemini surfactant and minerals is of the electrostatic type leading to considerable loss of these surfactants, particularly under high salinity conditions. As high multivalent conditions like calcium or magnesium ions, which are major deterrents for anionic surfactants in EOR processes, are common in

real production, these surfactants cannot be used alone in EOR and have to be mixed with others for optimum performance. It must, however, be noted that the cationic Gemini surfactants can be ideal reagents for lime stone reservoirs since the rock surface is positively charged.

Our study with dodecyl maltoside (DM) clearly shows that sugar based surfactants are promising candidates for EOR process because of their high tolerance to inorganics, particularly multivalent ions and more importantly because of their environmentally benign nature. Hydrogen bonding between the sugar rings and the surface hydroxyl groups is the major mechanism that dominates adsorption of DM on mineral surfaces and is not affected by electrostatic interactions. There is no significant depletion or loss of dodecyl maltoside in simulated adsorption processes. Besides, its adsorption under high temperature and low pH conditions is lower than that under ambient conditions, which will reduce chemical loss even more under such extreme conditions.

Increasing requirements for environmental protection and an escalating demand from consumers has made “going green” an inevitable and inescapable trend for the industries. Sustainability of chemical products in a future environmentally conscious market will favor only products certified to have been made in an environmentally responsible way. Sugar based surfactants are manufactured from renewable starting materials and are readily bio-degradable, which make them some of the best green surfactants. Application of this type of novel green surfactants in industry is suggested.

Surfactant mixtures or surfactant/polymer mixtures have vast potential because of the possibilities for synergism between them. The behavior of conventional surfactant/green surfactant mixtures and polymer/green surfactant mixtures at both liquid solid interface and at bulk solvent was studied in detail. Novel techniques such as analytical ultracentrifuge have been used for the first time to elucidate the mechanism of micellar evolution in the bulk fluid.

In the case of the anionic surfactants, their mixtures with a sugar based nonionic surfactant and an ionic surfactant have been evaluated in this work. The studies show antagonistic or synergistic interactions among the surfactants depending on the test conditions. Such antagonism and synergy can be used to control chemical losses.

Mixtures of polymers and ionic surfactants have also been evaluated. The study shows strong interactions between polymer and surfactant species. Hydrophobic moieties of modified polymers tend to form local hydrophobic domains with the carbon chains of the ionic surfactants aggregating around the domains to composite domains. The composite domains can serve as local reservoirs of the ionic surfactants, keeping them from adsorbing on the minerals. The domains can serve to solubilize and thus mobilize oil. This mechanism can contribute to minimizing chemical loss and at the same time enhancing oil extraction efficiency.

Based on our studies, the following guidelines for surfactant selection are proposed.

Guidelines in Surfactant selection

Rock Type	Surfactants types	
	Recommended	Not Recommended
Sandstone	Anionic+/non-ionic (ex. SDS, DM)	Cationic (ex. Gemini or alkyl amines)
Sandstone in a Ca-containing reservoir	Anionic (ex. SDS)	Cationic alkyl amines or gemini, Cationic+non-ionic (ex. Gemini+DM)
Sandstone + Limestone rocks	Anionic (ex. SDS)	Cationic alkyl amines, Cationic+non-ionic (ex. Gemini+DM)
Sandstone + Pyrite	Anionic+/non-ionic (ex. SDS, DM)	Cationic alkyl amines
Oxide-rich minerals	Ionics+/Non-ionics (ex. SDS, DM)	Non-ionics – pH not close to oxides' isoelectric point
Limestone	Cationic (Gemini, alkyl amines) +/Non-ionic (DM)	Anionic (SDS)

INTRODUCTION

There is considerable amount of oil trapped, together with water and gas, in reservoirs made up of porous and permeable rocks after the traditional oil production. Surfactant/polymer flooding is one of the promising techniques to recover additional oil from domestic oil reservoirs. In this regard, there is a need for cost-effective reagent schemes to increase the oil recovery under investigation in a number of places. The key criterion for the successful application of techniques using surfactant mixtures is minimal loss of surfactants on reservoir rocks by adsorption and precipitation. To design such optimal systems, a fundamental understanding of the mechanisms of between minerals and chemicals is essential. It was the aim of this project to conduct systematic studies on the role of reservoir minerals and surfactant/polymer chemistry in the adsorption and retention of these reagents on minerals in enhanced oil recovery particularly in the presence of relevant semi-soluble minerals.

It is well known that surfactants can interact to form aggregates in solutions (micelles) and at interfaces (hemimicelles) and these aggregation phenomena can have drastic effects on oil recovery processes. Research has shown that the aggregation behavior of some surfactant mixtures is quite unusual both in that more than one type of mixed micelles can form and possibly co-exist in the solution. This finding has both theoretical and practical implications. It has potential for applications to minimize the interfacial tension between the oil and the flooding media to facilitate oil liberation and, at the same time, to reduce adsorption of surfactants on reservoir rocks. It is to be noted that adsorption of surfactants, including polymeric ones, on minerals is determined by a large number of system variables such as chemical and structural properties of the minerals including solubility and interfacial charge, chemical and physical properties of solution such as salinity, hardness, pH, temperature, and the chemical composition and structure of the surfactants. A thorough understanding of the interactions between polymer and surfactant species and the mineral surfaces, the role of the dissolved species with

the respect to their effects on adsorption, desorption, wettability and interfacial tension at relevant interphases, is the key to alleviate the chemical loss in EOR processes.

EXPERIMENTAL

MATERIALS

Surfactants

Several typical nonionic and ionic surfactants were selected for this study.

Nonionics:

The non-ionic sugar-based surfactant, n-alkyl-β-D-maltoside (>95% purity by TLC) that was used was obtained from Calbiochem. The structure of n-dodecyl-β-D-maltoside (DM) is shown in Figure 1. The growing applications of sugar-based surfactants (alkylmaltosides and alkylglucosides) have been due to their favorable performance properties as well as good biodegradability and the fact that these surfactants are produced from renewable resources.

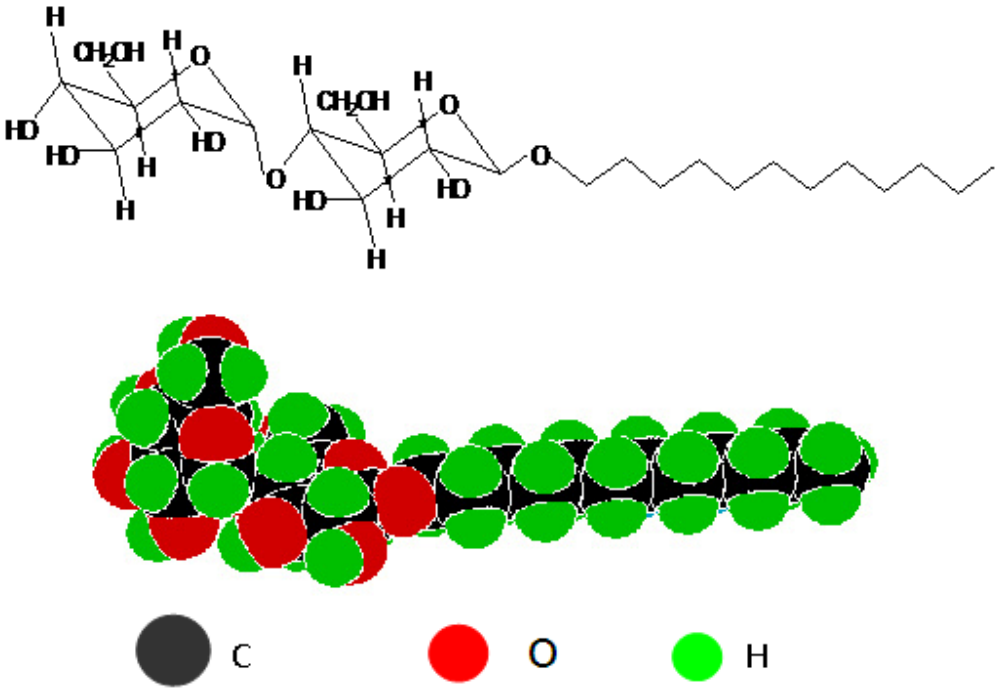

Figure 1: The Chemical Structure and molecular model of Sugar-based Surfactant n-dodecyl-β-D-maltoside (DM)

Anionics**:**

Sodium dodecyl sulfonate (C12SO3Na) of ≥99.0 purity was purchased from TCI Chemicals, Japan.

Sodium bis(2-ethylhexyl) sulfosuccinate (AOT) of purity ≥99.0 (using TLC), were purchased from Fluka was used as such.

Disodium laureth 3 sulfosuccinate (SLE3) in aqueous solution form, supplied by Rodia, was used as received

Cationics:

Dodecyl trimethyl ammonium bromide (DTAB) and didodecyl dimethyl ammonium bromide (DDAB) were purchased from TCI, America (G. R. quality) and were used as such.

Dodecyl trimethyl ammonium chloride (DTAC) of greater than 99% purity purchased from TCI Chemicals, Japan and were used as such.

Synthesized cationic Gemini surfactants

Cationic Gemini surfactants, butane-1,4-bis(quaternary ammonium chloride), represented as C_{12}-C_4-C_{12} and C_{14}-C_4-C_{14}, have been synthesized by the reaction of 1,4-dichlorobutane with corresponding alkyl dimethyl amines, as illustrated in Figure 2. After solvent evaporation, crude white paste product obtained was recrystalized in THF and then in ethanol/ethyl acetate solvent several times. The purified products were white powder, and were stored in a desiccator under vacuum for the complete removal of the solvent. High purity of the synthesized Gemini surfactants was confirmed by their proton NMR spectrums, as shown in Figure 3. There is only a slight amount of hydroxyl salt in the C_{12}-C_4-C_{12} and C_{14}-C_4-C_{14} Gemini, presumably due to the ion-exchange or replacement reaction with alcohol, and no other impurity was found by NMR in either Gemini surfactant.

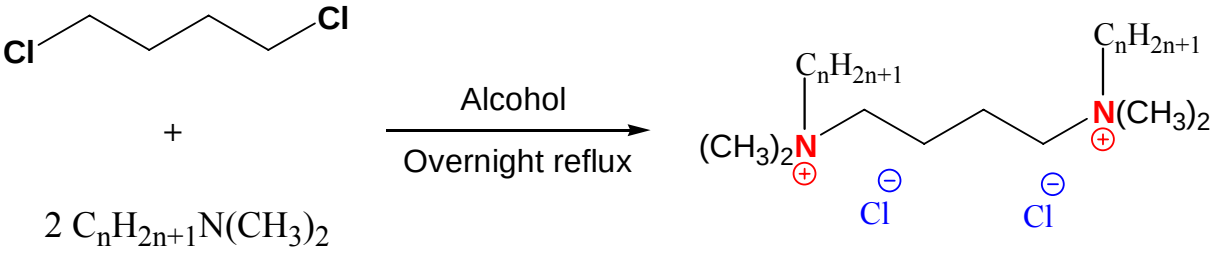

Figure 2. Synthesis of cationic Gemini surfactants C_n-C_4-C_n, n: alkyl chain length.

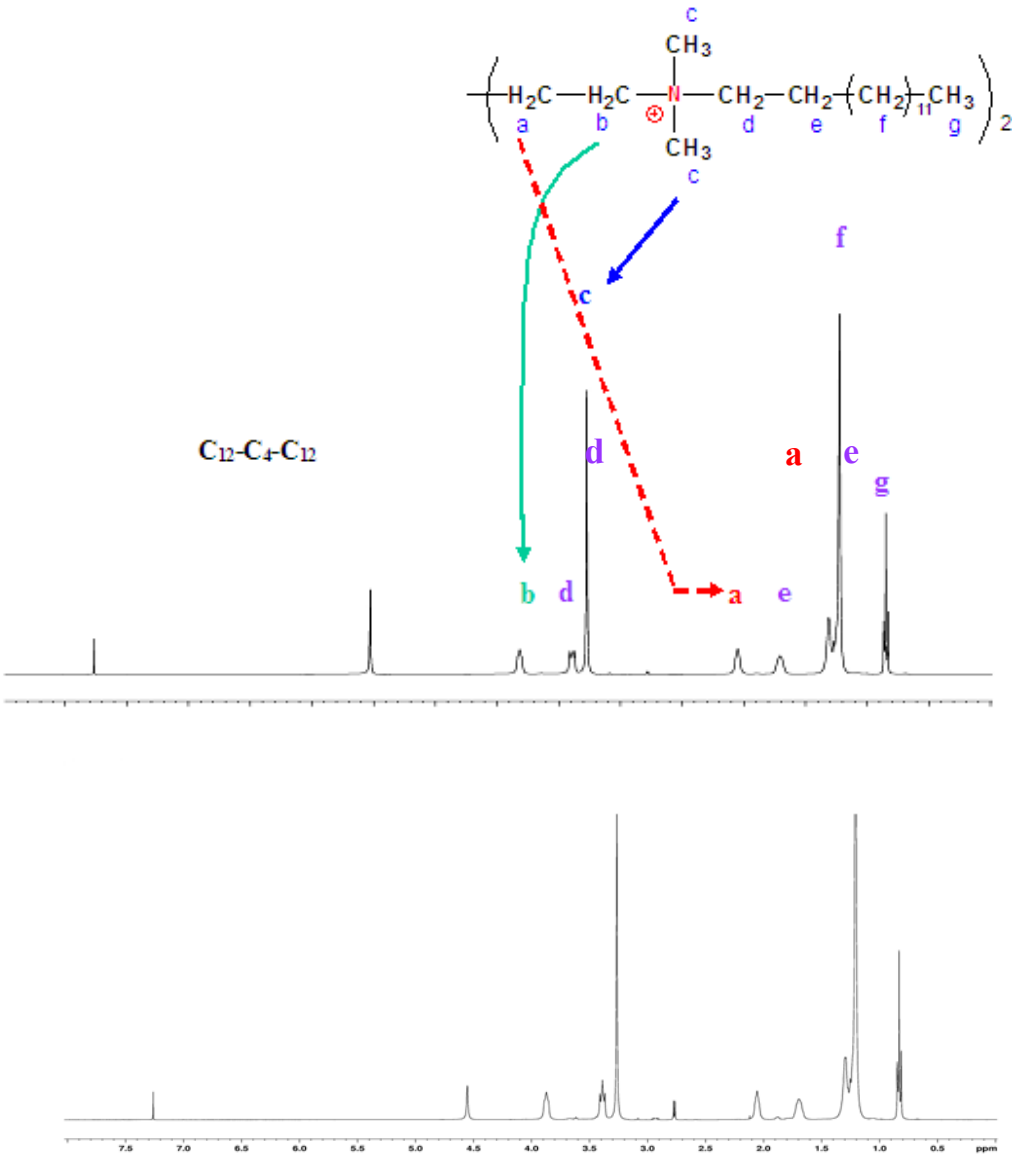

Figure 3: Characterization of synthesized Gemini surfactants C_{12}-C_4-C_{12} and C_{14}-C_4-C_{14}, their ^{1}H NMR spectrums show high purity of the products

The hydrophobically modified polymer, PMAOVE, provided by International Specialty Products, Inc., was synthesized using free-radical polymerization of a 1:1 mole ratio of maleic anhydride and octyl vinyl ether in toluene with Vazo-69 (azo bis-valeryl nitrile) as initiator. The products were purified twice by first dissolving in acetone (5% wt) followed by precipitation with an excess of *tert*-butanol (40 times in volume). Residual solvent was removed in vacuum at 50^0C to a constant mass. The anhydride moiety of the polymer was then hydrolyzed in triple distilled water to make approximately 5% wt solution. The solution was stirred at 500rpm at 70^0C for about 12 hours, and then freeze-dried. As determined by gel permeation chromatography, the weight average molecular weight (M_w) was 160,000 Daltons with a polydispersity index of 1.23.

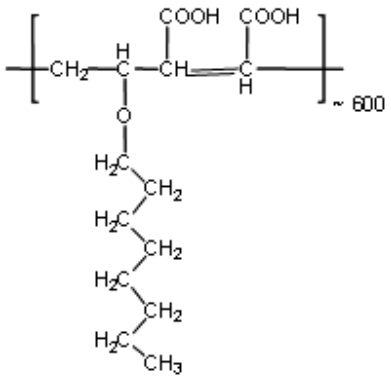

PMAOVE

Figure 4 molecular structure of polymers PMAOVE

Other Reagents:

HCl and NaOH, used for pH adjusting, are of A.C.S. grade certified (purity > 99.9%), from Fisher Scientific Co. To study the salt effect on surface tension, micellization and adsorption, salts such as LiCl, NaCl, KCl, $CaCl_2$, $AlCl_3$, Na_2SO_4, and Na_3PO_4 from Fisher Scientific Co.; NaBr and NaI from Aldrich Chemical Company, Inc.; and sodium citrate from Amend Drug & Chemical Company will be used as received. They are all A.C.S. certified. Water used in all the experiments was triple distilled, with a specific conductivity of less than $1.5\mu\Omega^{-1}$ and was tested for the absence of organics using surface tension measurements.

METHODS

Adsorption experiments

Adsorption experiments were conducted in capped 20 ml vials. 2 gram mineral samples were mixed with 10 ml of triple distilled water for 2 hours at room temperature. The pH was adjusted as desired and then 10 ml of the surfactant solution was added, and the samples were equilibrated further for 16 hours with pH adjustment. The samples were centrifuged for 30 min at 5000 rpm and the clear supernatant parts were then pipetted out for analysis.

Electrokinetics

The electrophoretic mobility of the solid particles (zeta potential) was determined using a Pen Kem Laser Zee Meter. After the surfactant adsorption, the samples were diluted with its own supernatants to make dispersions of suitable solid concentration.

Wettability

The sample for determining the relative hydrophobicity were prepared in the same way as those for the adsorption experiments and the wettability was determined using liquid-liquid extraction technique (using water and toluene as the two liquids). After 16 hours of equilibration of the mineral sample with the surfactant solution, 20 ml of the slurry was transferred to a separatory funnel to which 15 ml of toluene was added. The mineral–surfactant–toluene dispersion was shaken for 1 min manually and then allowed to settle for 1 hour. The bulk of the aqueous phase with hydrophilic solids, as well as the toluene phase with hydrophobic solids, were emptied out of the funnel separately. The two phases containing the solids were evaporated and the weight of mineral was recorded. The relative percentage hydrophobicity was determined as: (Weight of mineral in toluene phase) / (Weight of mineral in toluene phase + weight of mineral in aqueous phase) x 100%.

Surface tension

Measurements were performed by the drop volume method using a glass syringe, with appropriate correction factors applied. The syringe was calibrated using triple distilled water. Sets of measurements were taken for the aqueous surfactant solutions to ensure appropriate accuracy.

Fluorescence

Sample preparation. For fluorescence measurements in solutions, the surfactant solutions were mixed with desired amounts of pyrene, to make the final pyrene concentration ~ 1.0 μM. Surfactant solutions containing pyrene were shaken overnight at room temperature before taking fluorescence spectra. For fluorescence measurements at solid/solution interfaces, the same adsorption procedure was followed as in the experiments conducted in the absence of probe. Desired amount of pyrene probe from stock solutions containing known amounts of pyrene was added into adsorption sample solution, to make the pyrene concentration ~ 0.2 μM. After separating the supernatant and the solid slurry by centrifugation, the solid slurry was taken for direct fluorescence measurements.

Steady-state experiments. Steady-state emission spectra were obtained using a Horiba Jobin Yvon Fluorolog FL-1039 spectrophotometer. A portion of the solid slurry sample from the adsorption experiments or the surfactant solution sample containing pyrene was transferred to quartz cells, and the sample was excited at 335 nm and the emission between 360 and 500 nm recorded.

EPR Measurements: EPR spectra were recorded using a Bruker EMX spectrometer operating at X band (9.5 GHz). All EPR spectra were recorded at 22 ± 1 ^{0}C. The concentration of the probe molecule (5-DSA) used in all the studies was 10^{-4} M. The EPR spectra were analyzed by computer simulation of the spectral line shape by means of the procedure by Schneider, Freed, and Budil et al.

Analytical Ultracentrifuge

A Beckman Optima XL-1 analytical ultracentrifuge with scanning optics and an interference system was employed to perform sedimentation velocity experiments. The interference optical system provides total concentration by measuring the refractive index difference between the sample cell and the reference cell at each radial position as indicated by the vertical displacement of a set of evenly spaced horizontal fringe. The running condition was set at a motor speed 40,000 rpm, and the temperature at 25^{o}C. Software *Sedfit* developed by Peter Shuck was used to analyze the sedimentation data.

Density Measurement

To obtain the specific volume of surfactant micelles, density of surfactant solution was determined density meter, Anton Paar, DMA 5000.

Ultrafiltration

Ultrafiltration. All ultrafiltration tests were done at room temperature (22°C) using Amicon, YM-3, membranes, specified to exclude molecules with molecular weights greater than 3000. The filtration was carried out using an Amicon model 8050 filter at a 380 mmHg nitrogen pressure. The YM-3 membrane was used to separate dodecyl maltoside and sodium dodecyl sulfonate monomers from single and mixed surfactant micellar solutions.

Cryo-TEM

A thin film of the samples was prepared in the environment vitrification system (CEVS) to control the humidity and temperature. The thin film was cooled rapidly in liquid ethane to form a vitrified sample and then it was transferred to liquid nitrogen below -166 ^{o}C. All images were recorded on a high-resolution cooled CCD camera at magnifications of up to 50,000.

Analytical Techniques:

In adsorption experiments, cationic Gemini residual concentration was determined using a two-phase titration method using an anionic surfactant, sodium dodecyl sulfonate ($C_{12}SO_3Na$), as the titrating solution. The residual concentration of the anionic surfactant after adsorption was determined also by a two-phase titration method using a cationic surfactant, dodecyl trimethyl ammonium chloride (DTAC), as the titrating solution. Concentration of the sugar-based surfactant after adsorption was determined by colorimetric method through phenol-sulfuric acid reaction. In the case of the ionic/nonionic surfactant mixtures, the total residual surfactant concentration after adsorption was obtained by adding the individual component surfactant concentration, which was measured by either the two-phase titration or the colorimetric method.

RESULTS AND DISCUSSION

Characterization of the Mineral Samples:

Solid substrates selected for the study were alumina, silica, kaolinite, sandstone, limestone, gypsum and pyrite.

Alumina AKP-50 obtained from Sumitomo had a mean diameter of 0.2 μm. The BET specific surface area measured using nitrogen/helium with a Quantasorb system was 10.8 m^2/g and the isoelectric point (iep) was 8.9.

Silica obtained from Geltech was of a mean diameter of 0.2 to 0.3 μm, the specific surface area of 12.2 to 12.9 m^2/g and the isoelectric point around 2.

Kaolinite with the specific surface area of 23.12 m^2/g and limestone with the specific surface area of 0.96 m^2/g were obtained from the Wards Scientific Corporation. All these solids have relatively homogeneous surfaces and show low solubility in aqueous solutions. They were used as received.

The other natural minerals of sandstone, gypsum and pyrite, were obtained from Wards Scientific Corporation in stone form. They were ground to fine powder in the laboratory by using mortar grinder from Fisher Scientific Co. The BET specific surface areas, measured using nitrogen/ helium with a Quantasorb system were; sandstone: 1.39 m^2/g, gypsum: 2.64 m^2/g, and pyrite: 0.40 m^2/g. The measured isoelectric point of sandstone was 2.

SEM images of these minerals are shown in Figure 5. From SEM images, it can be seen that only kaolinite shows a porous like structure, with the others having crystal-like surfaces. The porous structure of kaolinite results in its higher specific surface area. Properties for these solids are listed in Table 1.

Table 1: List of Solids used in the Study

Name	Structure	Source	Mean particle size (μm)	Specific surface area (m^2/g)	Isoelectric point (iep)
AKP-50 Alumina	Al_2O_3	Sumitomo	0.2	10.8	8.9
Silica (Quartz)	SiO_2	Geltech	0.2 – 0.3	12.2 – 12.9	2
Limestone	$CaCO_3$	Wards	~ 2	0.96	N/A
Kaolinite	$Al_2Si_2O_5(OH)_4$	Wards	~ 1	23.12	--
Sandstone	SiO_2	Wards	~ 2	1.39	2
Gypsum	$CaSO_4 \bullet 2H_2O$	Wards	~ 2	2.64	N/A
Pyrite	FeS	Wards	~ 2	0.40	N/A

Gypsum

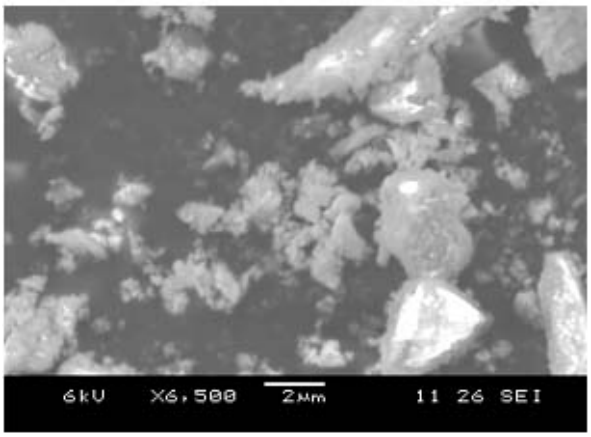

Kaolinite

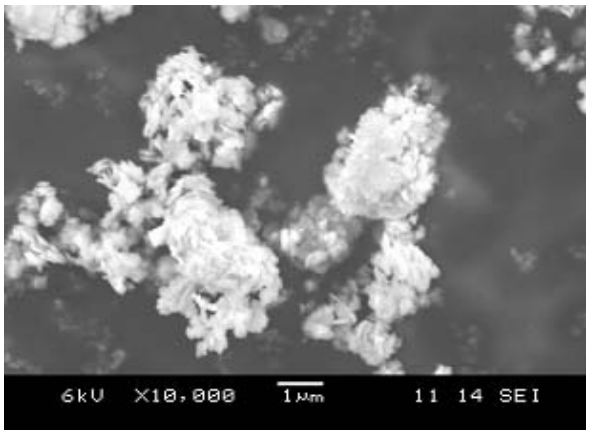

Limestone

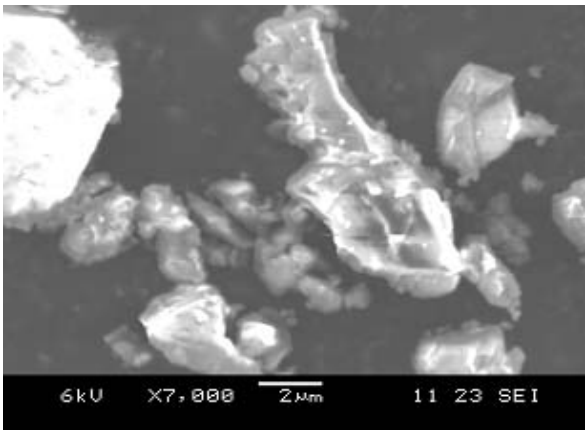

Pyrite

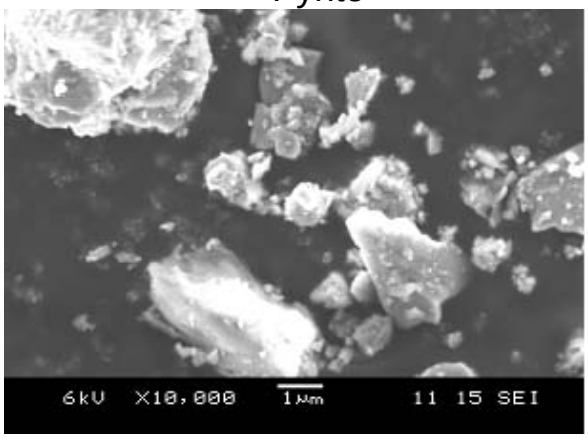

Sandstone

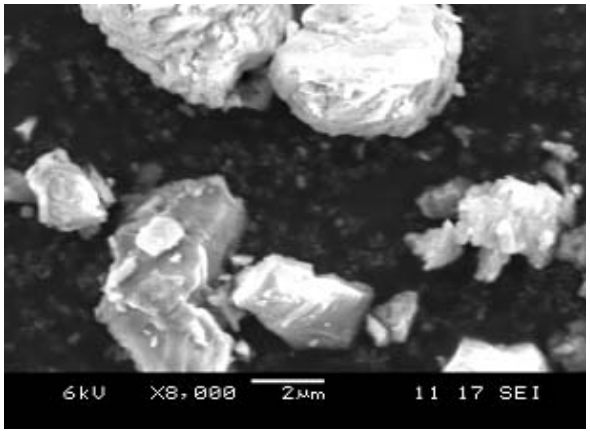

Figure 5: SEM images of the minerals gypsum, kaolinite, limestone, sandstone and pyrite in powder form

Adsorption of sodium dodecyl sulfate on gypsum and limestone

The role of minerals in governing the surfactant/mineral interactions was investigated by determining the adsorption isotherms of sodium dodecyl sulfate (SDS) on gypsum and limestone by depletion technique. Very high SDS adsorption was observed in the plateau range on both the limestone and gypsum (Figure 6). Compared to SDS adsorption on other minerals such as alumina, the plateau adsorption densities on gypsum and limestone were 20 times higher, which is attributed to the surfactant precipitation by the dissolved calcium ions from gypsum and limestone minerals.

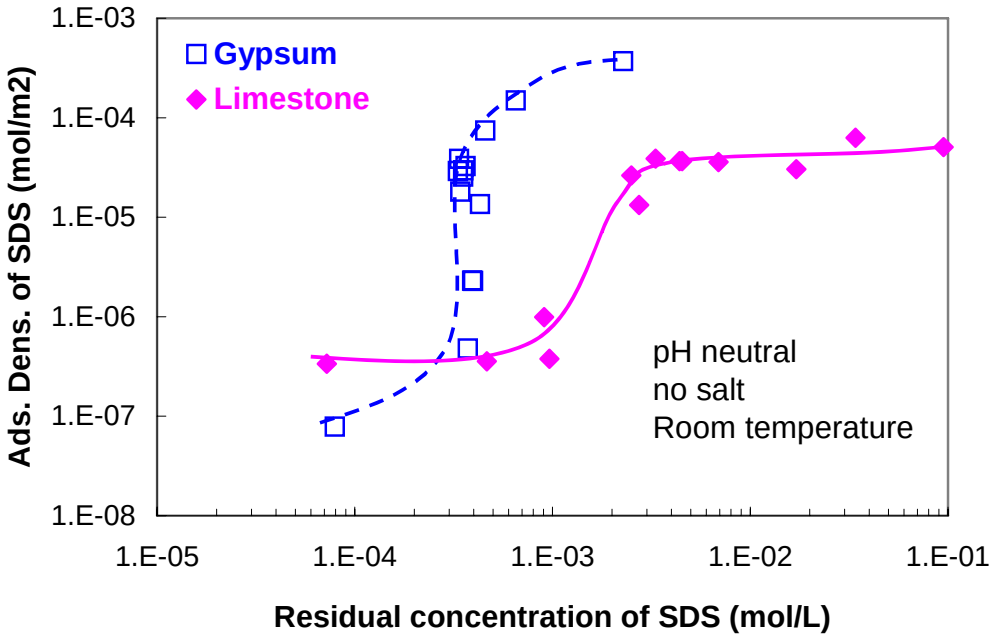

Figure 6: Effects of surface mineralogy on the adsorption of SDS

Adsorption of sodium dodecyl sulfate in the presence of multivalent ions

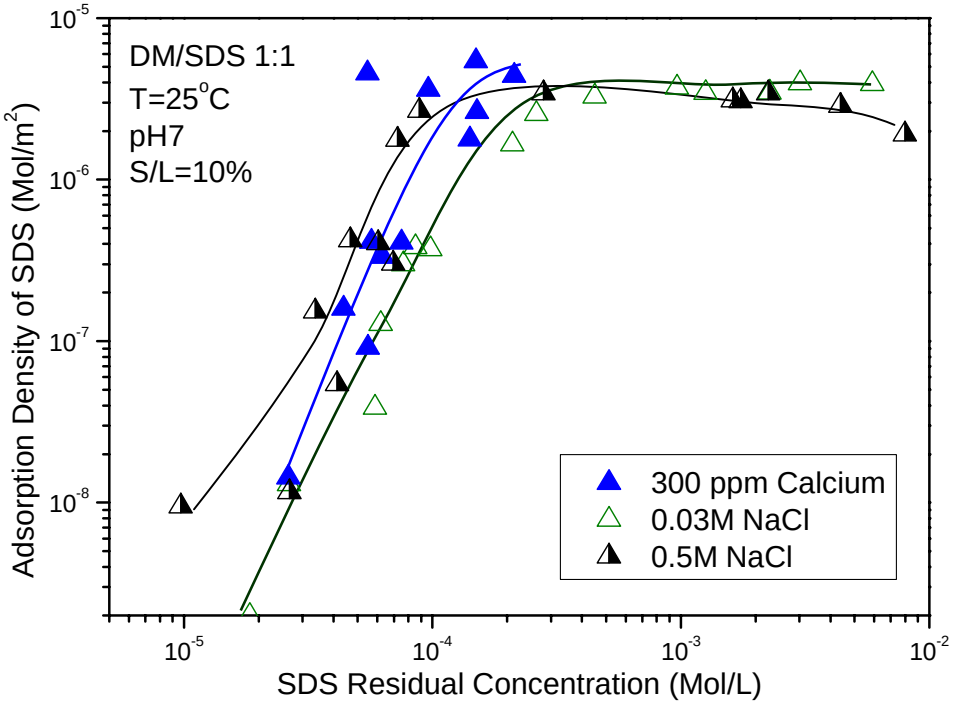

Figure 7: Adsorption of SDS from its mixture with DM on alumina at different ionic strength

Figure 7 shows the adsorption isotherms of SDS on alumina from its mixtures with DM. It can be seen that the adsorption of SDS changes significantly in the presence of sodium chloride and calcium. The divalent ion shows the highest effect on the adsorption of SDS, as the residual concentration of SDS was limited to 2×10^{-4} Mol/m^2 due to precipitation of calcium dodecyl sulfonate. In addition, it can be seen that the increase in NaCl concentration does not affect the adsorption of SDS much since the sodium ion only reduces the electrostatic forces and does not cause precipitation.

Adsorption of dodecyl maltoside on solids and the relationship between adsorption and surface ion concentration

Data shows that the adsorption of dodecyl maltoside on alumina changes dramatically with a variation in pH (Figure 8). The saturation adsorption at pH 7 was found to be 5.6×10^{-6} mol/m^2, while that at pH 4 is only 1.1×10^{-7} mol/m^2, which is only 2% of that at pH 7. Apparently, the adsorption decreases dramatically with pH from pH 7 to 3, while it remains constant from pH 7 to pH 11. This phenomenon was attributed to the pH-dependence of surface hydroxyl group, which is critical for the formation of hydrogen bonds. A similar adsorption drop was observed for dodecyl maltoside on hematite. The adsorption density at pH 3 was lower than that in the higher pH range. The low adsorption phenomena seen in the low pH range may help bring about a reduction of chemical loss in surfactant/polymer flooding.

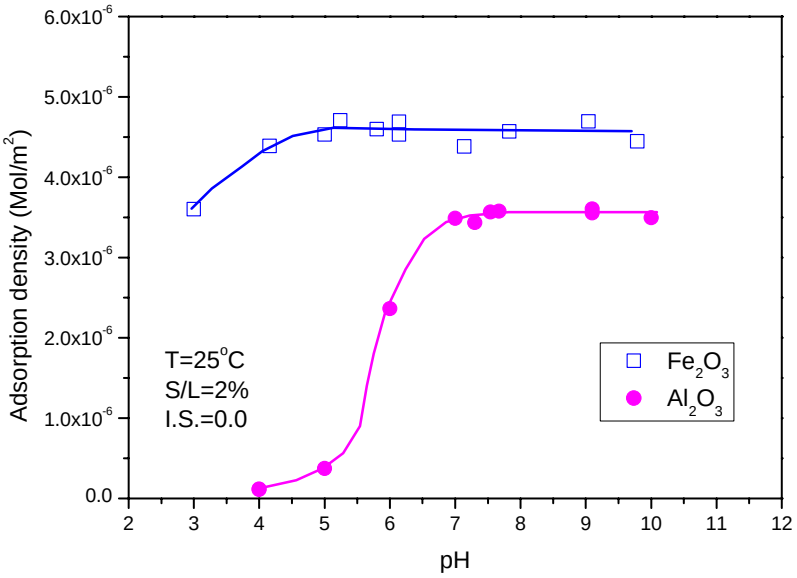

Figure 8: Adsorption of dodecyl maltoside on alumina and hematite as a function of pH

The driving force behind the adsorption of dodecyl maltoside on hydrophilic solid surface was proposed to be the hydrogen bonding between the surface hydroxyl group and the hydroxyl group on the sugar ring of the surfactant. The surface hydroxyl concentration was determined according to the following reaction:

$$-AlOH_2^+ \leftrightarrow -AlOH + H^+$$
$$-AlOH \leftrightarrow -AlO^- + H^+$$

The surface ionization constants can be obtained from zeta potential data and then the surface ion concentration can be obtained. The concentrations of alumina surface species, -AlOH, $-AlOH_2^+$ and $-AlO^-$ are plotted as a function of pH in Figure 9 along with the adsorption density of dodecyl maltoside. Interestingly, the adsorption density of dodecyl maltoside follows the same trend as the concentration of –AlOH, suggesting that there is a proportional relationship between them. The findings clearly demonstrate that the adsorption density of dodecyl maltoside is determined by the concentration of surface hydroxyl group on alumina.

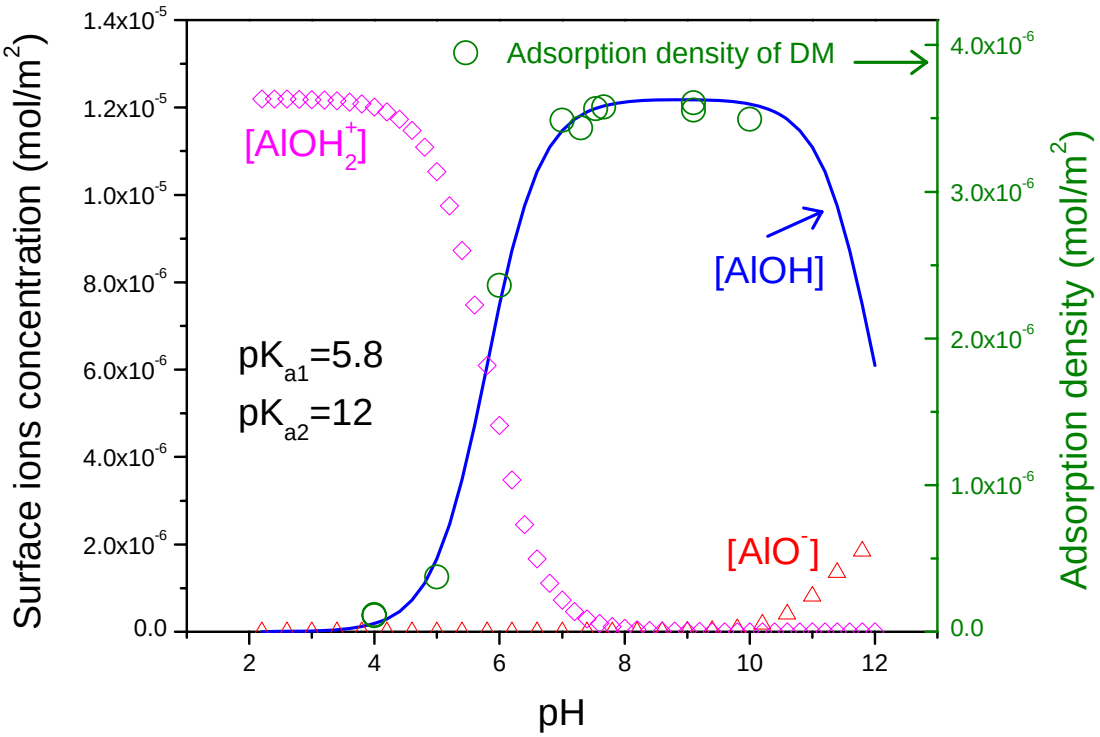

Figure 9: Surface ion concentration of alumina and adsorption of dodecyl maltoside on alumina

In Figure 10, the adsorption density of dodecyl maltoside on alumina is plotted as a function of concentration of –AlOH groups. The adsorption density increases linearly with the surface hydroxyl group concentration. The results obtained suggest a way to reduce chemical loss due to surfactant adsorption. If the surface hydroxyl group concentration can be controlled, the adsorption of surfactant can be reduced dramatically.

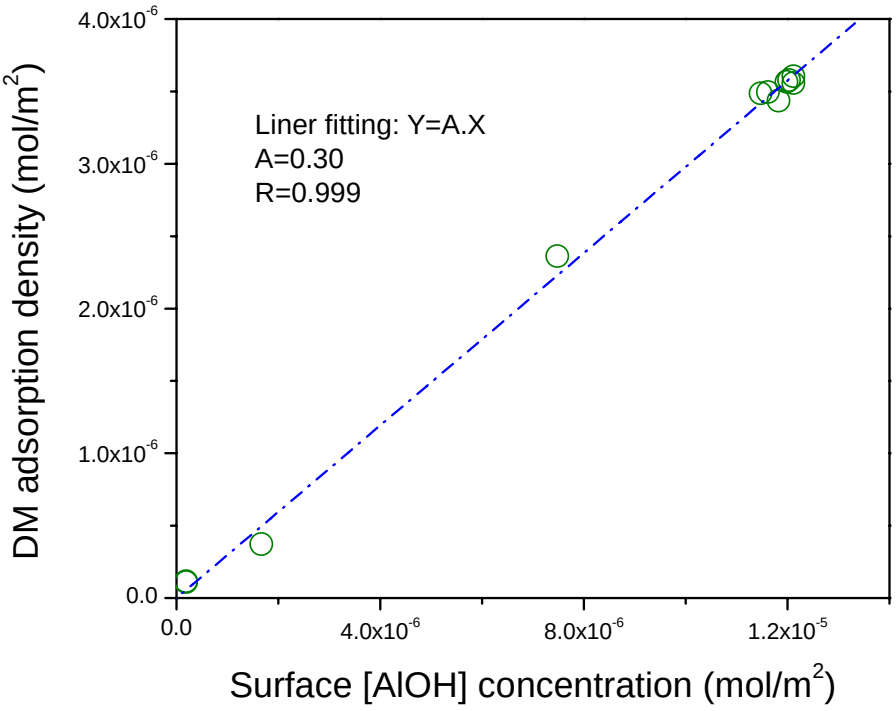

Figure 10: Surface ion concentration of alumina and adsorption of dodecyl maltoside on alumina

Similar phenomena were observed for dodecyl maltoside/hematite system. The surface –FeOH group concentration changes with pH and in turn affects the adsorption of surfactant, as shown in Figure 11. The adsorption density on hematite follows the same trend as the surface hydroxyl group concentration.

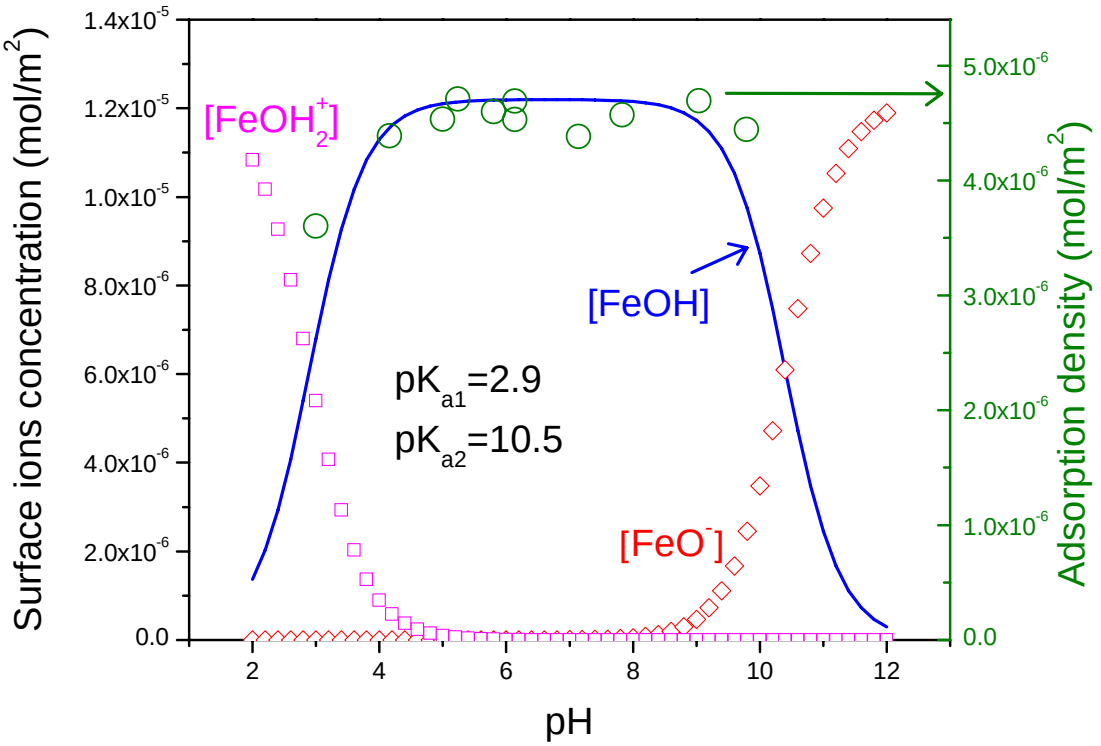

Figure 11: surface ion concentration of alumina and adsorption of dodecyl maltoside on alumina

Adsorption of dodecyl maltoside on solid at high temperature

To investigate the effect of temperature on surfactant adsorption, the adsorption experiments were done at a higher temperature. The tests were done in a hot box to maintain the sample temperature from the beginning to the separation of the supernatant and the slurry. The concentration of the supernatant was determined using TOC, and was used as the residual concentration. The adsorption of n-dodecyl-β-D-maltoside on alumina at 25 ℃ and 45 ℃ are shown in figure 12 respectively. The adsorption isotherm at 45 ℃ shows a typical three stage isotherm: low adsorption at low concentration below the critical aggregation concentration, a sharp increase in the concentration range close to critical

micellar concentration, and a plateau range above CMC. The isotherm is almost identical to that at 25 ℃ below the CMC. Surprisingly, the adsorption decreases significantly with temperatures above CMC, as the plateau adsorption density is 5.5×10^{-6} Mol/m^2 at 25 ℃ while it is only 4.5×10^{-6} Mol/m^2 at 45 ℃. The decrease in adsorption density can be attributed to the effect on the molecular packing at the solid/liquid interface. The average area per molecule may increase with temperature and it causes the decrease in adsorption density.

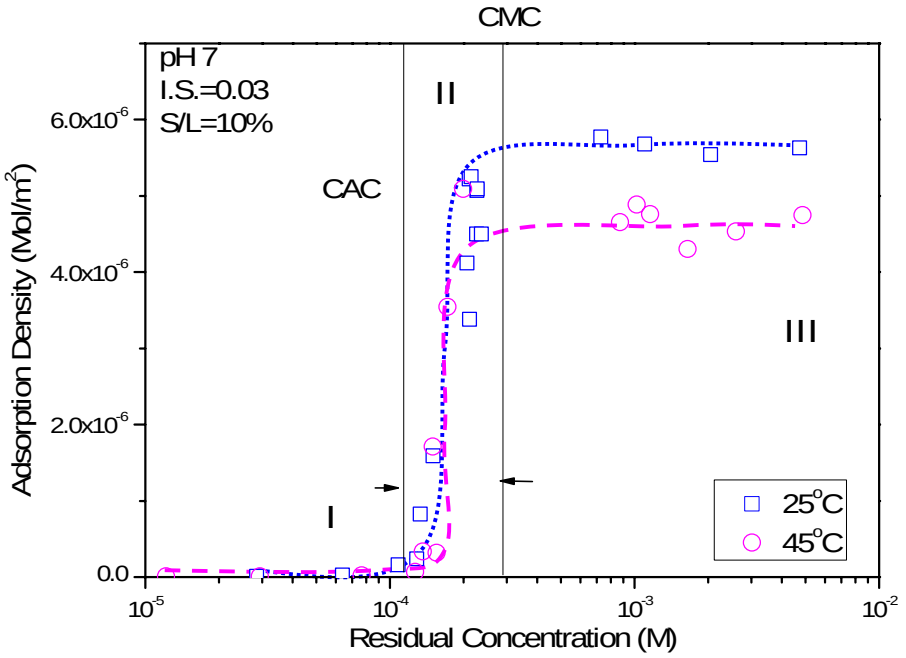

Figure 12: Adsorption isotherms of n-dodecyl-β-D-maltoside on alumina at 25℃ and 45 ℃

Adsorption of dodecyl maltoside in the presence of multivalent ions

In the oil reservoir, the dissolved mineral species can increase the ionic strength of the solution and the presence of the ions, especially multivalent ions, can cause significant precipitation and thus then chemical loss. To investigate the chemical loss of surfactant and surfactant mixture under practical conditions, the adsorption/precipitation tests of mixed DM/SDS on alumina was done in the presence of monovalent and divalent ions at different concentrations.

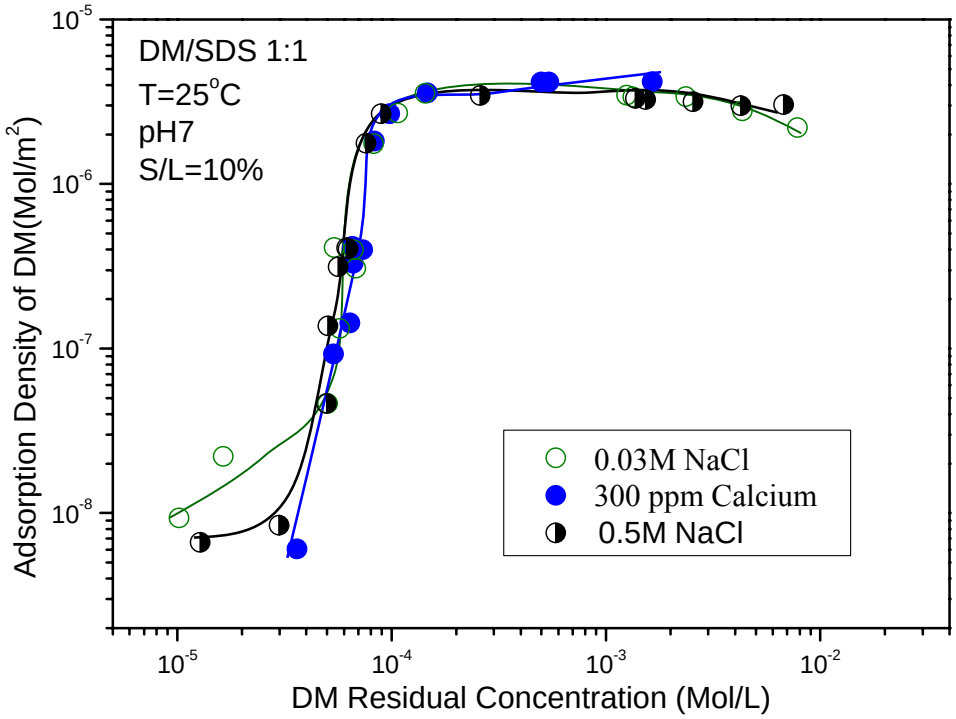

Figure 13: Adsorption of DM from its mixture with SDS on alumina at different ionic strength

The adsorption isotherms of DM on alumina from its mixture with SDS in the presence of different ionic conditions are plotted in figure 13. It can be seen that the isotherms lie on almost the same curve, suggesting that the adsorption of DM is independent of the monovalent and divalent ions. Also, the adsorption density does not change much when the sodium chloride concentration increases

from 0.03M to 0.5 M. This phenomenon can be attributed to the nature of the sugar based surfactants. This diagram clearly shows that, as a nonionic surfactant, DM has very good salt tolerance. In the case of adsorption the presence of monovalent or divalent ions, they affect the electrostatic force at the water/alumina interface and do not affect the adsorption of DM since the driving force for DM adsorption is hydrogen bonding, which has been found to occur between the hydroxyl groups on DM molecules and the hydroxyl groups on the alumina surface. It can predicted that the adsorption of this nonionic sugar based surfactant will not change much with dissolved species in the oil reservoir during the solution flooding process for enhanced oil recovery.

Adsorption of double hydrophobic chain Gemini and single chain general surfactants

Cationic Gemini surfactant butane-1,4-bis(dodecyl dimethyl ammonium chloride), C_{12}-C_4-C_{12}, with two hydrophobic and two hydrophilic groups in the molecule, could be viewed as a dimer of dodecyltrimethyl ammonium chloride (DTAC), which has a single hydrophobic and hydrophilic group. Figure 14 shows the structural relationship between C_{12}-C_4-C_{12} and DTAC. C_{12}-C_4-C_{12} is more surface-active than DTAC in terms of the micelle formation. The critical micelle concentration of C_{12}-C_4-C_{12}, 1.5mM, is 10 times lower than that of DTAC (20mM), due to the increased hydrophobicity of C_{12}-C_4-C_{12} with two hydrocarbon chains.

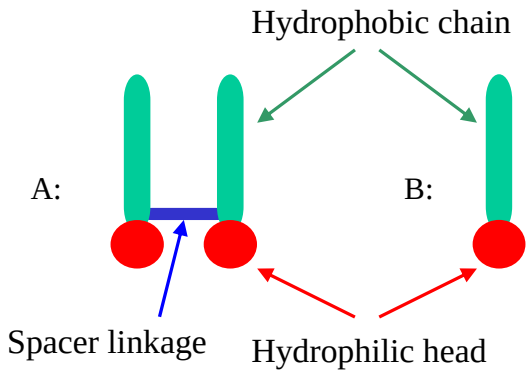

Figure 14. Structure comparison of cationic Gemini surfactant C_{12}-C_4-C_{12} (A) to DTAC (B), C_{12}-C_4-C_{12} is a dimmer of DTAC.

Adsorptions of Gemini C_{12}-C_4-C_{12} and DTAC on silica mineral were measured under the same conditions, and the results obtained are shown in Figure 15. Both C_{12}-C_4-C_{12} Gemini and DTAC reach the same saturation adsorption with approximate bilayer formation around their solution cmcs, because they share the same cross sectional area per hydrophobic chain. Adsorption of Gemini C_{12}-C_4-C_{12} in the low concentration range is markedly higher, which is attributed to the greatly increased electrostatic adsorption of C_{12}-C_4-C_{12} on the negatively charged silica, with the presence of **two** positively charged headgroups in the molecule.

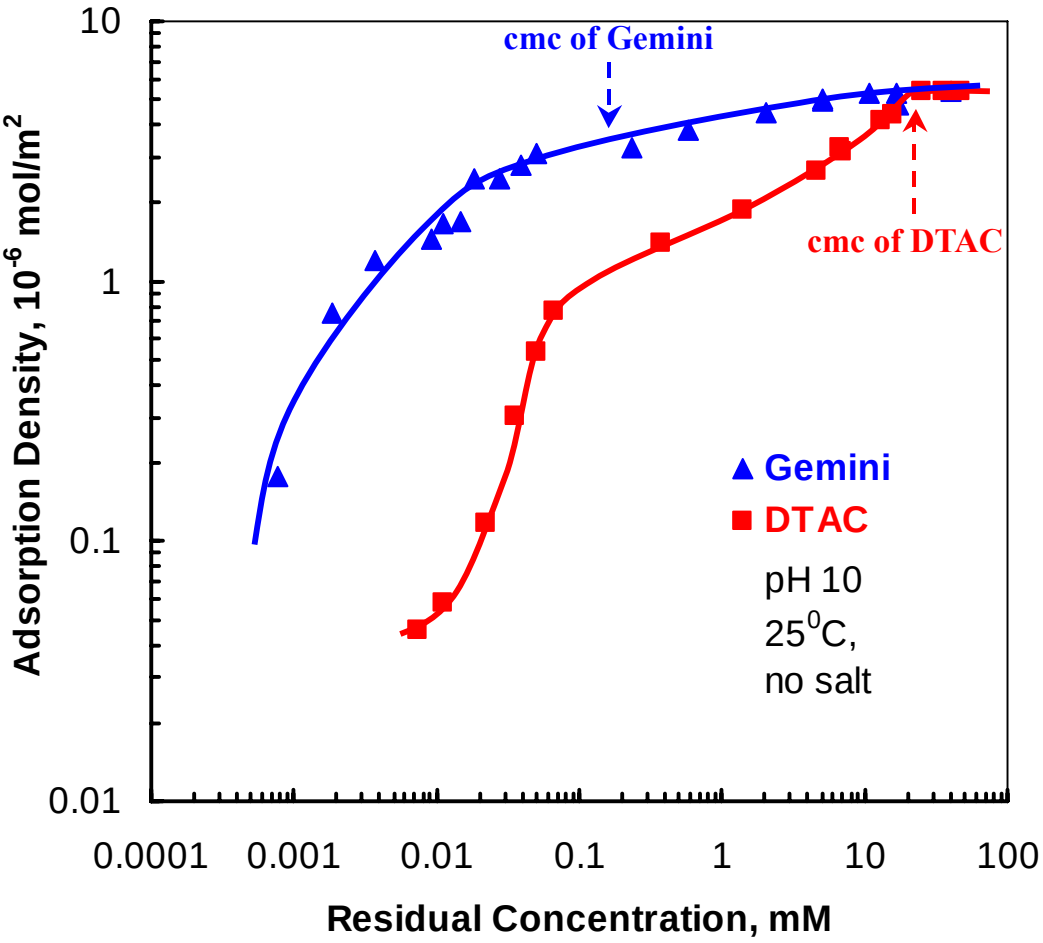

Figure 15. Adsorption of Gemini C_{12}-C_4-C_{12} and single chain DTAC on silica. Both adsorption density and residual concentration values are based on per hydrophobic alkyl chain in the surfactant molecule. For Gemini, there are two hydrophobic chains in every molecule.

pH Effect on the adsorption of cationic Gemini surfactant on silica

Figure 16 shows the adsorption of cationic Gemini surfactant C_{12}-C_4-C_{12} at different pH with out swamping amounts of salt. Clearly, pH has a remarked effect on the adsorption of the cationic Gemini on the negatively charged silica mineral. At pH 4, relatively low adsorption of C_{12}-C_4-C_{12} on silica was observed, with an S-shaped adsorption isotherm. At neutral pH, the adsorption of C_{12}-C_4-C_{12} on silica increases sharply in the low concentration range, because of

the strong mutual electrostatic attraction between the double positively charged headgroups on cationic Gemini and the negatively charged silica surface. Under basic conditions, a sharp increase of C_{12}-C_4-C_{12} adsorption was observed at lower concentrations.

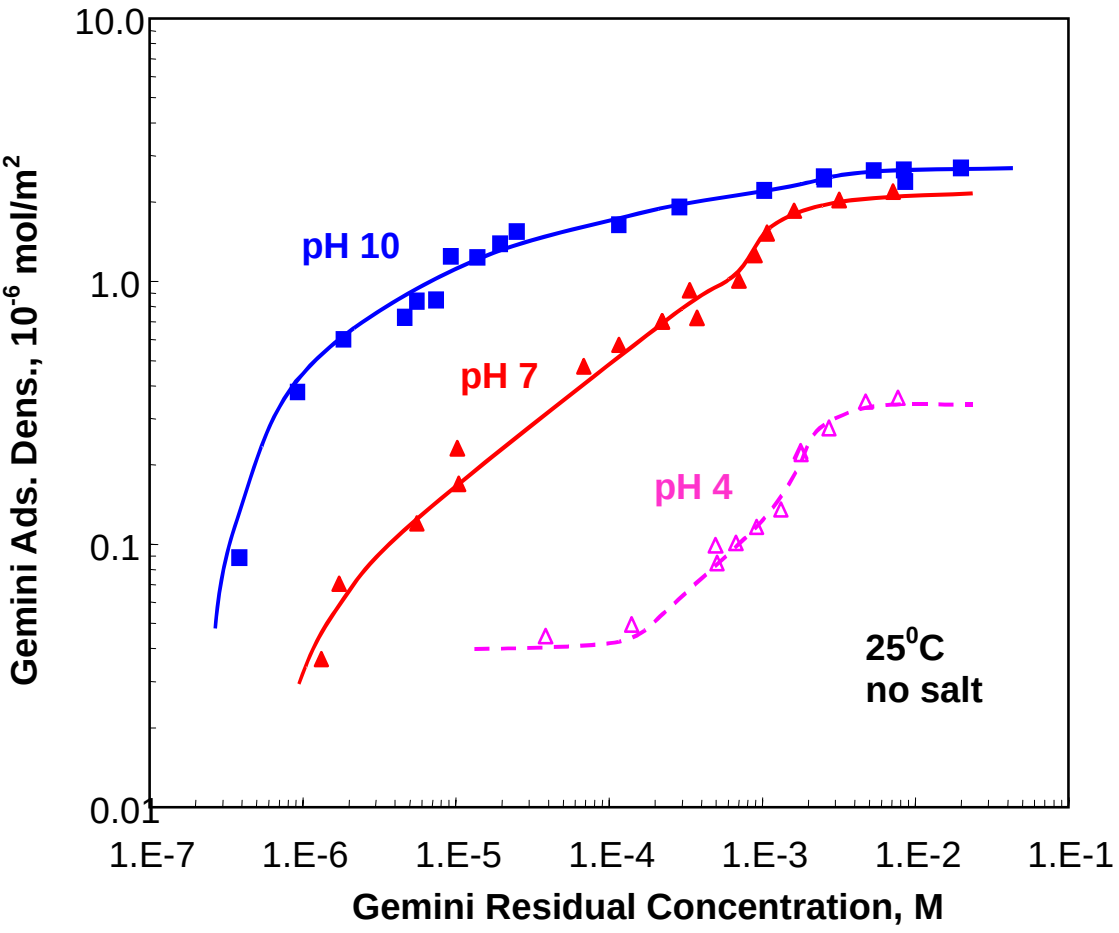

Figure 16. Effects of pH on adsorption of cationic Gemini surfactant C_{12}-C_4-C_{12} on silica at room temperature w/o salt. pH 4 △, pH 7 ▲, and pH 10 ■.

Effect on adsorption of double chain cationic surfactant on silica compared with single chain surfactant

The adsorption isotherm of single chain DTAB on silica was determined at two different salt concentrations and two different pH values. Fig. 17 and 18 show the isotherm at pH 5 and 9 respectively at the two salt concentrations of 5×10^{-3} mol/L and 5×10^{-1} mol/L. At the higher salt concentration, the sharply rising region becomes steeper possibly due to changes in the electrical double layer structure of the ions and their subsequent effects on the surface charge. Owing to the screening of electrostatic forces in the presence of high salt concentration, the formation of hemimicelles on the silica surface occurs in a narrow concentration range and it reaches saturation adsorption at a lower concentration. The fact that the maximum adsorption density in each case reaches the same value can provide an insight into the packing of the surfactant molecules on the surface.

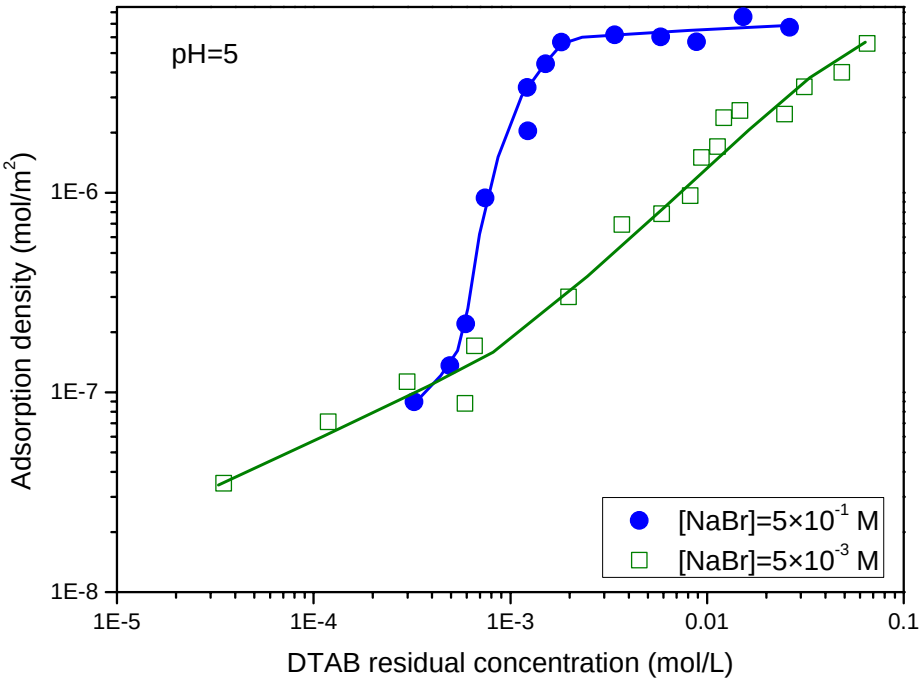

Figure 17 Adsorption isotherms of DTAB on silica at pH 5

At pH 9, the adsorption density in the low residual concentration range at 5×10^{-1} mol/L NaBr is lower than that at 5×10^{-3} mol/L. In contrast, the adsorption density in the higher residual concentration range is larger than that at 5×10^{-3} mol/L, suggesting that the role of electrostatic force changes with surfactant concentration. At low surfactant concentrations, the presence of salt neutralizes the negative charge on the silica surface and lowers the electrostatic attraction with the surfactant headgroup, thereby decreasing the adsorption density. At higher concentration, the adsorbed surfactant molecules reverse the surface charge and the presence of salt reduces the electrostatic repulsion among the surfactant molecules increasing the adsorption density.

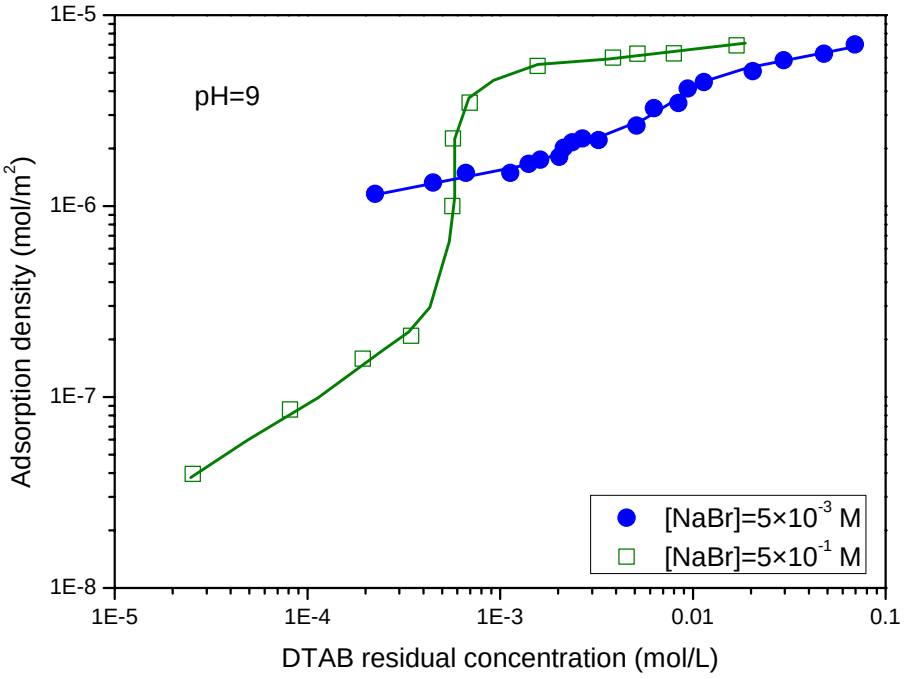

Figure 18 Adsorption isotherms of DTAB on silica at pH 9

Figure 19 illustrates the isotherms for double chain DDAB on silica at pH 5 and 9 at a salt concentration of 5×10^{-3} mol/L of NaBr. The isotherms at 5×10^{-1} mol/L NaBr could not be traced in this case since the maximum plateau values could not be reached due to the solubility limitations of DDAB at higher ionic strengths. Furthermore, even tests with a reduction in the solid content did not improve the prospect of attaining the plateau. The adsorption density increased sharply at a very low concentration, because of the formation of hemicelles on the surface. The double hydrocarbon chain produced much higher lateral associative interaction and thus enhanced the formation of aggregates at very low concentrations. The maximum adsorption density was observed to be the same at pH 5 and pH 9.

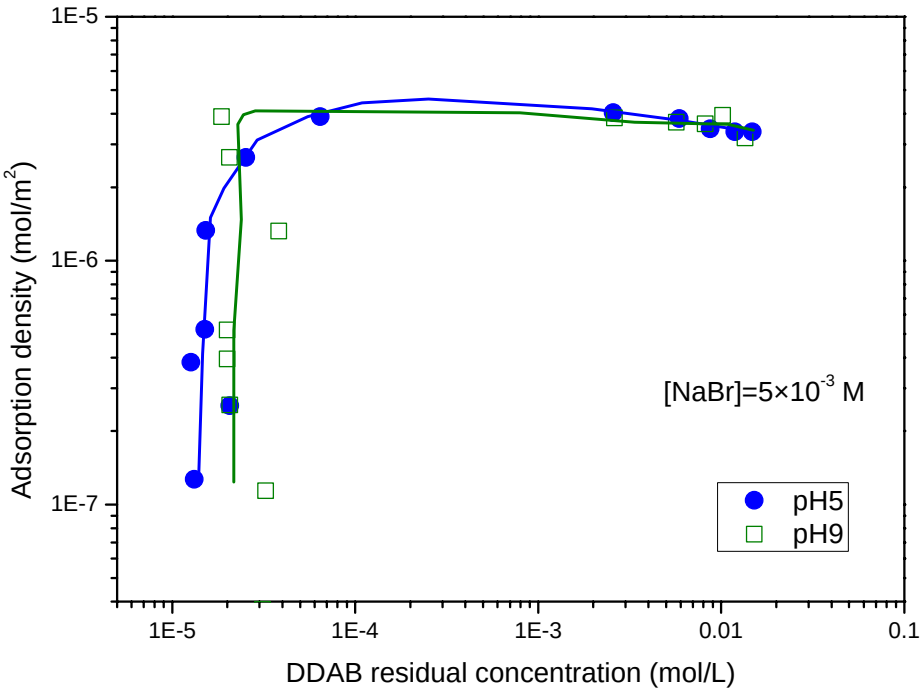

Figure 19: Adsorption isotherms of DDAB on silica at pH 5 and pH 9

In order to facilitate a comparison between the adsorption of single chain and double chain surfactants, the adsorption isotherms at pH 5 and a salt concentration of 5×10^{-3} mol/L are shown in Figure 20.

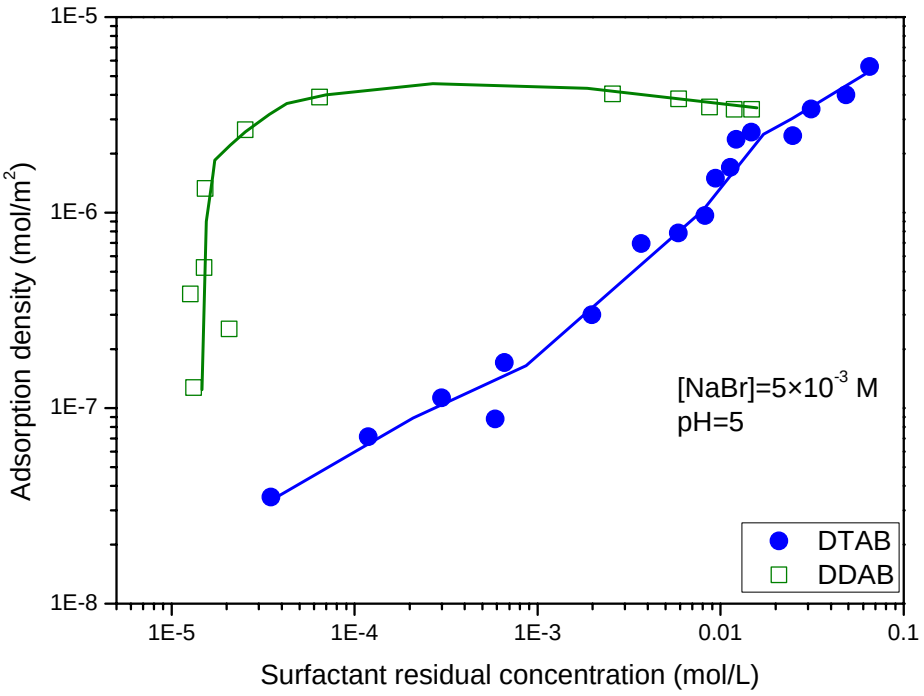

Figure 20: Adsorption isotherms of DTAB and DDAB on silica at pH 5

Table 2 lists adsorption densities at plateau for the two surfactants on silica at pH 5 and 9. Using the average headgroup areas DTAB yielded ~1.5 monolayers while DDAB yielded ~0.9 monolayers. The above numbers were based on the effective head group area obtained from the surface tension data. The effective head group area in the case of DTAB is 38 $Å^2$/molecule and in the case of DDAB, 37.4 $Å^2$/molecule.

Table 2 Adsorption densities at plateau for single chain and double chain surfactant.

	Saturation adsorption (mol/L)		Headgroup area ($Å^2$/molecule)	
	pH 5	pH 9	pH 5	pH 9
DTAB	6.25×10^{-6}	6.8×10^{-6}	26.6	24.4
DDAB	3.9×10^{-6}	3.9×10^{-6}	42.6	42.6

The above surface coverage data may be interpreted by considering the various aggregation possibilities that can drastically affect the wettability of the solid surface. The aggregation process can be visualized as follows: in the initial linear region the surfactant ions stick to the surface in a random manner. When the aggregation process commences on the surface, the molecules orient toward to the surface exposing more of their hydrophobic sites to the incoming molecules. When the aggregation process advances, some of the molecules adsorb on the aggregates with a reverse orientation, i.e. with the charged head group facing the aqueous phase. This region normally coincides with the charge reversal of the solid surface. The reverse oriented molecules, equivalent to a bilayer, impart hydrophilicity on mineral surface. The pseudo bilayer otained, however, cannot be as dense as a typical bilayer. The value of -1.5 monolayers for the adsorbed layer thickness is in line with the reverse orientation model, which should tend to a value of ~2 for a pure bilayer. The ~0.9 surface coverage value for the DDAB-silica system shows that in this case the DDAB aggregates to form monolayer surface coverage.

Zeta potentials of DDAB/silica system were determined at pH 2, 5 and 9 at a constant ionic strength of 5×10^{-3} mol/L. The zeta potential data is illustrated as a function of residual concentration and correlated with the adsorption isotherms. The adsorption densities corresponding to the point of zero charges in each case are 4.5×10^{-8}, 1×10^{-7}, and 3.5×10^{-6} mol/L for pH 2, 5 and 9 respectively. The points of zero charge occur well below the monolayer coverage.

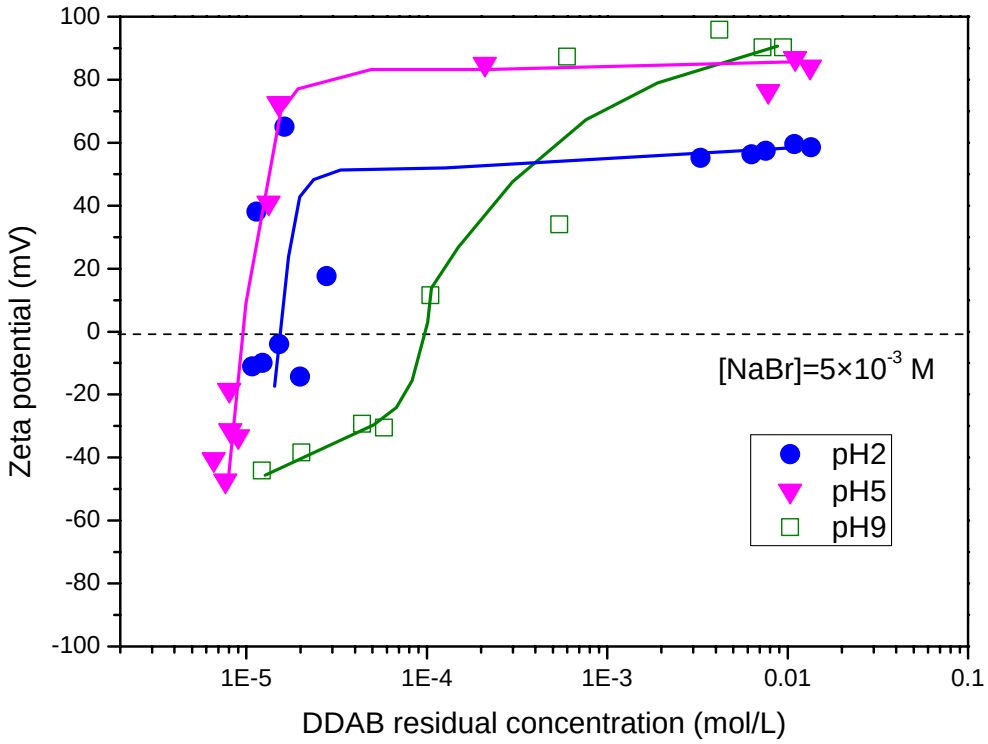

Figure 21: Zeta potential of silica with adsorption at various pHs

Adsorption of the mixtures of Gemini and sugar-based nonionic surfactants on solids

Surfactant mixtures have long been studied for both theoretical and practical interests. We investigated the adsorption behaviors of mixture systems of Gemini and sugar-based nonionic surfactants.

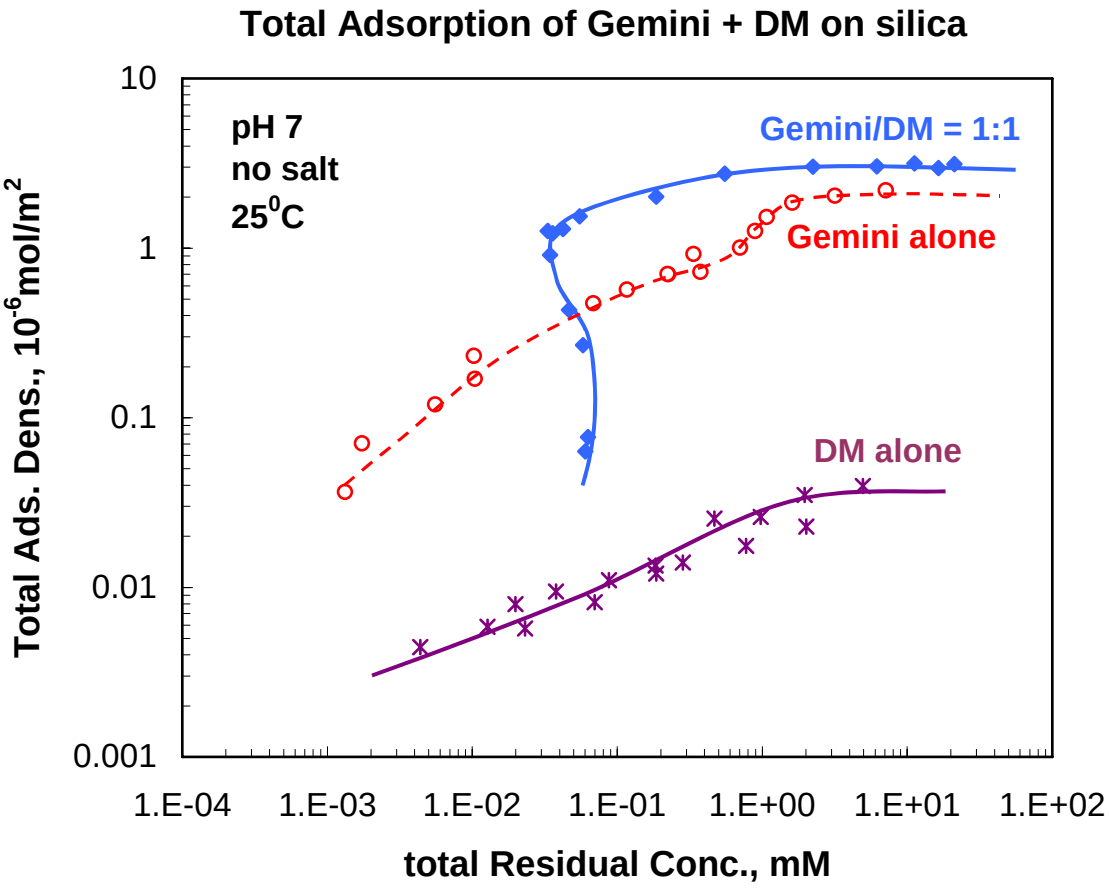

Figure 22: Total adsorption of mixtures of n-dodecyl-β-D-maltoside (DM) and cationic Gemini C_{12}-C_4-C_{12} and on silica, at pH neutral, no swamping amount of salt.

The results obtained for the total surfactant adsorption of both on silica at pH 7 from mixtures of cationic Gemini surfactant C_{12}-C_4-C_{12} and n-dodecyl-β-D-maltoside (DM) are shown in Figure 22. While DM shows negligible adsorption on silica at pH 7, cationic Gemini alone shows appreciable

adsorption under this condition. Apparently, in both the rising and saturation adsorption ranges, considerable synergistic adsorption exists. In the case of mixtures, lower concentration is required to reach saturation adsorption, because DM shows such lower concentration for the formation of aggregates at both the solid/liquid interfaces and the bulk solution. In Figure 23 the adsorption of DM from DM alone is compared with that from its mixture with C_{12}-C_4-C_{12}. With 1:1 Gemini/DM mixtures, the adsorption of DM on silica from the mixtures is 50 times higher than that of the adsorption of DM alone. Significant synergistic participation of DM in mixed adsorption is the major reason for the observed adsorption in this case. The synergy in the mixtures is proposed to result from the marked hydrophobic chain-chain interaction between DM and the adsorbed Gemini C_{12}-C_4-C_{12}. Since cationic Gemini C_{12}-C_4-C_{12} can easily adsorb on the negatively charged silica, adsorbed C_{12}-C_4-C_{12} molecules are proposed to act as nucleation sites for forming mixed aggregates with DM on silica surface, which would greatly increase DM adsorption.

In comparison to the increased DM and the combined mixture adsorption, adsorption of the cationic Gemini C_{12}-C_4-C_{12} on silica from its 1:1 mixtures with DM shows synergistic adsorption only in the rising part of the isotherm and some decreased saturation adsorption compared to the adsorption of Gemini alone (Figure 24). The increased Gemini C_{12}-C_4-C_{12} adsorption in the rising part is again attributed to be the hydrophobic chain-chain interaction between DM and C_{12}-C_4-C_{12}, while the decreased Gemini adsorption in the plateau regions is due to the significant competition of adsorption sites by DM (Figure 23).

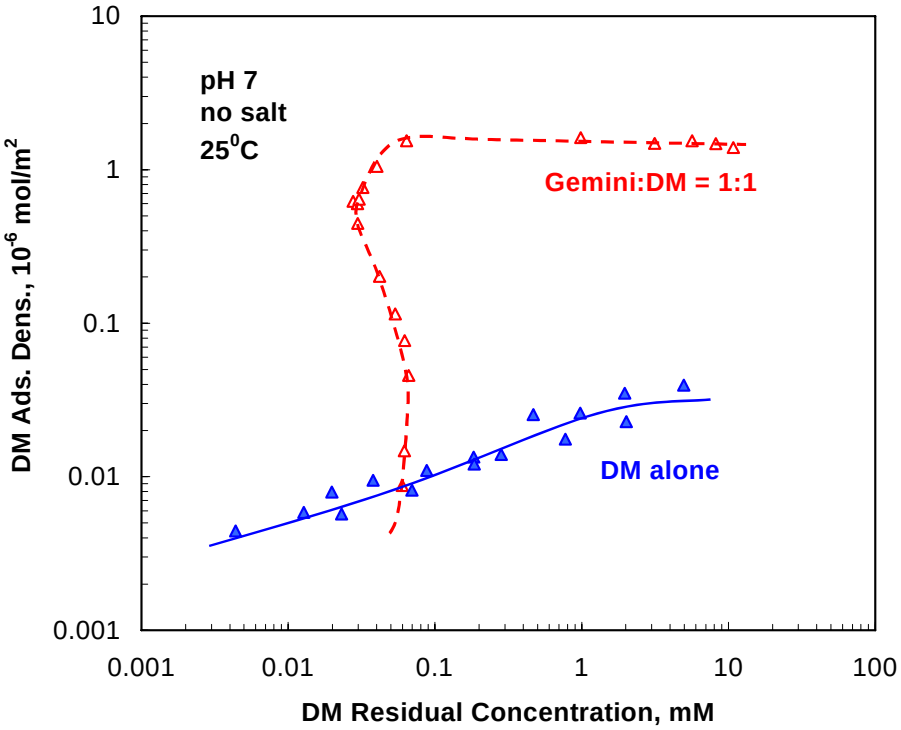

Fig23: Adsorption of n-dodecyl-β-D-maltoside (DM) from its mixtures with cationic Gemini surfactant C_{12}-C_4-C_{12} on silica, at neutral pH, no swamping amount of salt.

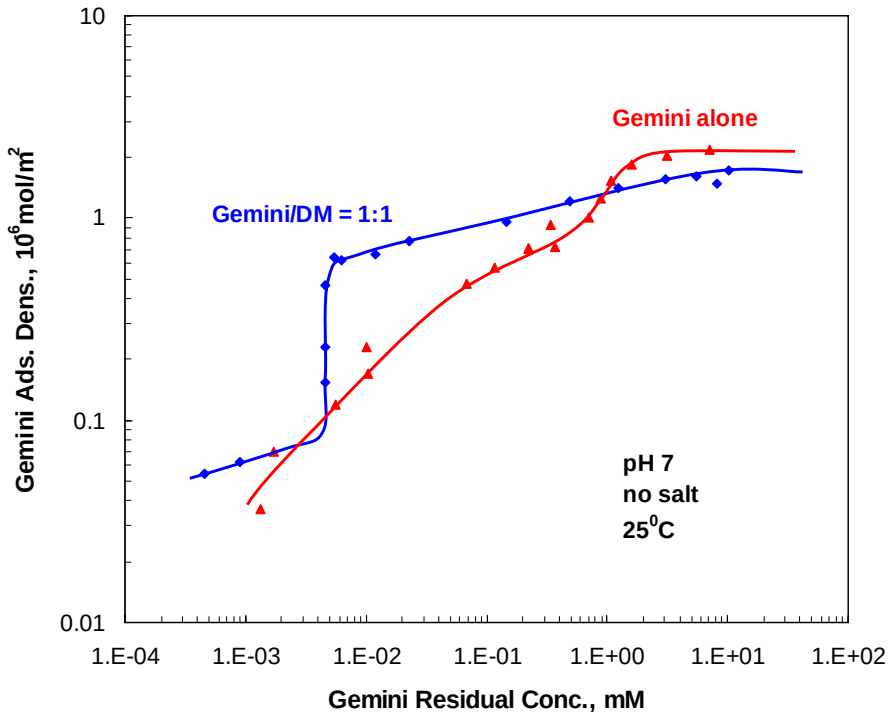

Fig24: Adsorption of cationic Gemini surfactant C_{12}-C_4-C_{12} from its mixtures with n-dodecyl-β-D-maltoside (DM) on silica, at neutral pH, no swamping amount of salt.

Effect of surfactant mixing ratio on the mineral-surfactant interactions at the solid/liquid interface

The effect of Gemini/DM mixing ratio on the adsorption of Gemini C_{12}-C_4-C_{12} on silica is illustrated in Figure 25. The residual Gemini concentrations after adsorption at different mixing ratios have been controlled to be the same in the rising part of the adsorption isotherms. A drastic increase in Gemini C_{12}-C_4-C_{12} adsorption has been observed with the increase of DM in the mixtures from DM/Gemini mixing ratio 1:10 to 1:1. Again, clearly the hydrophobic chain-chain interaction leads to significant synergy in adsorption in the rising part. In the plateau region competition for adsorption sites dominates and causes a decrease in C_{12}-C_4-C_{12} adsorption.

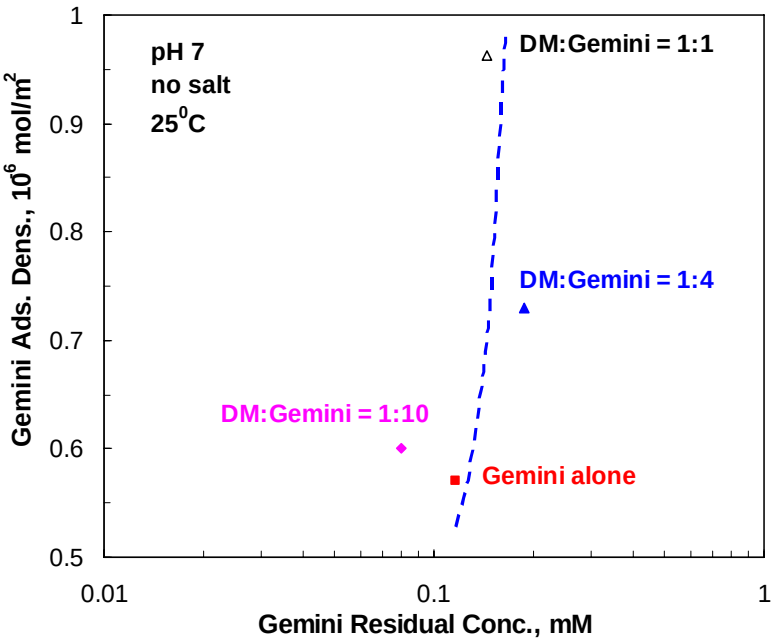

Figure 25: Effect of the mixing ratio on the adsorption of cationic Gemini C_{12}-C_4-C_{12} from its mixtures with n-dodecyl-β-D-maltoside (DM) on silica, at room temperature, neutral pH, no swamping amount of salt.

Results obtained for the total surfactant adsorption on silica at pH 7 from the mixture of cationic

C_{12}-C_4-C_{12} Gemini surfactant and n-dodecyl-β-D-maltoside (DM) are shown in Figure 26. DM shows relatively little adsorption on silica, compared to the cationic Gemini, which shows two orders of magnitude more adsorption at pH 7. Adsorption of the mixtures is higher than when present alone in the rising and saturation adsorption ranges, suggesting significant synergistic adsorption. Higher the DM mole fraction in the bulk solution, higher is the total adsorption and lower is the concentration required to reach saturation adsorption. Synergistic participation of DM in mixture adsorption is significant for the mixtures studied and this is clearly seen in Figure 27. At 1:4 Gemini/DM mixtures, the adsorption of dodecyl maltoside on silica from the mixtures is about 100 times higher than that of DM alone and 20 times higher than that from the mixtures with 10:1 Gemini/DM. For 1:4 Gemini/DM mixture, the saturation adsorption density of dodecyl maltoside is about 3.5×10^{-6} mol/m^2 and the surface area per molecule adsorbed is calculated to be 48 Å^2. When compared with the value derived from the surface tension data, this amount of DM surfactant adsorbed on the silica particles is estimated to be just enough to form a theoretical monolayer. A small amount of Gemini apparently acts as anchor molecules for adsorption of DM molecules around them. It would be useful to identify the optimum amounts of Gemini required for the optimal packing of the surfactant molecules in the adsorbed layers under relevant EOR conditions.

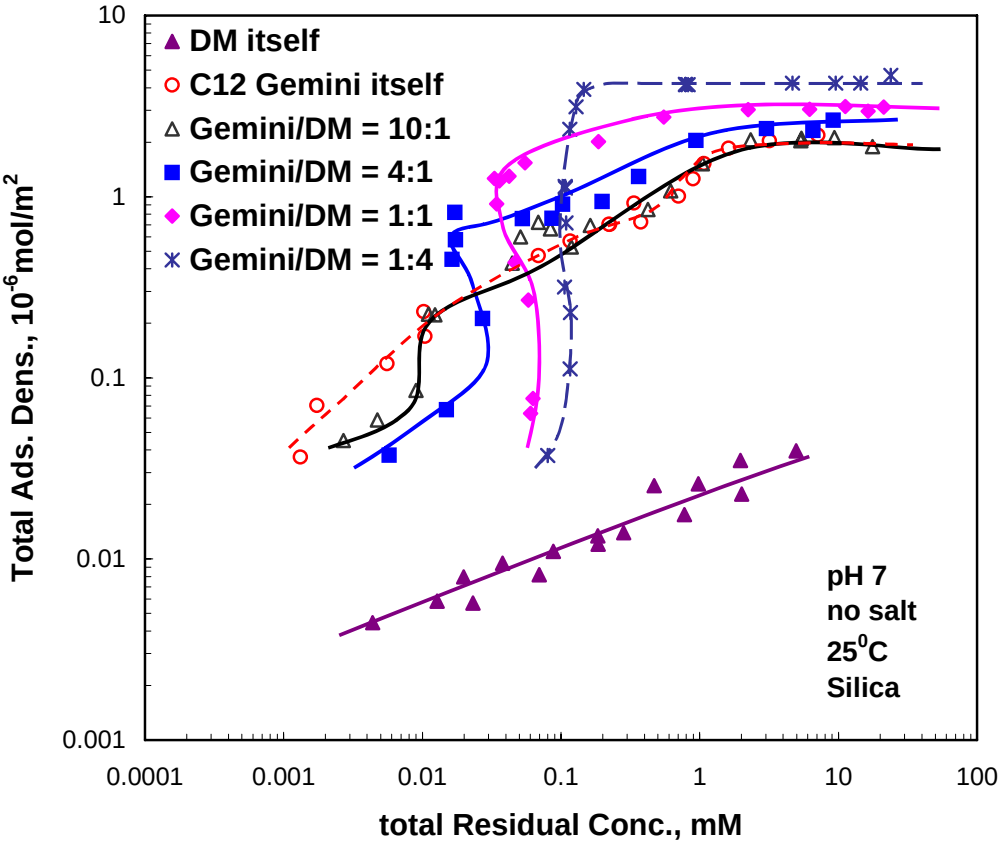

Figure 26: Effect of mixing ratio on total adsorption of mixtures of cationic C_{12}-C_4-C_{12} Gemini surfactant and n-dodecyl-β-D-maltoside (DM) on silica, at neutral pH and no swamping amount of salt.

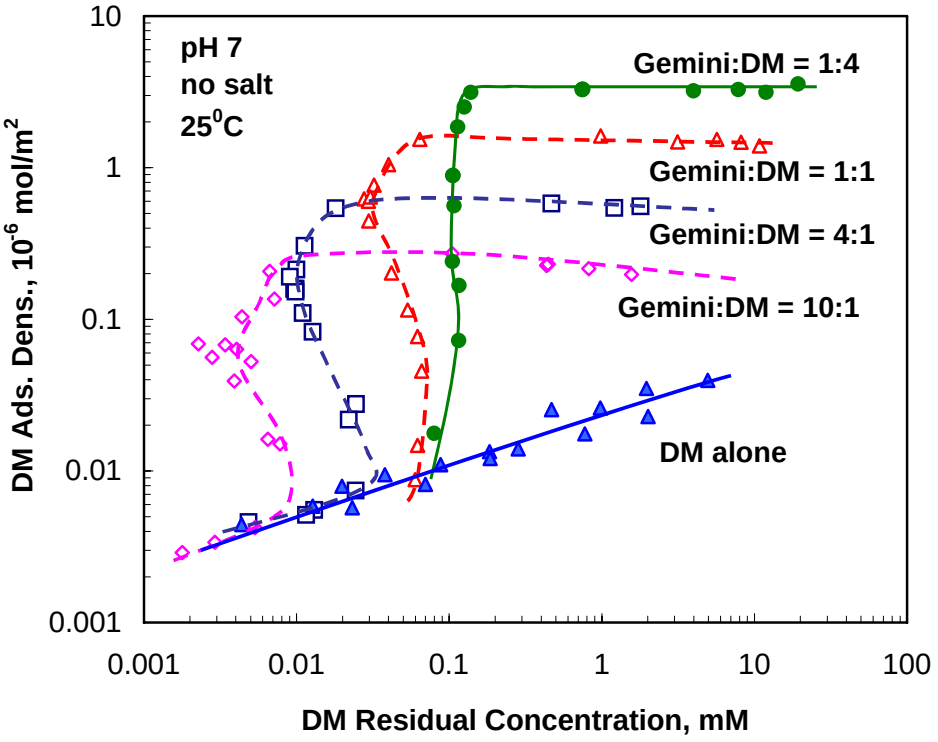

Figure 27: Effect of mixing ratio on the adsorption of n-dodecyl-β-D-maltoside (DM) from its mixtures with cationic C_{12}-C_4-C_{12} Gemini surfactant on silica, at neutral pH and no swamping amount of salt.

In contrast to the increased DM and total mixture surfactant adsorption, the adsorption of cationic C_{12}-C_4-C_{12} Gemini surfactant on silica from its mixture shows synergistic adsorption in the rising part of the isotherm, but decreased saturation adsorption compared to the adsorption of Gemini alone (Figure 28). Higher the DM molar fraction, more is the increase in the rising part of the Gemini adsorption, and higher is the decrease of the Gemini adsorption in the plateau region. This is attributed to the competition by dodecyl maltoside for adsorption sites. This suggests the possibility of obtaining desired interfacial properties by controlling the mixing ratios based on the type of information generated here.

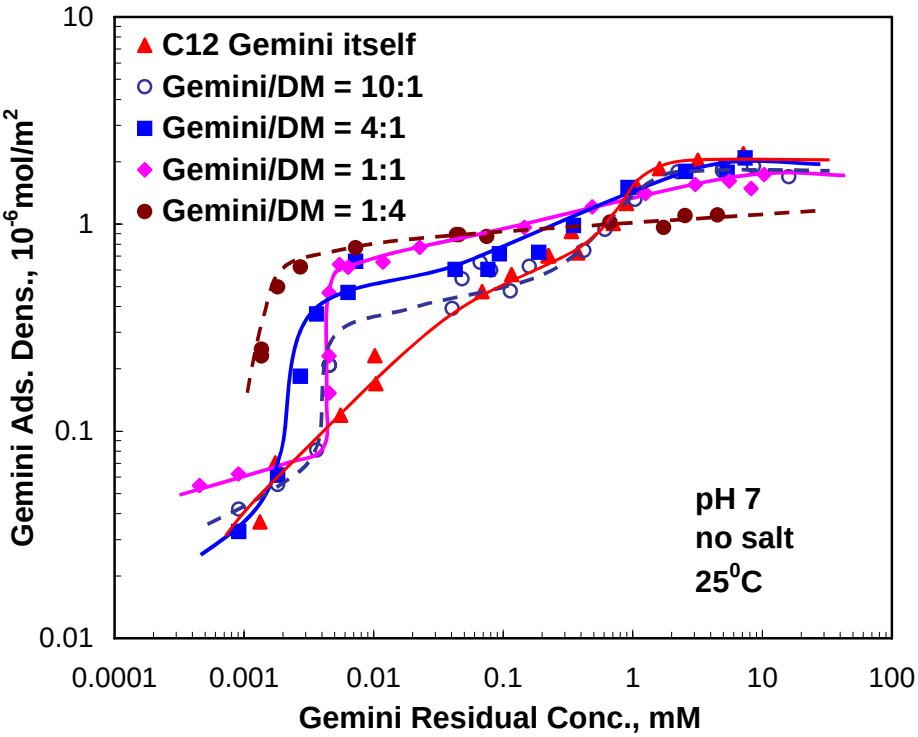

Figure 28: Effect of mixing ratio on the adsorption of cationic C_{12}-C_4-C_{12} Gemini from its mixtures with n-dodecyl-β-D-maltoside (DM) surfactant on silica, at neutral pH and no swamping amount of salt.

As discussed above, change in the mixing ratio in the C_{12}-C_4-C_{12}/DM systems has marked effects on mineral-surfactant interactions, especially the adsorption of DM on silica. The extent of this effect has been further studied by going to extreme mixing ratio conditions, to reveal how effective the surfactant mixing ratio can be. Figure 29 shows the adsorption of n-dodecyl-β-D-maltoside (DM) at such mixing ratio conditions. In Figure 29, the initial Gemini concentrations have been controlled so that at adsorption equilibrium the adsorption densities of Gemini are the same at all mixing ratios. We observed a continuous increase of the DM adsorption on silica with decrease of C_{12}-C_4-C_{12}/DM ratio from 10:1 to 1:100, even though DM barely adsorbs on silica by itself. This drastic increase of DM

adsorption in the presence of even very small amount of C_{12}-C_4-C_{12} Gemini has been attributed to the significant hydrophobic chain-chain interaction between DM and Gemini and the formation of mixed aggregates of Gemini and DM on silica surface, with Gemini acting as nucleation sites.

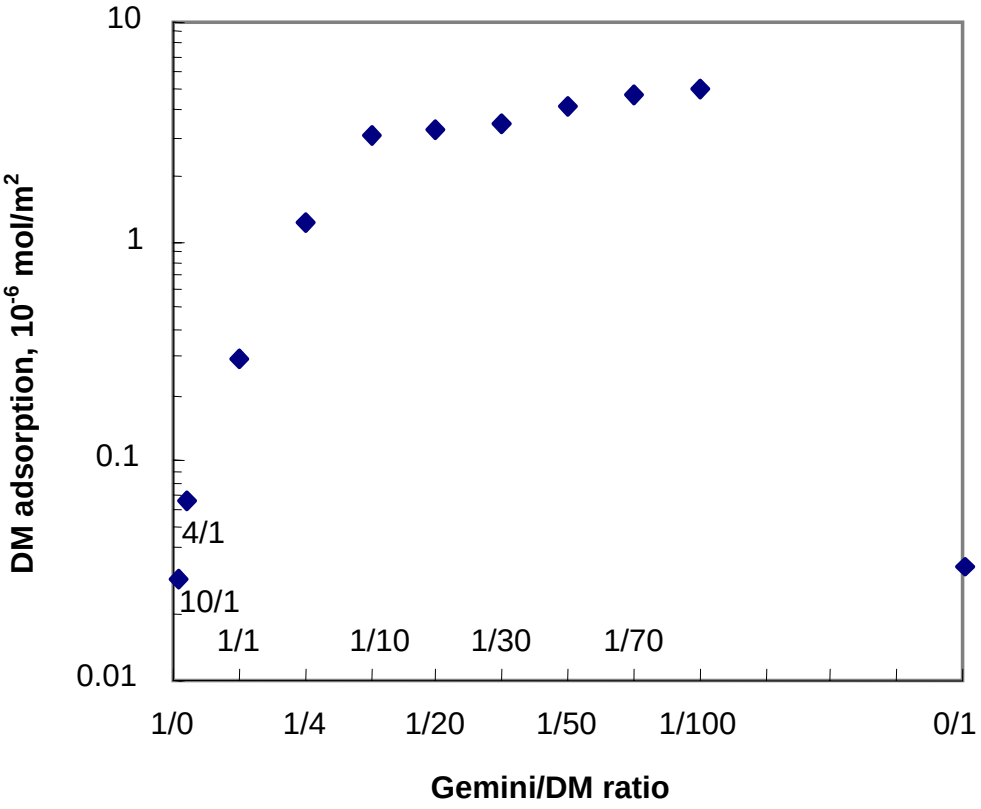

Figure 29: Effect of mixing ration on adsorption of dodecyl-maltoside (DM) from its mixture with cationic Gemini on silica, the adsorption density of Gemini has been controlled to be the same at all ratios.

Electrokinetics of silica in the mixtures of cationic Gemini and sugar-based surfactant solution

Surface charge of the minerals is one of the important factors determining the solid/solution interfacial processes such as adsorption and the efficiency of oil liberation from the mineral rocks in the IOR processes. Electrokinetic studies of silica mineral have been carried out during this period along with adsorption. The results obtained are shown in Figures 30 and 31. It is clear from Figure 30, that the zeta potential of silica is not altered significantly by the adsorption of DM surfactant alone, which is in accord with the nonionic nature of n-dodecyl-β-D-maltoside. Figure 30 also shows the zeta potential of the silica surface as a function of the amount of cationic Gemini C_{12}-C_4-C_{12} adsorbed on silica. The zeta potential of silica particles shows the same change with the Gemini adsorption from both individual surfactant solution and its mixture with DM, showing that the adsorption of the cationic Gemini C_{12}-C_4-C_{12} is the reason for the change in electrophoretic property of the mineral. The results show good correlation between the cationic Gemini adsorption and the zeta potential change.

Figure 31 shows the zeta potential change of silica as a function of residual Gemini concentration. The surface charge reversal of silica occurs at lower concentrations in the case of 1:1 DM/C_{12}-C_4-C_{12} mixture than in the case of the cationic Gemini C_{12}-C_4-C_{12} alone (DM adsorption making no significant contribution to the zeta potential change of the silica mineral), suggesting synergy between C_{12}-C_4-C_{12} and DM, with more Gemini C_{12}-C_4-C_{12} from the mixture adsorbed on silica at low Gemini residual concentrations (*i.e.* the rising part of Gemini adsorption isotherm).

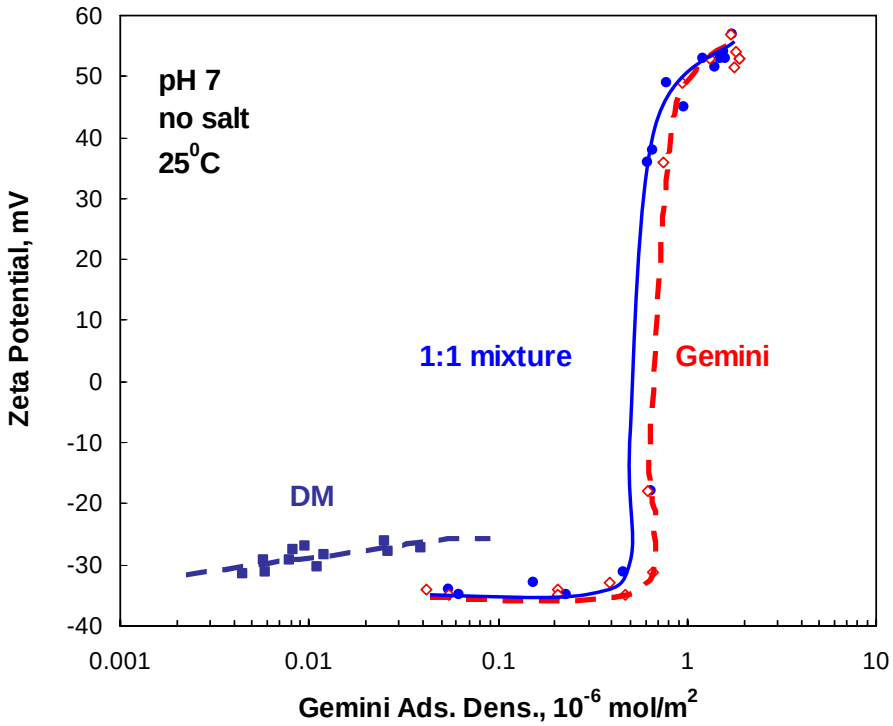

Figure 30: Effect of Gemini adsorption density on the zeta potential of silica due to mixture adsorption, pH 7, 25^{0}C, and no swamping amounts of salt.

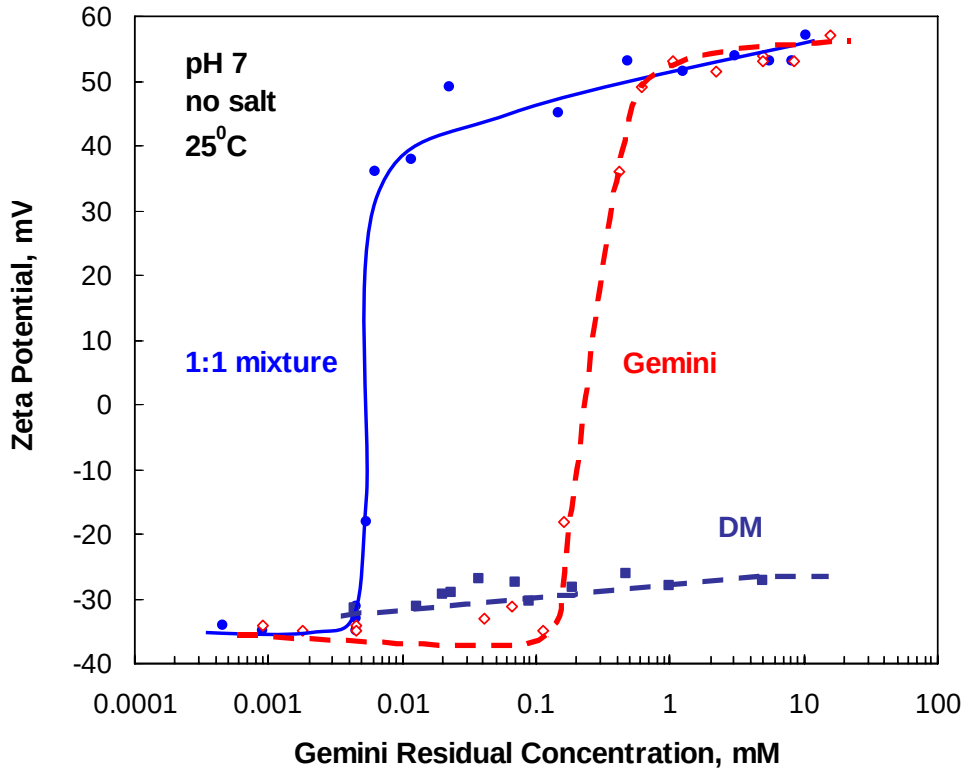

Figure 31: Effect of Gemini residual concentration on the zeta potential of silica due to mixture adsorption, pH 7, 25^{0}C, and no swamping amounts of salt.

Wettability of silica minerals due to the adsorption of surfactant mixtures

Adsorption of surfactants on silica minerals could dramatically change the wettability of the minerals. Wettability of minerals plays an important role in determining the efficiency of oil liberation from the mineral rocks as well as dispersion of mineral fines in EOR processes. Wettability of silica due to the adsorption of the mixtures of cationic Gemini and sugar-based surfactants was therefore determined along with the adsorption measurements.

The information on changes in relative hydrophobicity of the mineral surface due to surfactant adsorption can also shed light on the orientation of the surfactant species on the solid surface and help to elucidate the mechanisms involved. The effect of C_{12}-C_4-C_{12} Gemini adsorption on the wettability of silica is illustrated in Figure 32 along with the adsorption isotherm in both water and 0.03M NaCl media. In the absence of the surfactant, the silica exhibits complete hydrophilicity. With an increase in adsorption of C_{12}-C_4-C_{12} Gemini on silica, the mineral surface becomes hydrophobic due to increasing amount of surfactant adsorbing with their hydrophobic tails oriented toward the bulk solution. The hydrophobicity reaches a maximum and stays constant for a wide range of surfactant concentrations, suggesting that a complete monolayer formation is not necessary to reach maximum mineral hydrophobicity. The drop in hydrophobicity at higher surfactant concentrations suggests that the onset of the chain-chain interaction is causing more and more surfactant to orient with hydrophilic groups toward the aqueous phase. The minimum hydrophobicity of the silica in the plateau region is attributed to the bilayer adsorption, since that can render the silica mineral surface hydrophilic.

It can also be seen from Figure 32, that, C_{12}-C_4-C_{12} Gemini reaches adsorption plateau at much lower concentration in 0.03M NaCl than in water, because of the decreased critical micelle concentration. Decreased cmc also resulted in higher Gemini adsorption density under constant ionic strength conditions in the low residual concentration range, making the silica more amenable to change from

hydrophilic to hydrophobic surface. The Gemini concentration for hydrophilic - hydrophobic silica transition is much lower in 0.03M NaCl than in water.

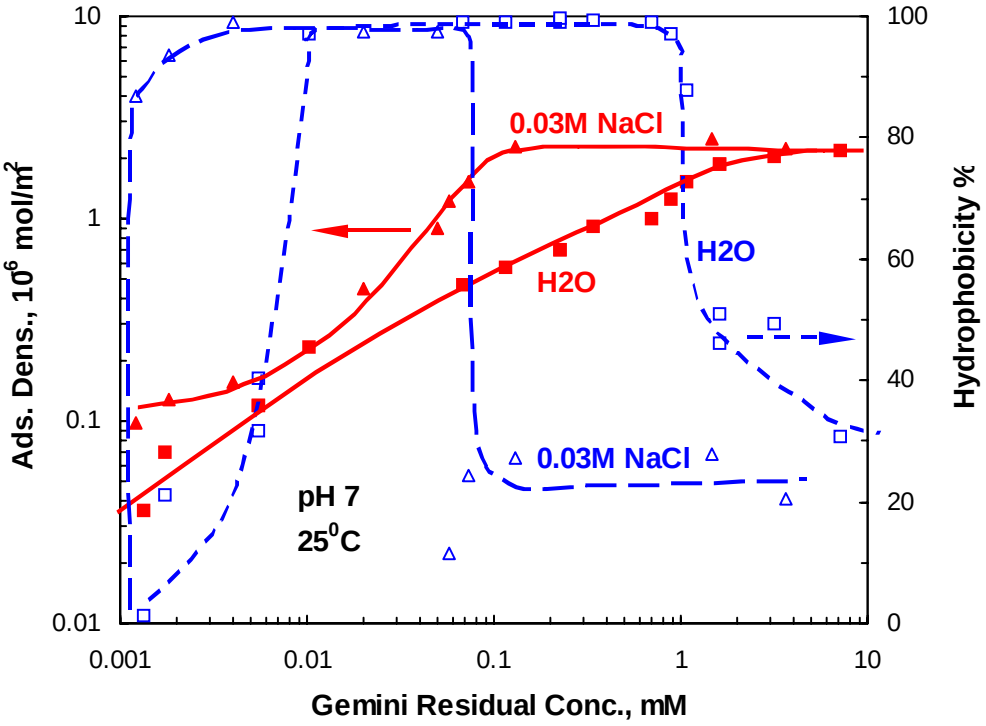

Figure 32: Wettability of silica due to the adsorption of C_{12}-C_4-C_{12} Gemini surfactant at pH 7, 25^{0}C, in both and 0.03M NaCl and H_2O.

As most commercial surfactants used in enhanced oil recovery processes consist of mixtures of surfactants or polymers, the wettability of mineral solid due to the adsorption of surfactant mixtures is more relevant than the effects of single surfactant. Wettability of minerals has been measured to determine how significantly the co-adsorption of n-dodecyl-β-D-maltoside (DM) and C_{12}-C_4-C_{12} Gemini surfactants would change the wettability of the silica mineral. Figure 33 shows the adsorption isotherms of C_{12}-C_4-C_{12} Gemini on silica from its mixtures with n-dodecyl-β-D-maltoside at different surfactant molar ratio along with the corresponding wettability curves. Similar to the single Gemini surfactant, the

wettability of silica changes from hydrophilic to hydrophobic with increase in surfactant adsorption, stays hydrophobic in a wide concentration range and then drops back to hydrophilic due to bilayer adsorption on the silica. It can be seen from Figure 34, that the wettability curve of silica shifts to lower Gemini adsorption density with increase of DM molar ratio in the mixture, indicating significant participation of n-dodecyl-β-D-maltoside in changing the wettability of the minerals. The fact that there is marked synergism/competition in the adsorption of mixtures of n-dodecyl-β-D-maltoside and C_{12}-C_4-C_{12} Gemini in different surfactant concentration ranges, offers valuable information to achieve desired mineral wettability by adjusting surfactant molar ratio in the mixture, and total surfactant concentrations.

From the previous section, it shows that electrophoretic property of silica mineral solids is affected only by the adsorption of Gemini but not by that of nonionic DM. Wettability of mineral solids is clearly affected by the total adsorption of both Gemini and DM, and hence it is possible to obtain both desired wettability and electrophoretic property of the mineral solids through the proper selection of surfactant mixtures, their mixing ratio and the total concentration.

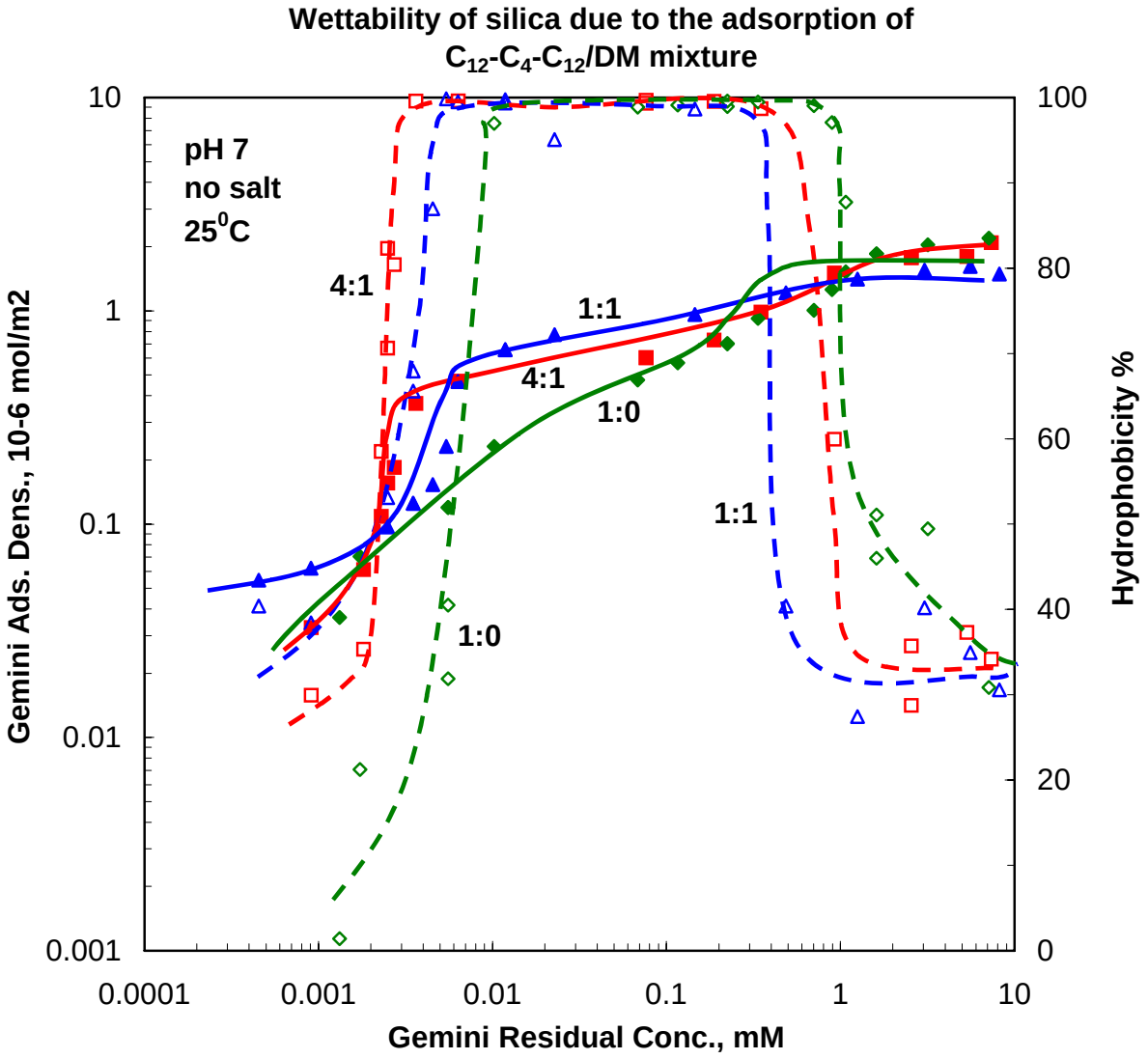

Figure33: Adsorption of the mixtures of n-dodecyl-β-D-maltoside (DM) and C_{12}-C_4-C_{12} Gemini surfactants on silica and its effects on the wettability of silica at pH 7, 25^{0}C, and no swamping amounts of salt. Solid lines for adsorption isotherms, dashed lines for hydrophobicilty curves.

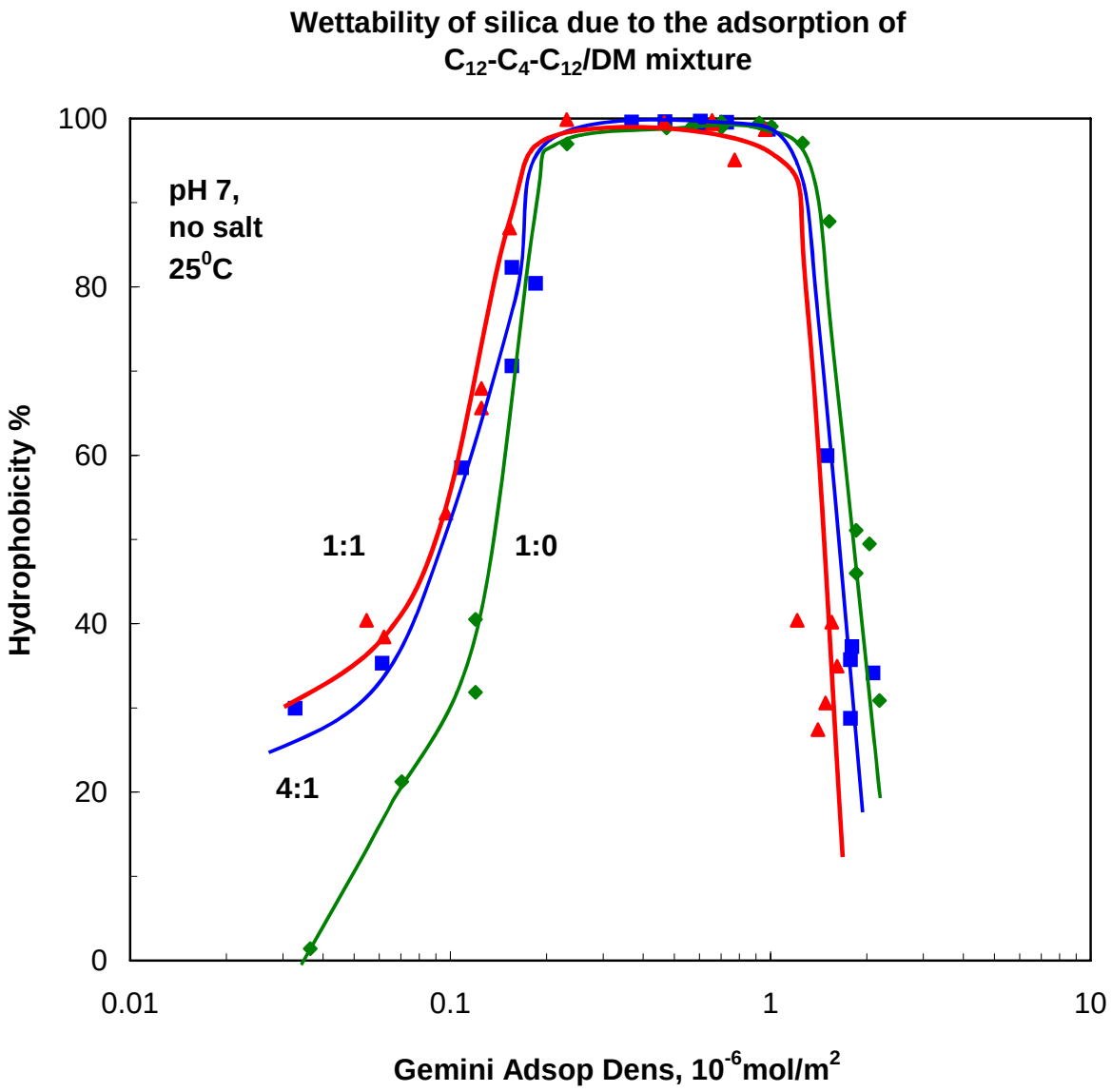

Figure 34: Wettability of silica due to the adsorption of n-dodecyl-β-D-maltoside (DM)/C_{12}-C_4-C_{12} Gemini mixture at pH 7, 25^{0}C, and no swamping amounts of salt. Gemini/DM molar ratio: 1:1 ▲, 4:1 ■, and 1:0 ◆.

Interactions between C_{12}-C_4-C_{12} Gemini and n-dodecyl-β-D-maltoside (DM) in solutions

Mineral-surfactant interactions are dynamic by nature with the adsorbed layers and the bulk phase solution tending towards equilibrium continuously. The behavior of surfactants and their mixtures in solution, such as surface activity and aggregate formation, affect the surfactant adsorption and the mineral-surfactant interactions. When mixed in solutions, surfactants usually show non-ideal mixing and exhibit the so-called synergism/antagonism, depending on the nature of the interactions among mixed surfactants. Interactions between C_{12}-C_4-C_{12} Gemini and n-dodecyl-β-D-maltoside (DM) in bulk solution were studied in this work using surface tensiometry and regular solution theory. Results obtained for the surface tension of aqueous solutions of individual C_{12}-C_4-C_{12}, DM and their mixtures are given in Figure 35. Critical micelle concentrations were determined from the surface tension curves and listed in Table 3. In H_2O, the cmc of the nonionic DM is lower than that of C_{12}-C_4-C_{12} Gemini, while the mixtures are generally not as surface active as DM alone. By regular solution approximation, the interaction parameter (β) for this binary mixed surfactant system was determined to be –1.5, indicating mild interaction between DM and Gemini in solution. Regular solution theory will be applied in the future to correlate changes in monomer concentration of the individual surfactants in the mixtures with their adsorption behavior.

Table 3: Critical micelle concentrations of C_{12}-C_4-C_{12} Gemini and n-dodecyl-β-D-maltoside (DM) mixtures of varying composition

Surfactant mixture mol ratio	cmc (kmol/m^3)
C_{12}-C_4-C_{12} alone	1.75×10^{-3}
4:1 C_{12}-C_4-C_{12} /DM	7.00×10^{-4}
1:1 C_{12}-C_4-C_{12} /DM	4.96×10^{-4}
1:4 C_{12}-C_4-C_{12} /DM	2.50×10^{-4}
1:10 C_{12}-C_4-C_{12} /DM	1.85×10^{-4}
DM alone	1.70×10^{-4}

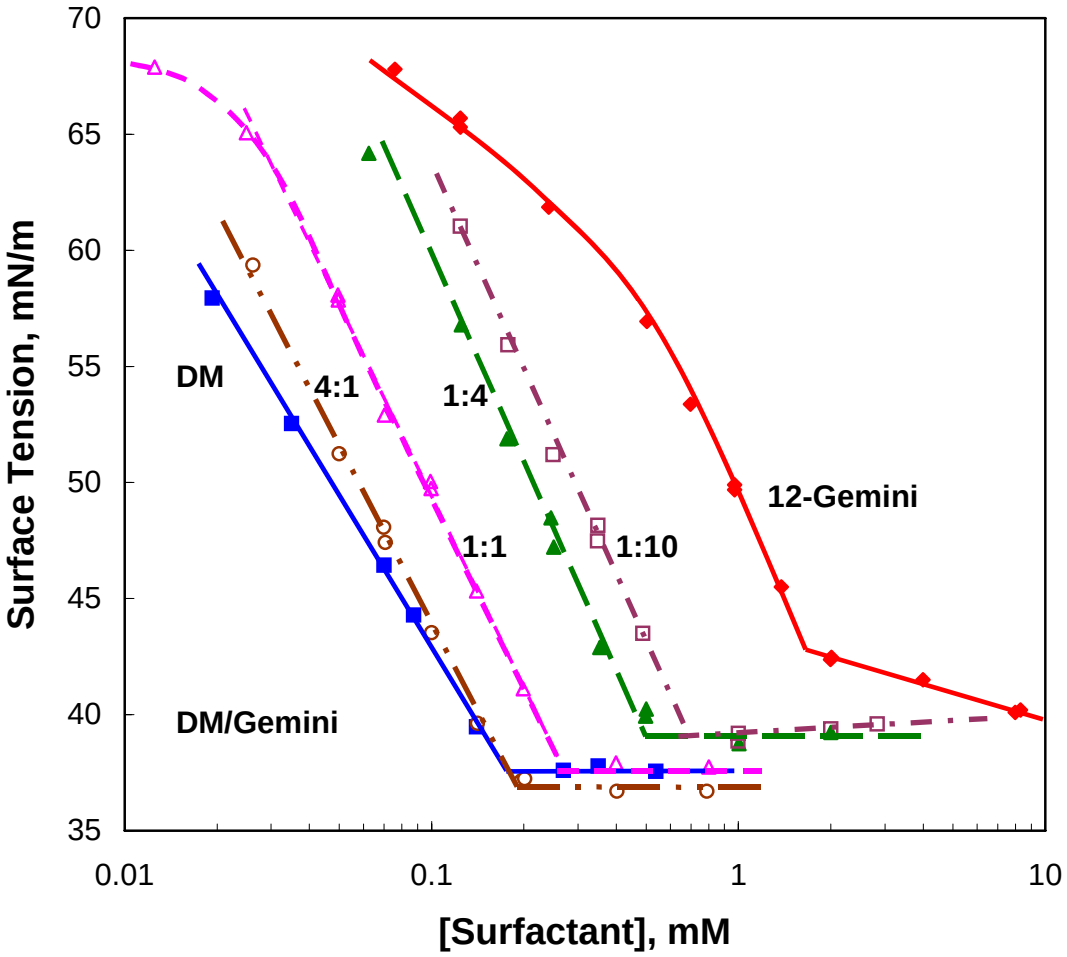

Figure 35: Equilibrium surface tension curves of individual C_{12}-C_4-C_{12} Gemini, n-dodecyl-β-D-maltoside (DM) and their mixtures of varying composition.

Adsorption of dodecyl sulfonate and sugar-based nonionic surfactant mixture on solids

To obtain optimal mineral-surfactant interactions and minimum chemical loss by adsorption in the enhanced oil recovery processes, the effects of solution pH, surfactant mixing ratio and addition of different salts on the mineral-surfactant interactions have been investigated for the mixed systems of anionic dodecyl sulfonate and sugar-based nonionic DM surfactants on alumina.

a) pH effects on DM adsorption

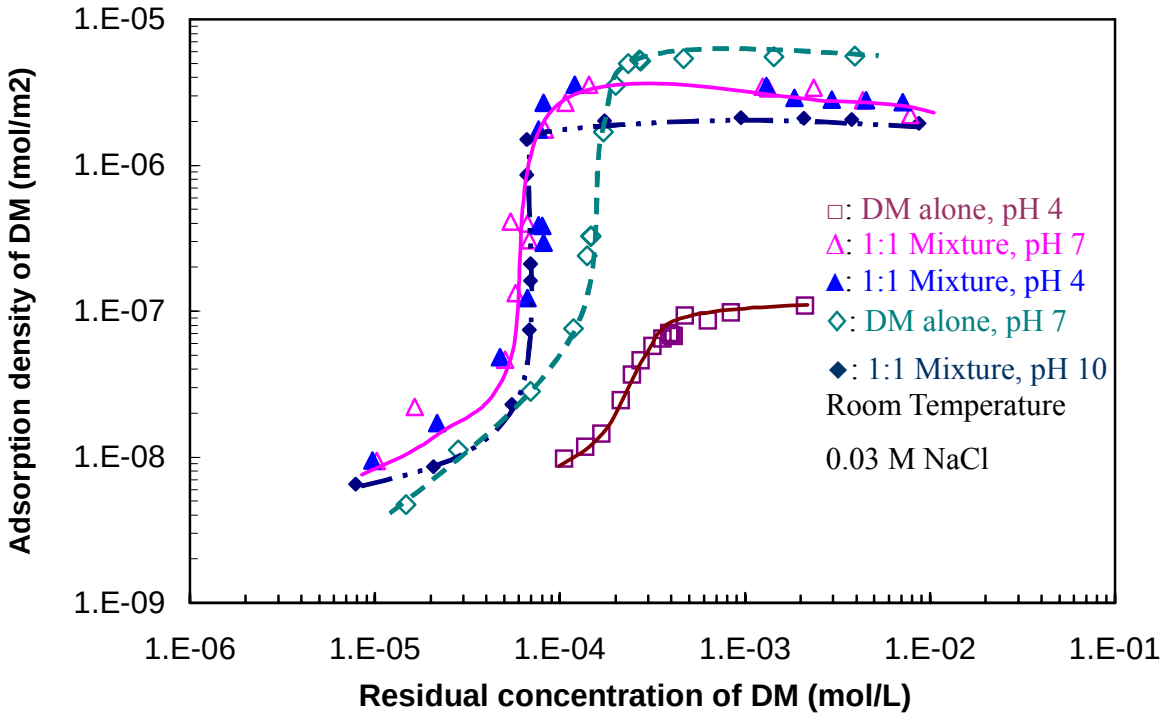

Figure 36: Effects of solution pH on the adsorption of n-dodecyl-β-D-maltoside (DM) on alumina from its mixture with dodecyl sulfonate ($C_{12}SO_3Na$) compared to DM alone.

The results obtained for the adsorption of n-dodecyl-β-D-maltoside (DM) on alumina from DM alone and from its mixtures with sodium dodecyl sulfonate ($C_{12}SO_3Na$) at different pH are shown in Figure 36. Adsorption of DM at pH 10 from mixtures with sulfonate at a mixing ratio of 1:1 shows much

stronger competition between DM and sulfonate in the plateau range. Saturation adsorption of DM from its mixtures with sulfonate is less than that in the case of DM alone system. Theoretically, sulfonate with negatively charged head group is not expected to adsorb on alumina at pH 10, due to the mutual electrostatic repulsion. However, the adsorption of DM was affected significantly by the sulfonate at pH 10. Since the adsorption of the nonionic surfactant DM does not affect the surface charge of alumina, the driving force for sulfonate adsorption in this case is proposed to be due to hydrocarbon chain-chain interactions between the dodecyl maltoside and the dodecyl sulfonate.

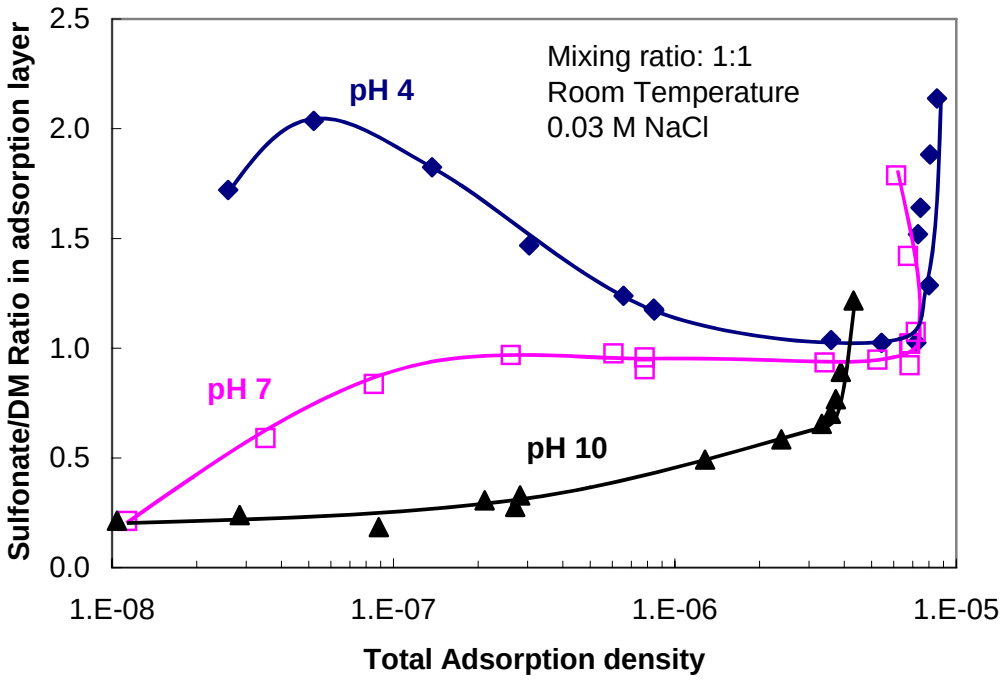

Figure 37: Sulfonate/DM molar ratios in adsorption layer at different pH.

It is apparent that different types of interactions play a part in determining the adsorption of sulfonate/DM mixtures on alumina at different pH. The ratio of sulfonate/DM in the adsorption layer was calculated and is shown in Figure 37 as a function of the total adsorption density. We propose that

hydrogen bonding is the driving force for sugar-based surfactant adsorption on alumina. The driving force for anionic dodecyl sulfonate adsorption usually is electrostatic interaction at low pH. At pH 4 and 7 (Figure 37), the variation of the sulfonate/DM ratio in the adsorption layer shows a three-stage trend: a steady ratio change at the beginning of mixture adsorption, a flat range with ratio in the adsorbed layer close to the initial ratio in the bulk solution, and a sharp increase of the ratio above saturation adsorption. The changes in the sulfonate/DM molar ratio suggest that different interactions exist between the two surfactants in the adsorbed layer in different adsorption stages. At pH 4, the sulfonate/DM ratio in the adsorption layer is higher than the initial mixing ratio in the bulk solution for the whole adsorption range, with the ratio decreasing first, followed by a sharp increase at saturation adsorption. At pH 7 and 10, the sulfonate/DM ratio in the adsorbed layer increases with increase in total surfactant adsorption, suggesting increased hydrophobic chain-chain interactions between dodecyl sulfonate and DM with increase in the total surfactant adsorption.

b) Mixing ratio effects on DM/sulfonate mixture adsorption.

The effect of mixing ratio on mixture adsorption is shown in Figure 38 as a function of pH. Interestingly pH shows opposite effect on DM adsorption, when it is adsorbed from a mixture of it with dodecyl sulfonate than from its solution without sulfonate (Figure 38). In these experiments, the initial concentration of DM was fixed at 4×10^{-3} mol/L. From Figure 38, adsorption of DM from its mixtures is much higher than that from DM alone below pH 7, which is due to the neutralization of positive charges on alumina surface by the anionic sulfonate. DM adsorption is almost the same at mixing ratio of 3:1 as that at 1:1 mixing ratio from pH 4 to pH 7, with much lower DM adsorption observed for 3:1 ratio at pH 3. The increased DM adsorption indicates synergism between dodecyl sulfonate and DM in the pH range of 3 to 7.

On the other hand, in the pH region of 7 to 11, DM adsorption decreases in the presence of sulfonate due to antagonism between the two surfactants. In the case of 1:1 mixture, DM adsorption decreases markedly from pH 7 to pH 11, and in the case of 3:1 mixture, DM adsorption decreases slightly in this pH range. Because of the competition for the adsorption sites on alumina, the more the sulfonate adsorption, the less is the DM adsorption.

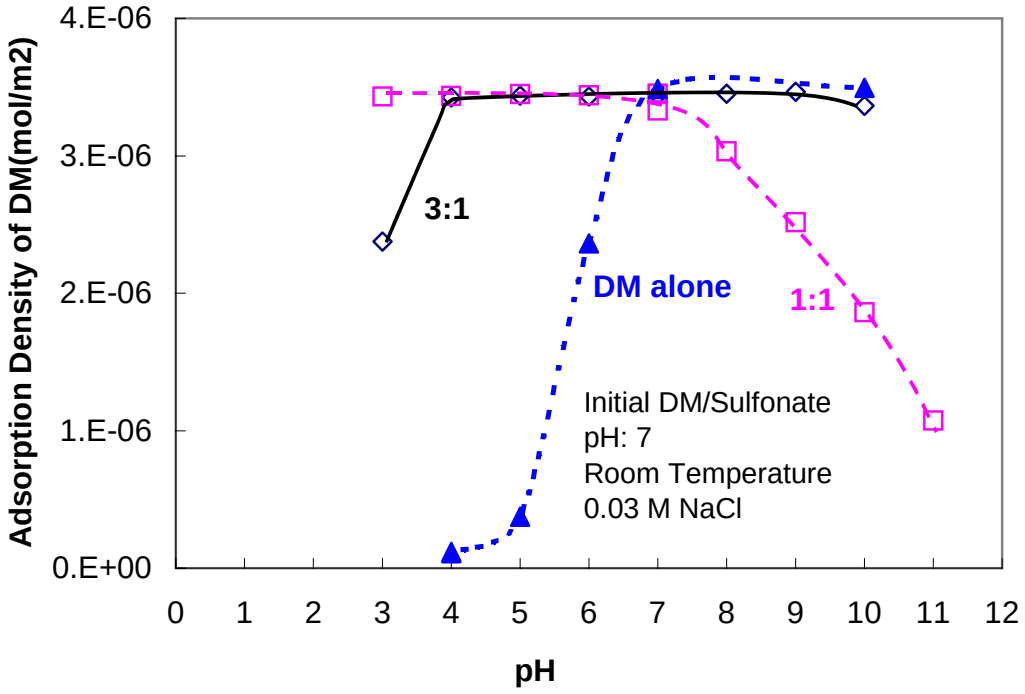

Figure 38: Adsorption of n-dodecyl-β-D-maltoside (DM) from its mixtures with $C_{12}SO_3$ on alumina as a function of pH.

The effect of solution pH on sulfonate adsorption is illustrated in Figure 39. Adsorption density of sulfonate decreases sharply with increase in pH, and almost no sulfonate adsorption observed above pH 9, due to the alumina being negatively charged. In the case of the 3:1 mixture, even less sulfonate adsorption is observed with the adsorption decreasing only slightly with increase in pH. Clearly, solution pH and surfactant mixing ratio play a major role in determining surfactant/mineral interactions on

reservoir rocks. Indeed the adsorption of DM is reduced under saturation conditions at high pH and this is beneficial for the enhanced oil recovery.

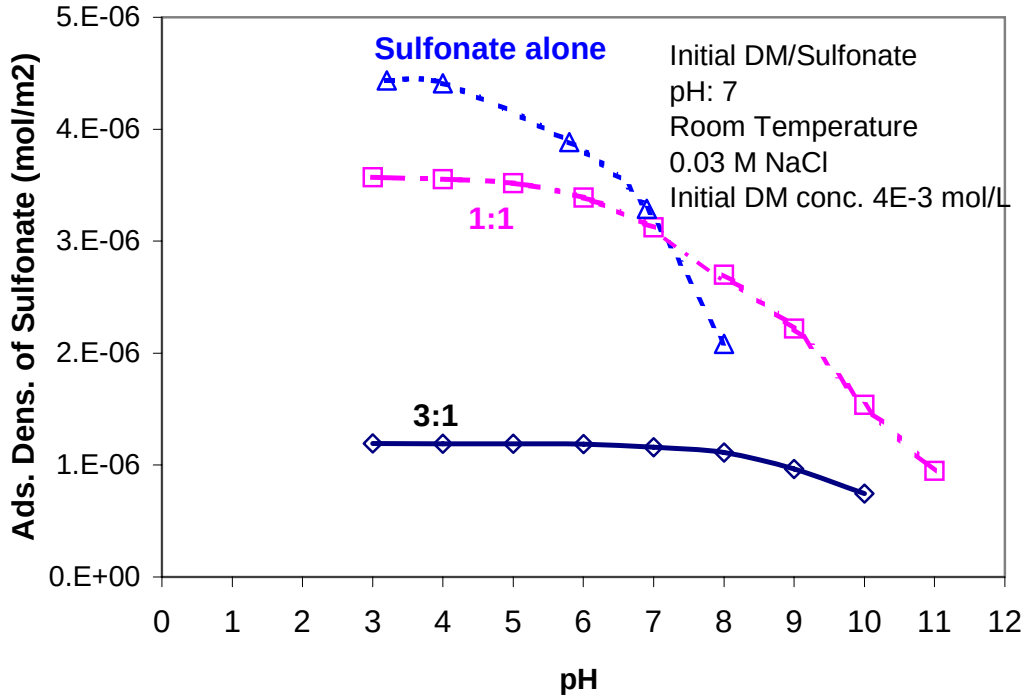

Figure 39: Adsorption of sodium dodecyl sulfonate from its mixtures with DM on alumina as a function of pH.

Adsorption of mixtures of sugar-based n-dodecyl-β-D-maltoside (DM) and anionic dodecyl sulfonate (C12SO3NA) at other different mixing ratios was investigated at pH 7 and 0.03M NaCl again, and the results obtained are shown in Figures 40 and 41. It was observed that saturation adsorption of DM decreases with increase of dodecyl sulfonate, and this suggests the competition for adsorption sites by the sulfonate. The mixtures reach adsorption plateau at higher concentrations with increased sulfonate molar fraction due to their higher CMC. The difference of plateau adsorption density of each surfactant corresponds to the DM/sulfonate ratio from 3:1 to 1:3. Such effects are relevant for enhanced oil recovery or flotation processes where it will be beneficial to arrive at saturated adsorption at lowest surfactant concentrations.

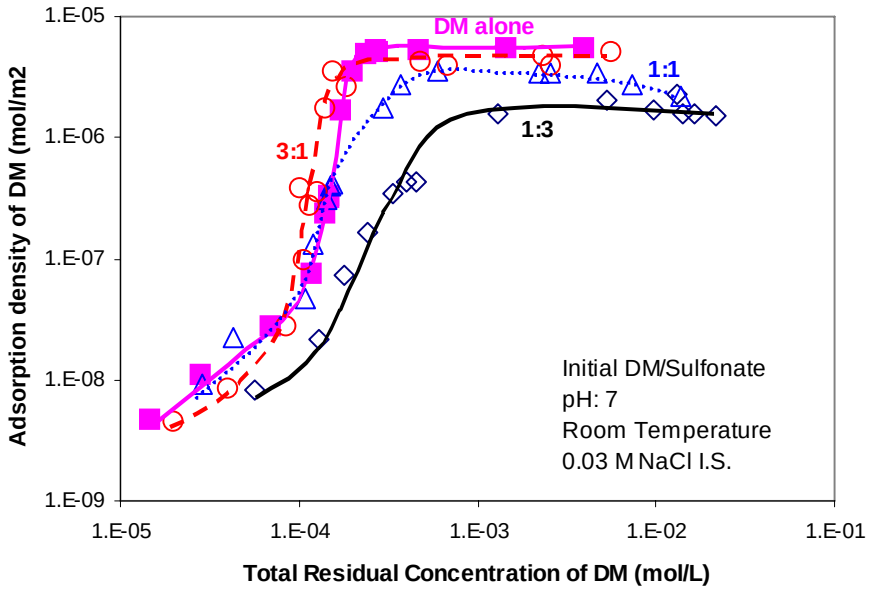

Figure 40: Effect of mixing ratio on the adsorption of n-dodecyl-β-D-maltoside (DM) from its mixtures with anionic C12SO3NA on alumina, at pH 7 and 0.03M I.S.

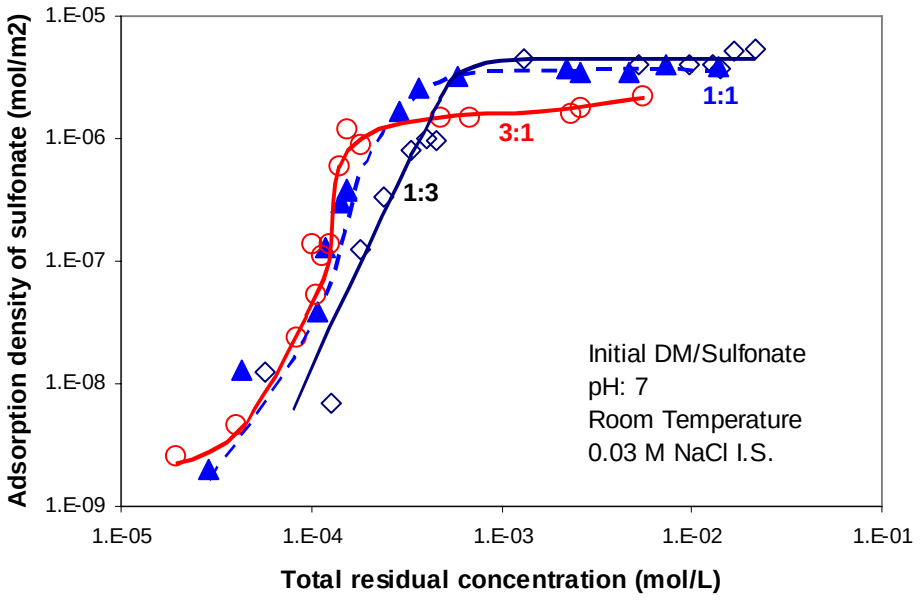

Figure 41: Effect of mixing ratio on the adsorption of C12SO3NA from its mixtures with n-dodecyl-β-D-maltoside (DM) on alumina, at pH 7 and 0.03M I.S.

On the other hand, the saturation adsorption of C12SO3NA on alumina also decreases along with the increase of dodecyl maltoside ratio in the mixture. However, it was noticed that the sum of saturation adsorption density of dodecyl maltoside and C12SO3NA remains fairly constant with variable mixing ratio, and the this can be attributed to the fact that the total adsorption area on the solid surface is fixed. In addition, this observation also suggests the relative value of interactions among surfactants and the minerals surface. The interaction between the two surfactant and alumina are almost at the same level at pH 7, so the ratio of the surfactant in adsorbed layer depends mainly on the ratio of that surfactant in the bulk. This conclusion is in good agreement with the results reported previously, in which pH 7 seems like a critical point for adsorption of dodecyl maltoside and dodecyl sulfonate mixture on alumina and below pH 7 dodecyl sulfonate is more attractive to the solid surface, whereas dodecyl maltoside adsorbs more above pH 7 than dodecyl sulfonate. Quantifying the interaction among surfactants and minerals is

of critical importance to the modeling of adsorption of surfactant mixtures on minerals.

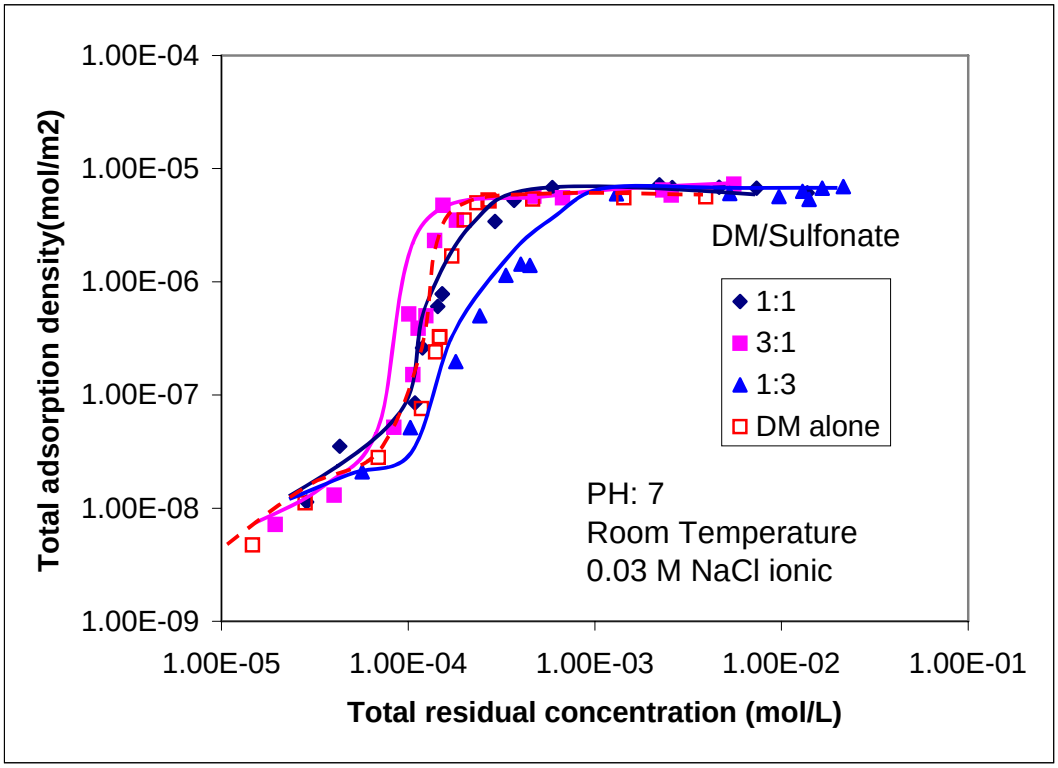

Figure 42: Effect of mixing ratio on the total adsorption of C12SO3NA and n-dodecyl-β-D-maltoside (DM) on alumina, at pH 7 and 0.03M I.S.

To identify the synergism or antagonism between DM and sulfonate, additional adsorption tests were done as a function of the mixing ratio under different pH. The initial concentration of DM was fixed at 5×10^{-3} mol/L. In figure 43, the three curves at low pH exhibit two stages with a linear increase followed by a decrease. As discussed above, DM does not adsorb much on alumina below pH 7 without the sulfonate. Sulfonate can therefore be considered to enhance DM adsorption in the first stage due to the chain-chain interaction and neutralization of the positively charged alumina surface. However in the second stage, DM adsorption decreases since the total available adsorption sites on the solid surface are limited, causing competitive interaction to dominate. The curve for pH 10 exhibits continual trend of decrease, showing no enhancement of DM adsorption.

More interestingly, the maximum adsorption point shifts to left with decrease in pH, with good linearity in each stage suggesting a quantitative relationship between DM adsorption and concentration of the sulfonate. This fact will prove helpful while developing a model for of synergism and antagonism.

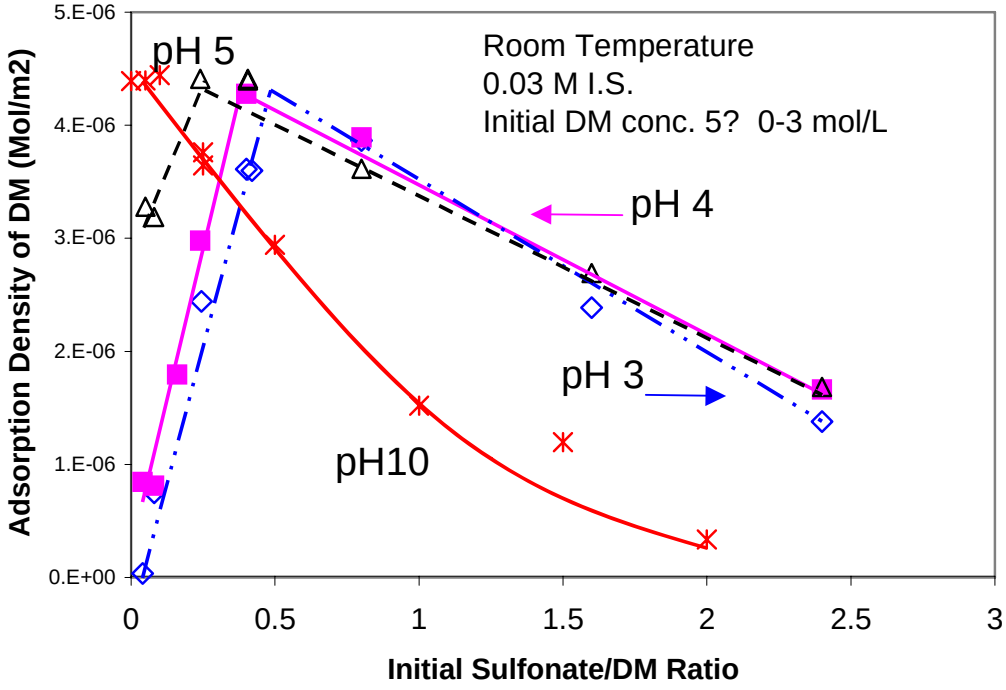

Figure 43: Adsorption of dodecyl maltoside as a function of mixture ratio at varied pH

Adsorption of dodecyl maltoside and dodecyl sulfonate mixture as a function of mixing ratio at different pH.

Adsorption of mixed dodecyl maltoside(DM) and dodecyl sulfonate on alumina was measured by depletion technique and the results are shown in figure 44~46. The initial surfactant concentration was maintained at 6 mM. Figure 40 shows that adsorption density of DM increases with DM ratio but decreases at pH 4. It is known that DM at pH 4 has only 2% adsorption of that at pH 7, but in the presence of dodecyl sulfonate, DM at acidic pH could adsorb as much as at higher pH due to the hydrophobic chain-chain interaction and neutralization of alumina surface by sulfonate adsorption. Below a ratio 0.60, DM has almost the same adsorption density at pH 4 and 7, but the adsorption decreases sharply due to the absence of deodecyl sulfonate above this ratio. On the other hand, the adsorption density at pH 10 lies below that at pH 7, regardless of the fact that the adsorption isotherms of DM are identical in the pH range 7~10. The existence of dodecyl sulfonate in the adsorption layer blocks the packing of DM molecules and thus reduces the DM adsorption density.

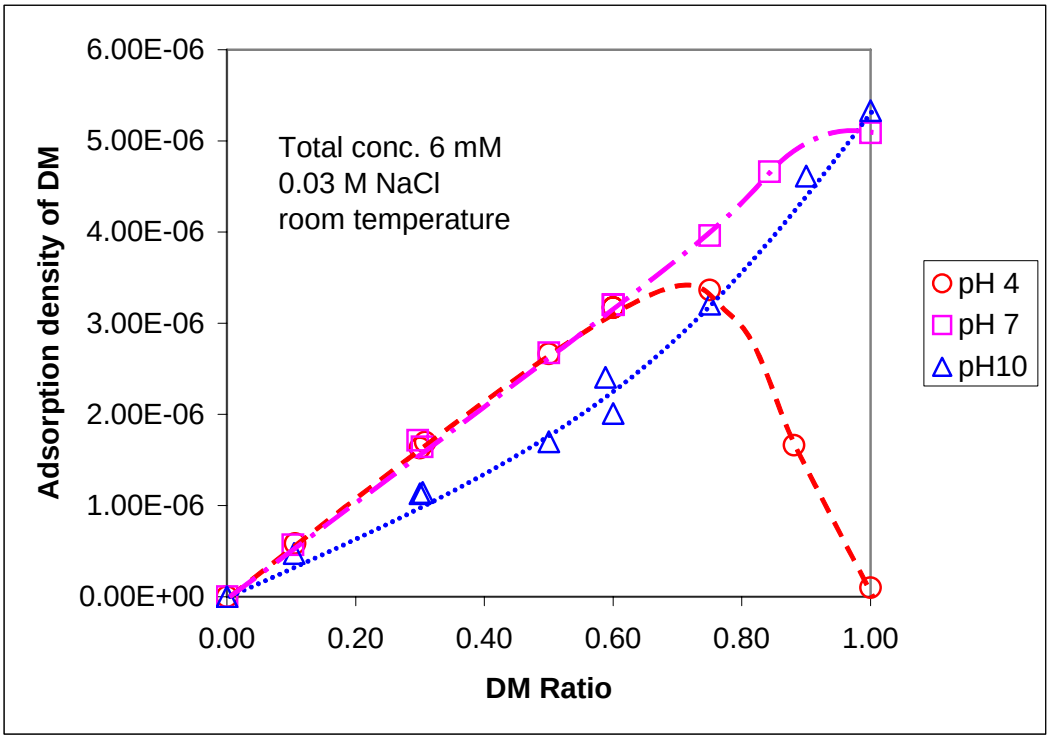

Figure 44: Adsorption of dodecyl maltoside on alumina as a function of mixing ratio at different pH.

Adsorption density of dodecyl sulfonate in the same experimental system was also determined and the results are shown in figure 41. The most significant observation is that dodecyl sulfonate does adsorb on the negatively charged alumina at pH 10 in the presence of dodecyl maltoside in comparison to zero adsorption density of dodecyl sulfonate in the absence of the latter. The hydrophobic chain-chain interaction between dodecyl maltoside and dodecyl sulfonate in the adsorption layer, in which DM is in the bottom layer and dodecyl sulfonate in the upper layer oriented toward the bulk, overcomes the electrostatic repulsion force between the negative head group and the negatively charged alumina. This proposal is supported by the hydrophobicity results given below. On the other hand, adsorption density decreases linearly at pH 4 and 7, because of the decrease in dodecyl sulfonate ratio. Higher adsorption at pH 4 than at pH 7 is because the lower the pH, the higher is the positive charge density on the solid

surface.

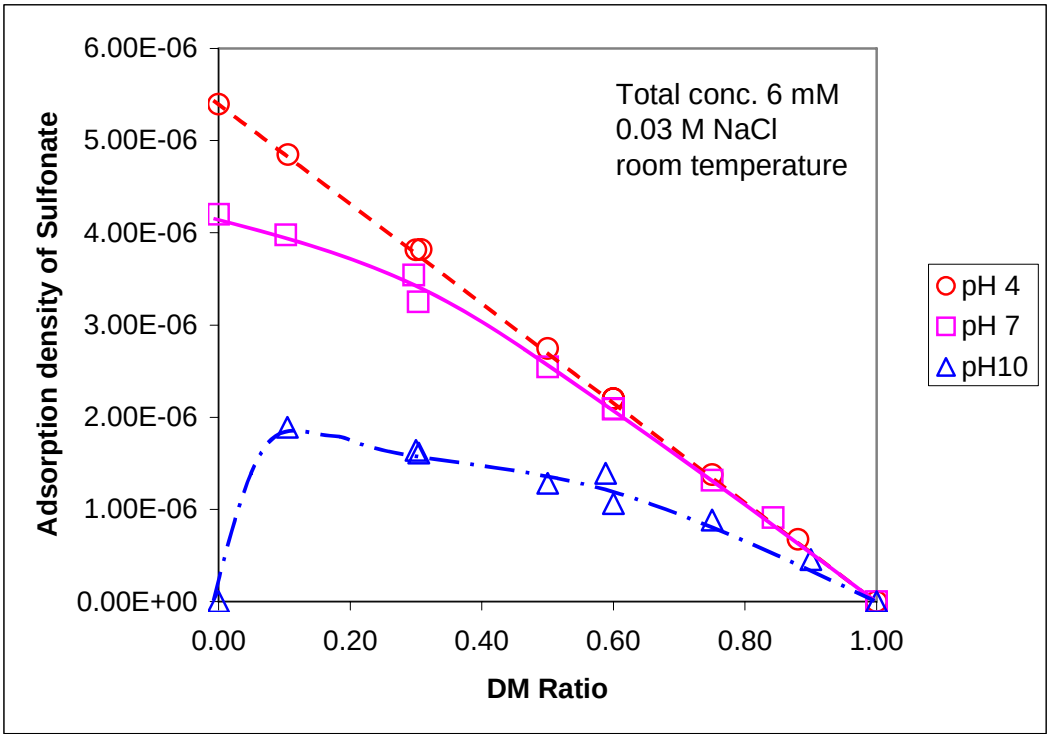

Figure 45: Adsorption of dodecyl sulfonate on alumina as a function of mixing ratio at different pH.

The total adsorption of both surfactants was summed in figure 42. The results reveal how the total adsorption is affected by pH and mixing ratio. At pH 4, adsorption decreases sharply above ratio 0.6, because DM alone has little ability to absorb. At pH 7, adsorption keeps increasing slowly with DM ratio because DM has a more compact aggregate structure than the dodecyl sulfonate aggregates at water/alumina interface. On the other hand, at pH 10, because dodecyl sulfonate blocks the packing of dodecyl maltoside, the total adsorption is reduced remarkably. Obviously, the total adsorption or each individual surfactant adsorption can be easily controlled by changing the pH and the mixing ratio. This is of importance for enhanced oil recovery. For example, at pH 10, passive (the component that does not adsorb by itself) dodecyl sulfonate dramatically decreases the adsorption of dodecyl maltoside, which is

more expensive than dodecyl sulfonate. Based on the adsorption mechanism and the quantitative analysis, the conditional parameters and mixing ratio could be optimized to reduce the cost and improve the performance of surfactant mixtures in oil recovery.

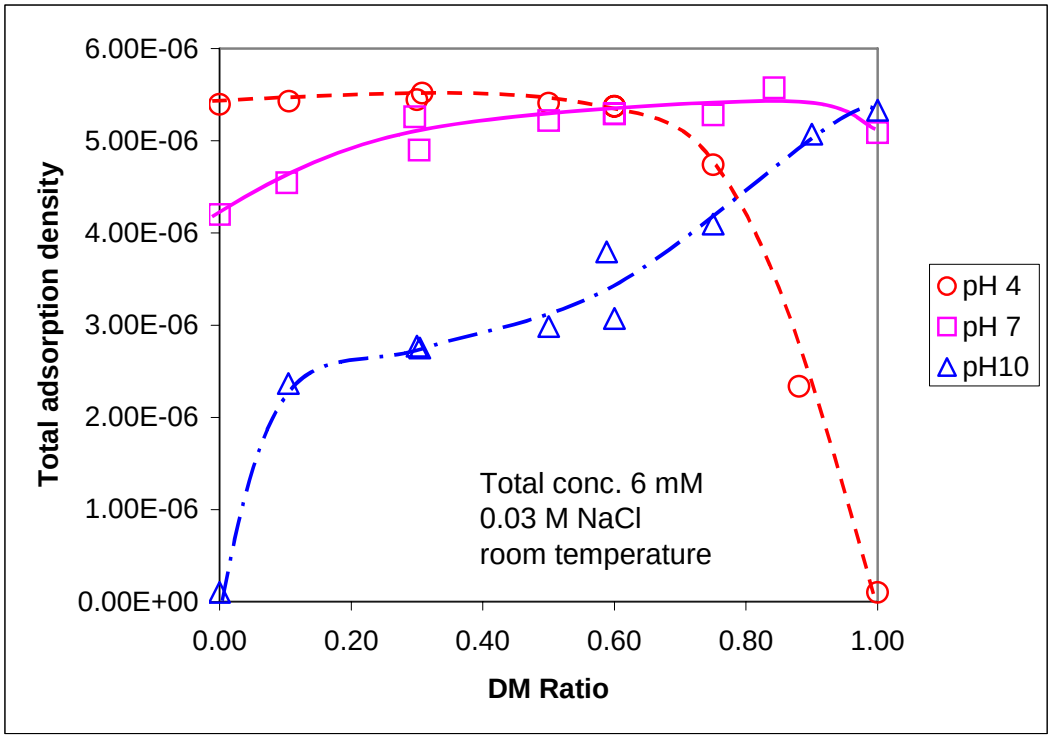

Figure 46: Total adsorption on alumina as a function of mixing ratio at different pH

Wettability of the solid due to the adsorption of surfactant mixtures

Adsorption of surfactants on solids could dramatically change the wettability of the surface. Wettability of alumina particles due to the adsorption of dodecyl sulfonate and DM mixtures has been investigated using two-phase extraction and deplection techniques. The information on changes in wettability of the surface due to surfactant adsorption can also shed light on the orientation of the surfactant species on the solid surface and help to elucidate the relationship between molecular packing and structures.

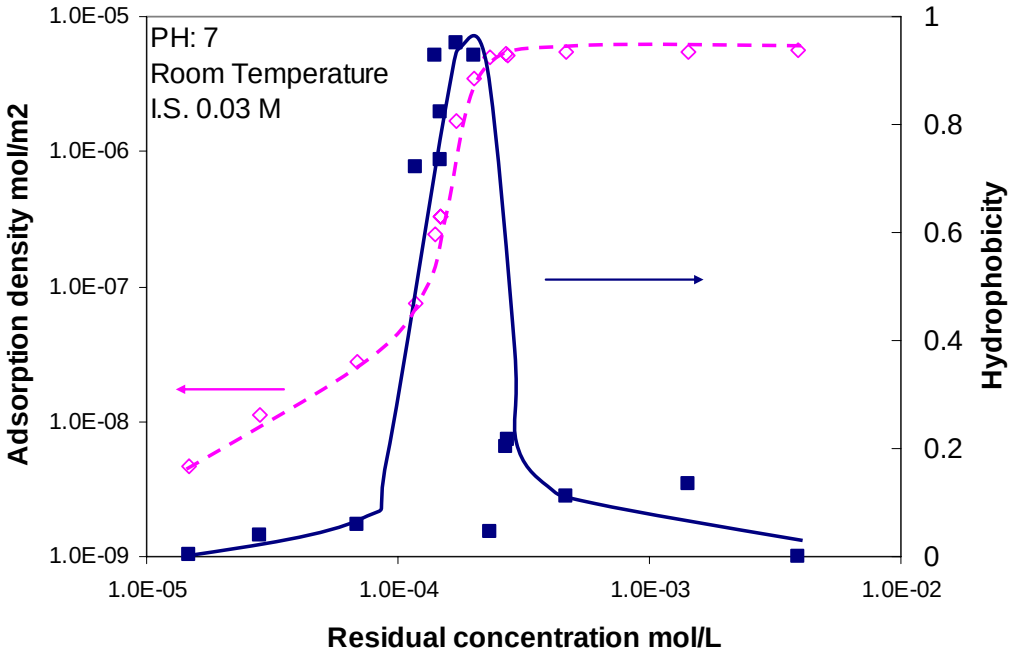

Figure 47: Hydrophobicity of alumina along with adsorption at pH 7

The effect of DM adsorption on the hydrophobicity of alumina is illustrated in figure 47 along with the adsorption isotherm at pH 7. Alumina becomes hydrophobic with the adsorption of DM and reaches

maximum hydrophobicity around the CMC. Interestingly, the alumina remains hydrophobic only within a very narrow range and becomes hydrophilic again at higher surfactant concentrations. The drop in hydrophobicity suggests that additional surfactant molecules with hydrophilic groups orient towards the aqueous phase at higher concentrations. Evidently, in the low concentration range, a monolayer is formed with the surfactants adsorbed with the hydrocarbon tails oriented towards bulk and at higher concentration a bilayer with orientation of the hydrophilic head towards the bulk.

Hydrophobicity obtained in the case of mixed $C_{12}SO_3Na$/DM is shown in figure 48. In this case, the alumina surface exhibits hydrophobicity even in the low residual surfactant concentration range (below CMC), because of the strong adsorption of dodecyl sulfonate due to the electrostatic attraction. When the residual concentration reaches CMC, the alumina surface becomes hydrophilic again due to the formation of a bilayer.

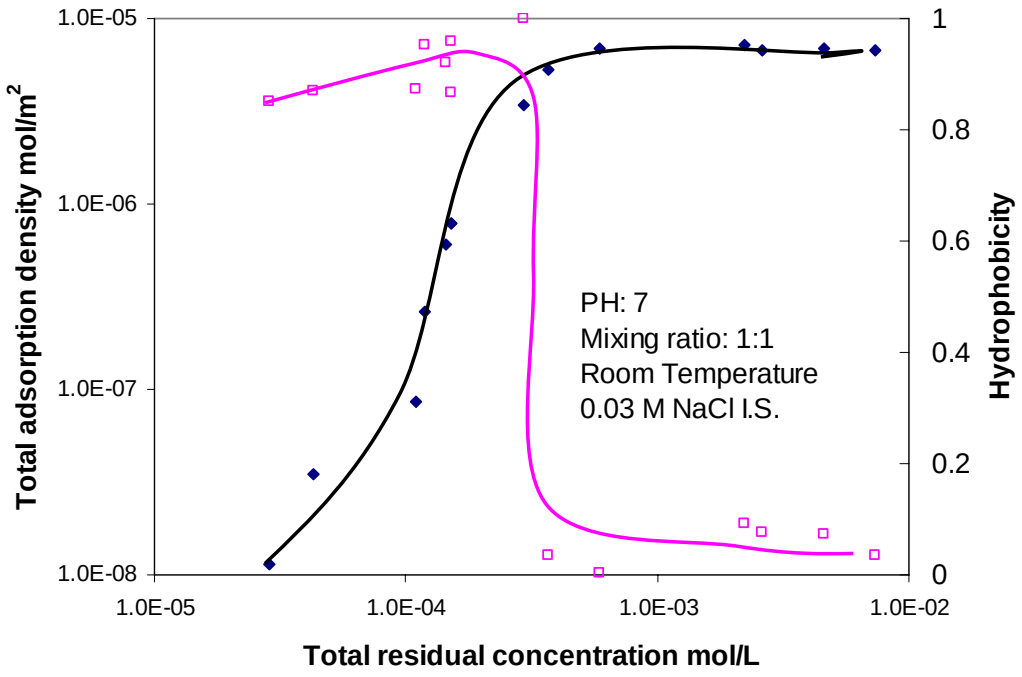

Figure 48: Effect of DM/sulfonate mixture adsorption on the hydrophobicity of alumina

The effect of relevant parameters such as pH was studied next. It can be seen that pH has a marked effect on the adsorption of mixed $C_{12}SO_3Na$/DM on alumina. DM adsorbs fifty times less on alumina at pH 4 than at pH7, even though the adsorption isotherms have the same typical three-stage S shape (figure 49). The sharp increase at CMC indicates the formation of hemimicelles at the solid/liquid interface; however, the surfactant layer does not change the hydrophobicity of the surface due to the low surface coverage. The surface remains hydrophilic in the tested concentration range as shown in figure 49.

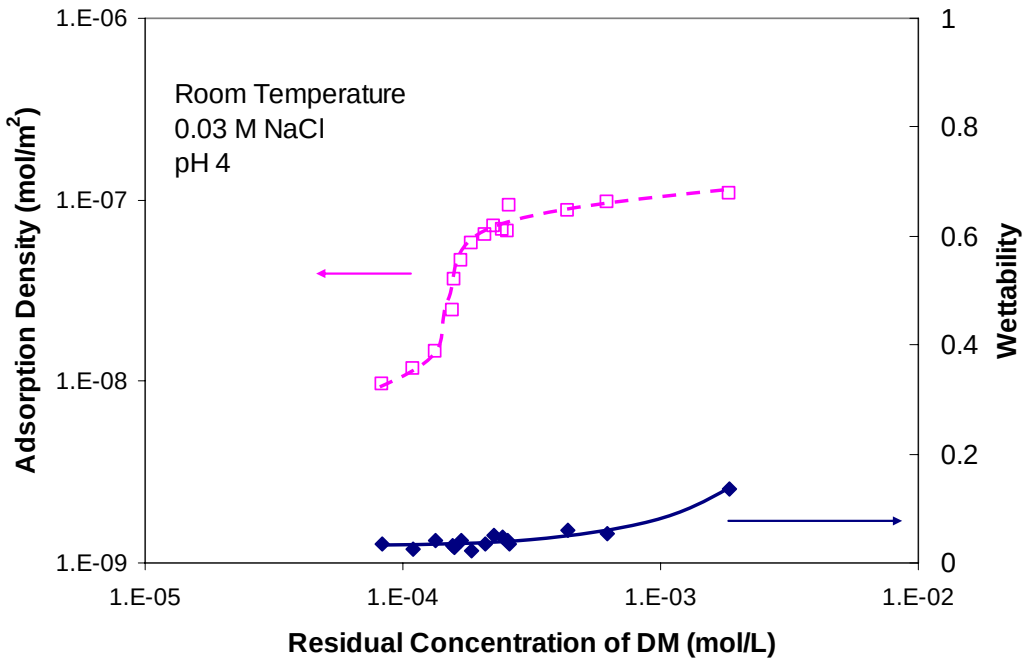

Figure 49: Effects of DM adsorption on hydrophobicity of alumina at pH 4

Wettability of alumina with mixture ratio of surfactants adsorbed on the surface

Hydrophobicity of alumina particles with surfactant adsorption on surface was determined by the two-phase extraction method. The result is plotted with adsorption density in figure 50 to 52. The forming of bilayer makes the solid surface hydrophilic at low DM ratio, but, with decrease in adsorption density, alumina particle becomes hydrophobic and reverts to hydrophilic again. At low DM ratio, the solid surface is occupied fully by surfactant molecules, which then forms a bilayer with head groups oriented toward the bulk solution and thus make solid surface hydrophilic.

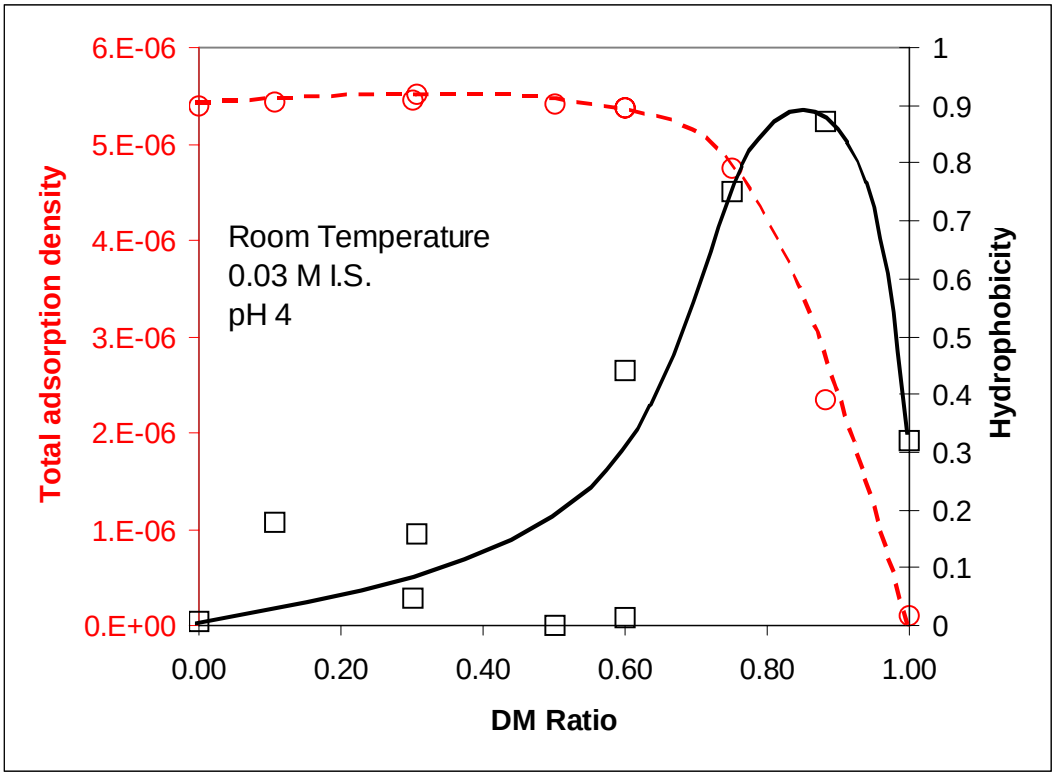

Figure 50: Hydrophobicity of alumina particles with surfactant adsorption at pH4

Hydrophobicity of alumina particles at different mixing ratios are shown in figures 51 and 52 for pH 7 and 10 respectively. At pH 7, total adsorption density is at a relatively higher level of around 5×10^{-6}mol/L, at which a bilayer should be forming according to the cross sectional areas of dodecyl maltoside and dodecyl sulfonate as determined from surface tension measurement. In the case of ratio of >0.50, the

mineral surface is hydrophilic, which is favorable for the release of trapped oil from the surface of the minerals. Result obtained at pH 10 is shown in figure 52. The total adsorption density is less than 50% of that at pH 7 below a mixing ratio of 0.6, but the mineral surface is surprisingly hydrophilic, which suggests that the head groups of surfactant molecules are oriented towards the bulk solution. This condition again is beneficial for chemical flooding.

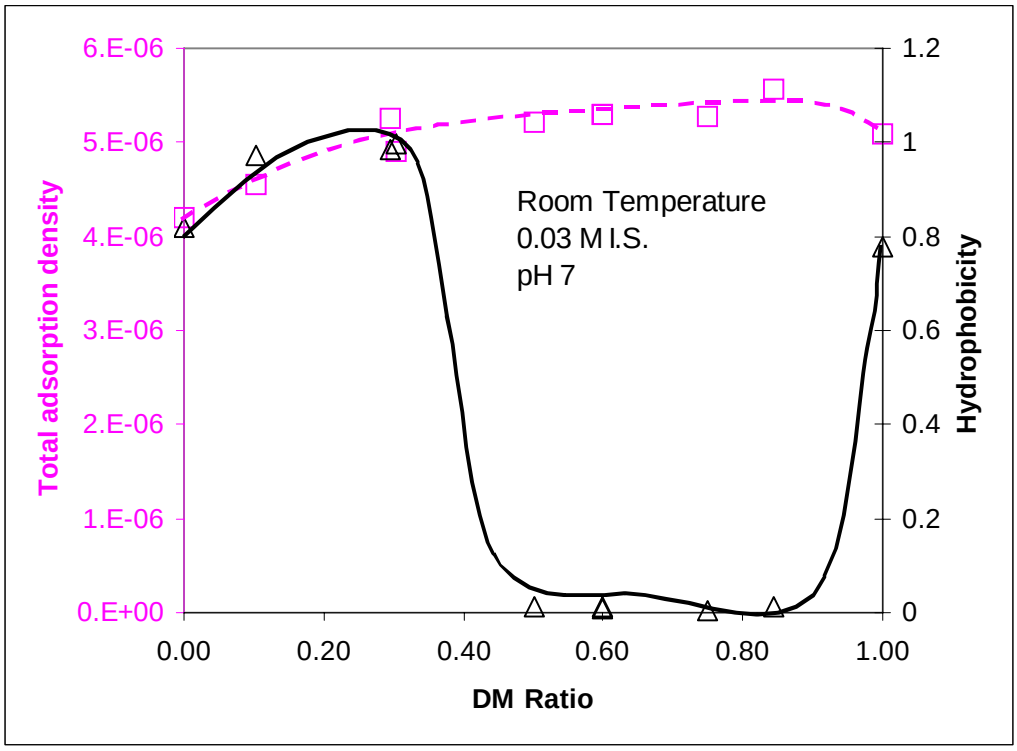

Figure 51: Hydrophobicity of alumina particles with surfactant adsorption at pH7

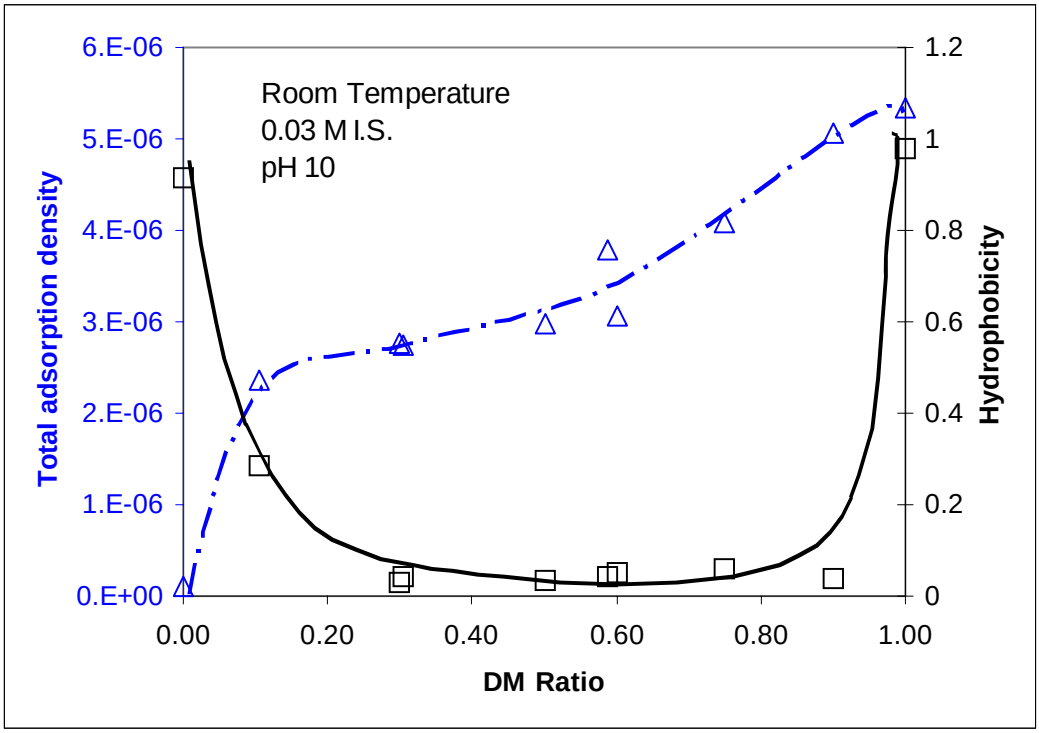

Figure 52: Hydrophobicity of alumina particles with surfactant adsorption at pH10

Adsorption of surfactant mixture in the presence of multivalent ions

In the oil reservoir, the dissolved mineral species can increase the ionic strength of the solution and the presence of the ions, especially multivalent ions, can cause significant precipitation and thus chemical loss. To investigate the chemical loss of surfactant and surfactant mixture under practical conditions, the adsorption/precipitation tests of mixed DM/SDS on alumina was done in the presence of monovalent and divalent ions at different concentrations. The adsorption experiments were done in the presence of calcium sodium salts. A significant difference was observed in terms of adsorption and precipitation. The isotherms are shown in the following figures.

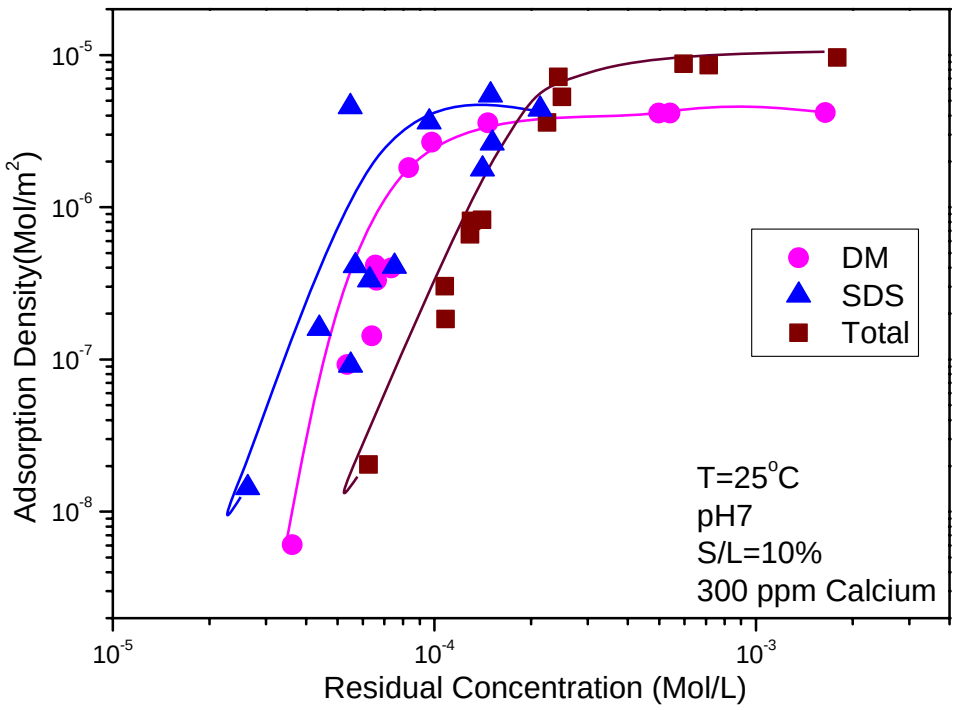

Figure 53: Adsorption of DM/SDS mixture on alumina in the presence of calcium ions

Figure 53 shows the adsorption isotherms for mixed DM/SDS on alumina at pH 7 in the presence of 300 ppm calcium. The mixing ratio was fixed at 1:1. It can be seen that the adsorption increases

sharply in the initial concentration range. The adsorption of SDS is much higher than that of DM possibly due to the precipitation between SDS with calcium. On the other hand, the presence of calcium ions reduces the electrostatic repulsion between the SDS head groups themselves resultingin a tight molecular packing in the adsorbed layer. In the plateau adsorption range, the total adsorption density reaches 1×10^{-5} Mol/m^2. In other words, the area per molecule is about 16 Å^2, which is much smaller than the area per molecule for DM or SDS obtained based on surface tension measurements. It can be concluded that the chemical loss is due to both adsorption and precipitation of this surfactant mixture in the presence of calcium ions.

To further understand the effect of ions on the adsorption/precipitation of this surfactant mixture on alumina, the adsorption isotherms for DM, SDS and the total are compared in the following figures, 54~56.

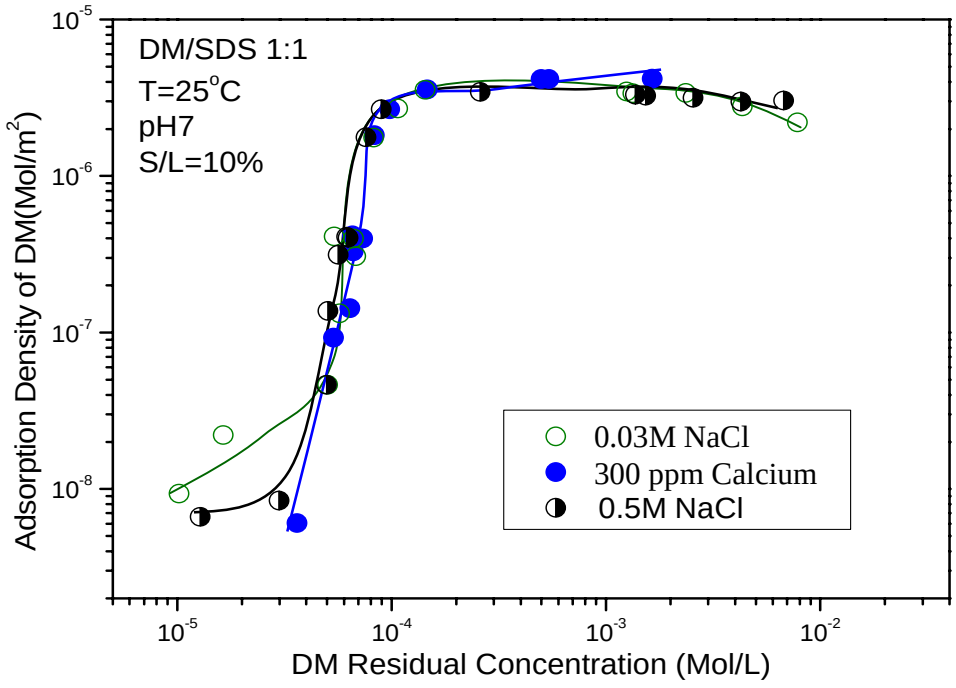

Figure 54: Adsorption of DM from its mixture with SDS on alumina at different ionic strength

The adsorption isotherms of DM on alumina from its mixtures with SDS in the presence of different ionic conditions are plotted in figure 54. It can be seen that the isotherms lie on almost the same curve, suggesting that the adsorption of DM is independent of the monovalent and divalent ions. Also, the adsorption density does not change much when the sodium chloride concentration is increased from 0.03M to 0.5 M. This phenomenon can be attributed to the nature of the sugar based surfactants. As reported previously, as a nonionic surfactant DM has shown very good salt tolerance. In the case of adsorption of mixed DM/SDS on alumina, the presence of monovalent or divalent ions affects the electrostatic force at the water/alumina interface and does not affect the adsorption of DM since the driving force for DM adsorption is hydrogen bonding. It can predicted that the adsorption of this nonionic sugar based surfactant will not change much with dissolved species in the oil reservoir during the micellar flooding process for enhanced oil recovery.

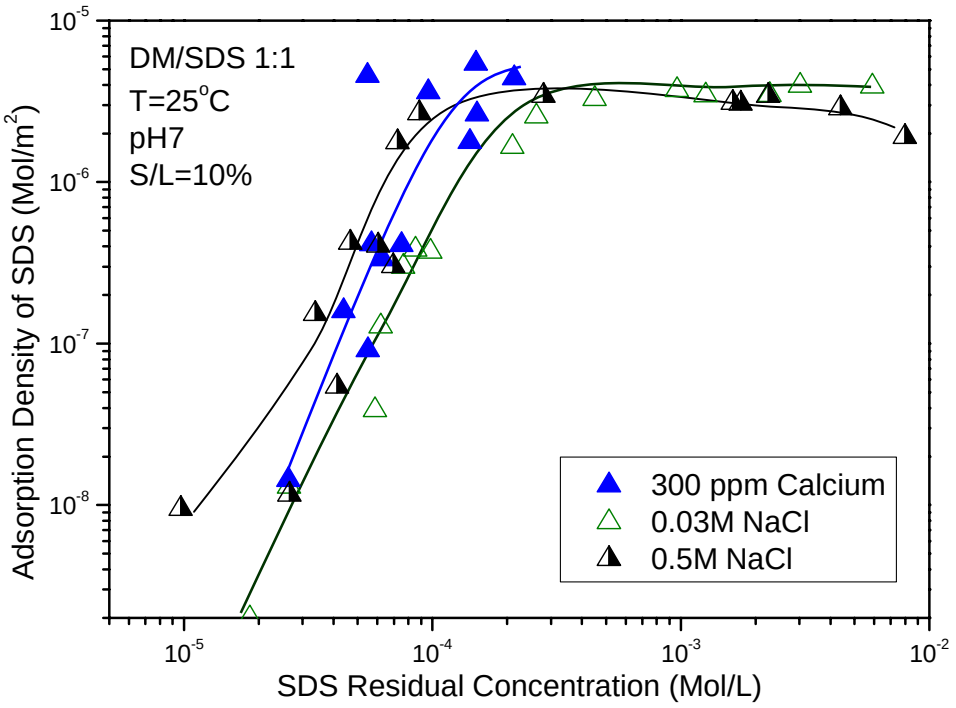

Figure 55: Adsorption of SDS from its mixture with DM on alumina at different ionic strength

Figure 55 shows the adsorption isotherms of SDS on alumina from its mixtures with DM. It can be seen that the adsorption of SDS changes significantly in the presence of sodium chloride and calcium. The divalent ion shows the highest effect on the adsorption of SDS, as the residual concentration of SDS was limited to 2×10^{-4} Mol/m^2 due to precipitation of calcium dodecyl sulfonate, which has a low solubility at room temperature. In addition, it can be seen that the increase in NaCl concentration does not affect the adsorption of SDS much since the sodium ion only reduces the electrostatic forces and does not cause precipitation. Furthermore, it can be concluded that the alumina surface is not affected by the calcium dodecyl sulfonate precipitation since the adsorption of DM is not changed in the presence of calcium. This can be attributed to two factors: a) the precipitates are formed in the aqueous phase and

removed in the separation process by centrifugation; and b) there is not enough precipitate to cover the alumina surface.

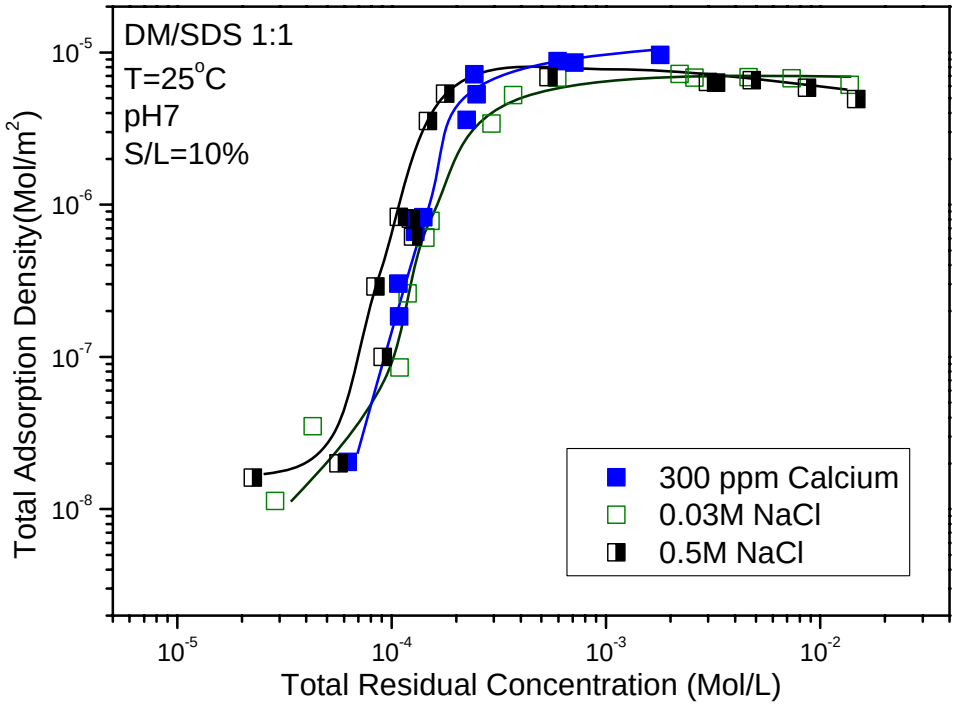

Figure 56: Adsorption of DM/SDS mixtures on alumina at different ionic strength

The total adsorption of isotherms of mixed DM/SDS on alumina in the presence of 0.03 M NaCl, 0.5M NaCl and 300 ppm calcium are shown in figure 56. At low residual concentration, the adsorption density increases with the salt concentration and the divalent calcium promotes the adsorption more effectively than the monovalent NaCl, while in the plateaus range, the adsorption isotherms show different trends, as the calcium promotes the adsorption significantly due to possible precipitation and the NaCl shows little impact on the total adsorption.

Micellization of surfactant mixtures in solution studied by analytical ultracentrifuge (AUC)

A unique tool to obtain information on the shape and the size of micellar aggregates is analytical ultracentrifuge. This technique was used in the current project to obtain useful data on surfactant aggregation of single and mixed surfactant systems. Given that the sedimentation velocity of the surfactant micelles is determined mainly by the density of the surfactant micelles, data for partial specific volume was required for the analysis of the analytical ultracentrifugation data. The partial specific volume of the surfactant micelle, defined as the volume of unit weight of micelle, is a quantity essential for acquiring information such as the sedimentation coefficient and the micelle mass. The partial specific volume $\bar{v}$ is obtained empirically from the density gradient using the following equation:

$$\bar{v} = \frac{1}{\rho_0}\left(1 - \frac{d\rho}{dC}\right) \qquad (1)$$

where C is the surfactant volumetric concentration in grams per milliliter and ρ and ρ_0 are the densities of the solution and the solvent, respectively.

The density of DM and SDS solutions was measured using Anton Paar 5000A density meter and the results are shown in figures 57 and 58.

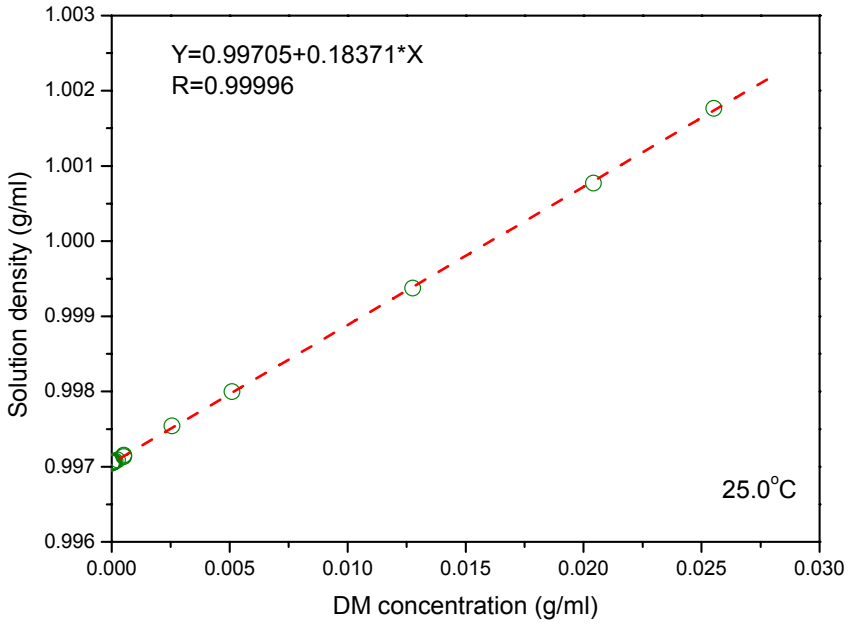

Figure 57 Density-concentration results for DM solutions

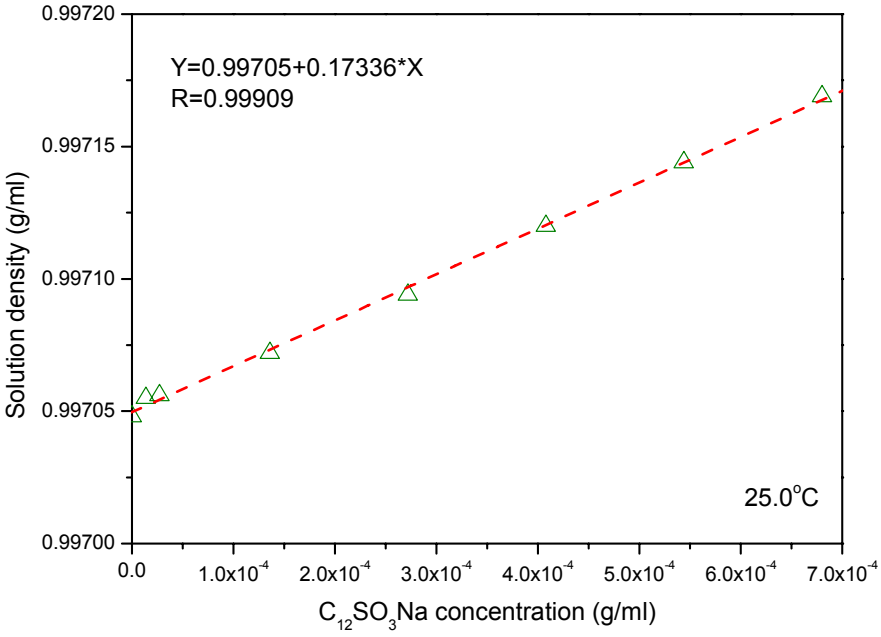

Figure58 Density-concentration results for SDS solution

By fitting the density-concentration data, the specific volumes for DM and SDS were calculated using equation (1) to be 0.833 ml/g and 0.826 ml/g respectively. Given that the values for these two surfactants are very close, the mixed DM/SDS micelles are estimated to have a specific volume around 0.83 ml/g/. This measurement was actually used for the data analysis of sedimentation velocity.

Size distributions of mixed DM/SDS systems

Information on the size and shape of the species can be obtained from the sedimentation process of micellar samples. The size distributions of mixed DM/SDS micelles at 10 mM are shown as a function of sedimentation coefficient in figure 59. In the case of DM alone, a single peak was observed around 3.6 S. Since SDS alone does not form micelles at this concentration, no sedimentation process was observed. The micellar distribution shifted to low sedimentation coefficient with increase in SDS molar ratio, suggesting a decrease in micellar size. The micellar evolution was attributed to the nature of the surfactant molecules. Since SDS molecule is charged (has a large parking area as revealed by the surface tension measurements), the electrostatic repulsion hinders the association of molecules, while the micellization of DM is determined only by the geometry of the molecule.

Interestingly, a second micellar peak was observed at DM/SDS ratio 9:1 and 3:1. Even though the coexistence of two types of micelles has been predicted, this is the first report of direct evidence for the coexistence of micellar species in mixed nonionic/anionic surfactant mixtures. This phenomenon can be understood using the schematic model proposed by Huang. At high DM ratios, the concentration of SDS (at 9:1 ratio, 1mM; at 3:1 ratio, 2.5 mM) is far below its CMC (12.5mM) and therefore SDS itself does not form a micelle and possibly the formation of mixed aggregates is due to the dissolution of SDS molecules into the DM micelles. The monomer ratio of SDS is larger

than that of the bulk, suggesting a low ratio of SDS in the micellar phase. Since the second peaks are very close to the peak of DM, it is proposed that some DM-rich micelles exist in equilibrium with the mixed micelles (first peak). In addition, it is seen that the area of the second peak is very small, indicating a low molar ratio of the second micellar species.

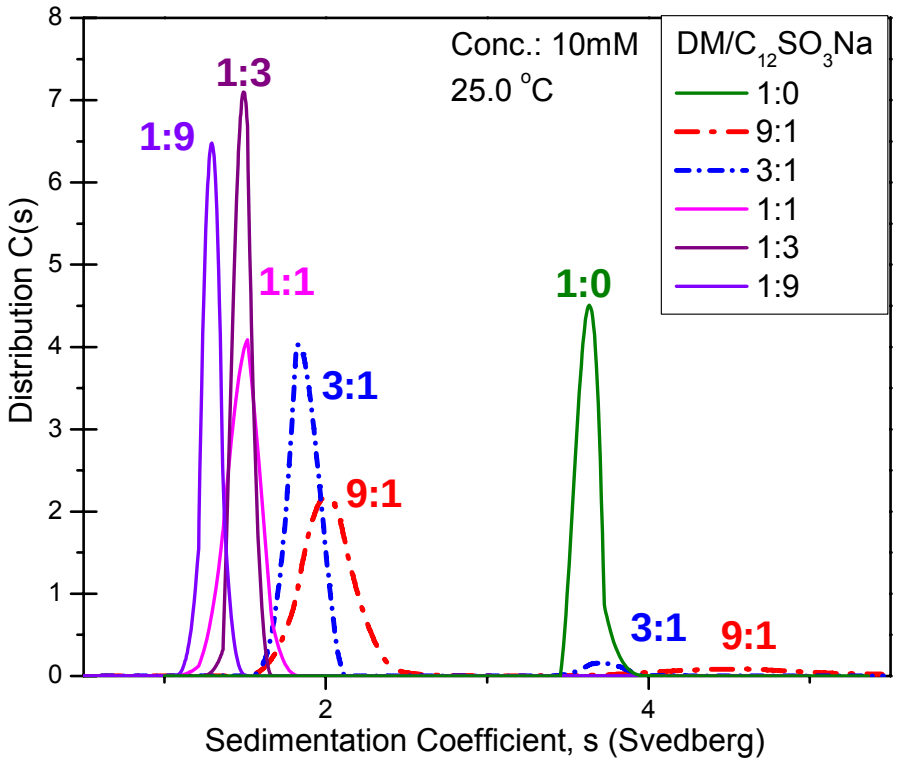

Figure 59 Size distributions over sedimentation coefficient for mixed DM/SDS system at 10 mM.

The size distributions of mixed DM/SDS at 50 mM are shown in figure 60. The results are similar to those at 10 mM, however the peaks appear at relatively low sedimentation coefficient. Since 50 mM is above the solubility of SDS at room temperature, the peak for pure SDS micelle was not obtained. The peaks were also found to shift from right to left with an increase in SDS

molar ratio. The coexistence of two types of micelles was also observed at 50mM at DM/SDS ratios of 9:1, 3:1 and 1:1. Again the phenomenon is proposed to be due to the existence of the DM-rich micelles.

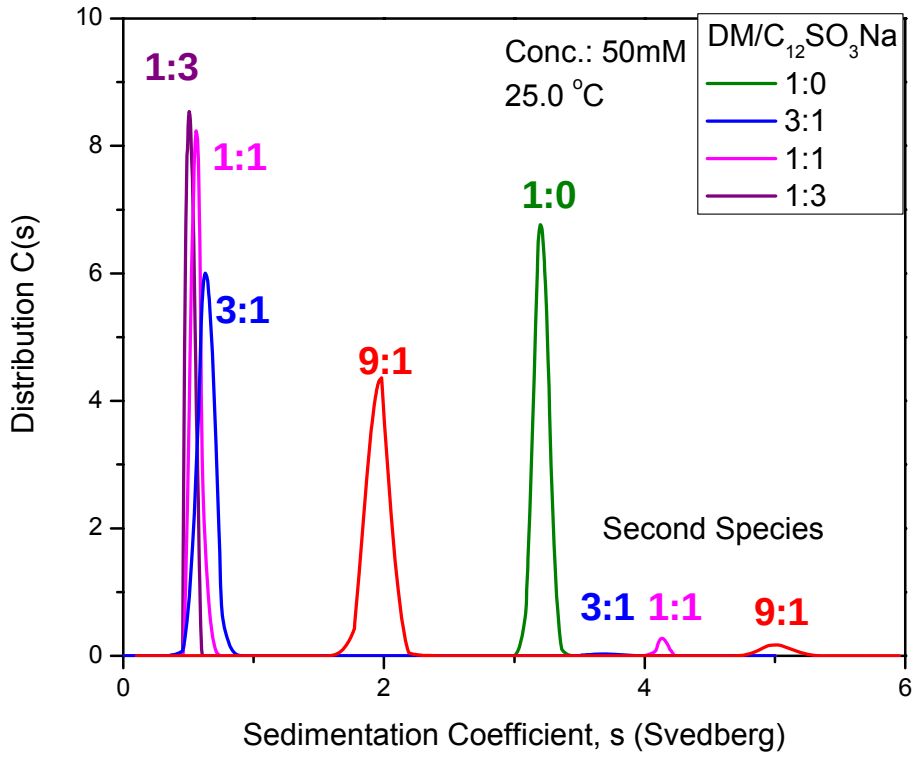

Figure 60 Size distributions over sedimentation coefficient for mixed DM/SDS system at 50 mM.

Aside from the size distribution, the shape of the mixed micelles was identified as spherical in the concentration range and mixing ratios tested. The shape is determined by the packing parameter. Since both DM and SDS have relatively large headgroups, the mixed micelle have a high packing curvature. The spherical shape of DM micelle was confirmed by Cryo-TEM technique (the image is shown in the next section). In the case of the mixtures, the mixed micelles still have a high curvature and possibly have a spherical shape even though synergistic interaction exists between

DM and SDS. It is to be noted that the size and shape of the aggregates are important in determining the colloidal properties such as viscosity in EOR systems.

Aggregation numbers of mixed DM/SDS systems

Aggregation number is a critical parameter for surfactant micelles. In the past, a number of techniques have been employed to determine the aggregation number of the surfactant mixture system, including small angle neutron scattering (SANS), light scattering, and static and life-time fluorescence spectroscopies. However, the accuracy does not appear to be very precise especially for spherical micellar systems. Based on the size distributions obtained in figures 59 and 60, the micellar mass was obtained and then divided by the molecular weight to obtain the aggregation numbers. In the cases of mixtures, the monomer concentrations were used to estimate the molar ratio in the micellar phase and thus the average molecular weight.

The aggregation number of the mixed DM/SDS systems at 10 mM is shown in figure 61 along with the DM ratios. The DM ratio in the micellar phase was found to increase along with its bulk counterpart. The aggregation number appears to be governed by the presence of SDS molecules. DM alone has an aggregation number above 100, but at a DM ratio of 0.1 the aggregation number is only 40, which is close to the aggregation number of pure SDS micelles reported in the literature. The aggregation numbers of the mixed micelles were observed to increase with DM ratio, but were limited to 60, suggesting that the presence of electrostatic repulsion reduces the association of surfactant molecules in micelles. This behavior can be used to explain the formation of the second micellar species. DM tends to form relatively large micelles, however the incorporation of surfactant micelles may be reduced by electrostatic repulsion caused by the SDS. Therefore, it is proposed that DM-rich micelles with a large aggregation number exist in the system.

The experimental results are in accordance with the proposed mechanism, as the second micellar specie has a much larger aggregation number (figure 61).

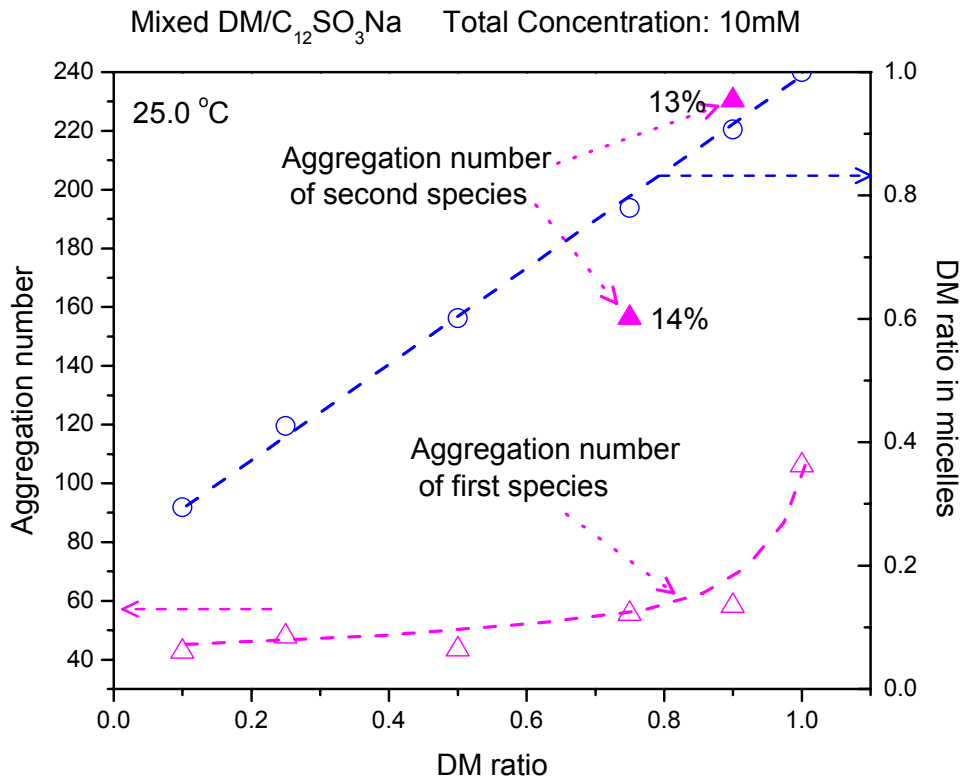

Fig 61 Aggregation numbers and DM ratio in micellar phase for mixed DM/SDS system at 10 mM.

The aggregation numbers at 50 mM are shown in figure 62 along with the DM ratios. A sharp increase in the aggregation number was found above the DM ratio of 0.75, below which the presence of SDS molecules produces enough electrostatic repulsion to limit the incorporation of additional molecules to the micelles. Even though, the second micellar species have a small ratio (lower than 5%), their aggregation numbers were found to be much larger than even those of DM alone.

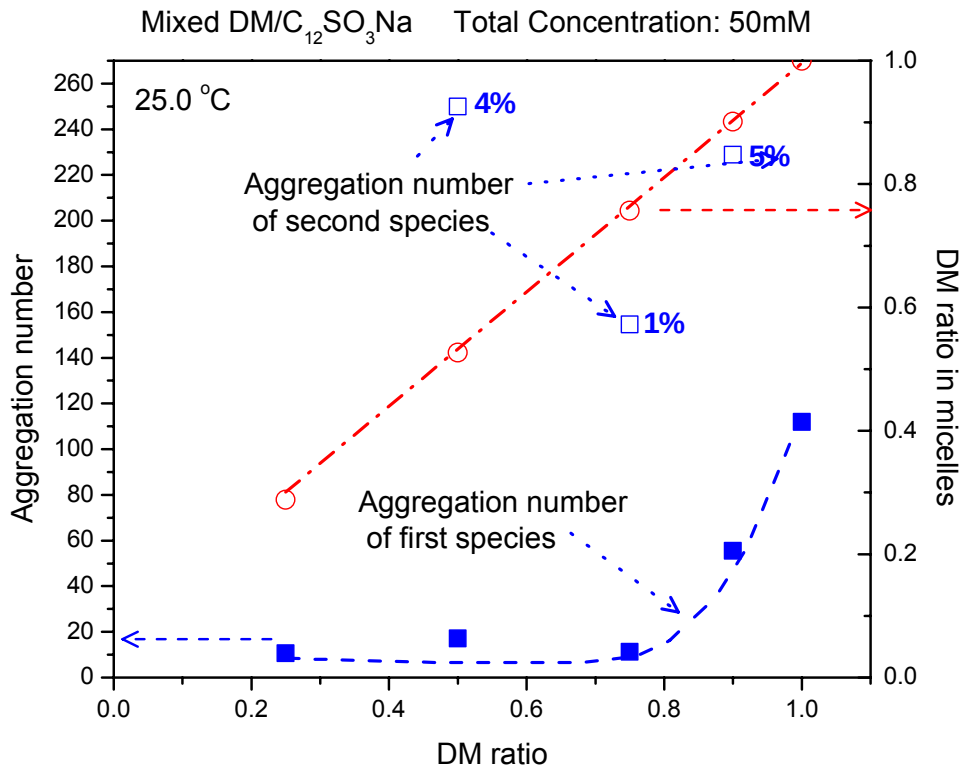

Fig 62 Aggregation numbers and DM ratio in micellar phase for mixed DM/SDS system at 50 mM.

Micellar evolution in mixed DM/SDS systems

From the results of aggregation numbers obtained at 10 mM and 50 mM, it can be seen that surfactant concentration plays a significant role in determining the micellar size and shape. To further understand the effect of surfactant concentration on the micellization of mixed DM/SDS system, surfactant solutions at 1 mM and 30 mM were also investigated using analytical ultracentrifugation. The results are shown along with the data at 10 mM and 50 mM in figures 63 and 64.

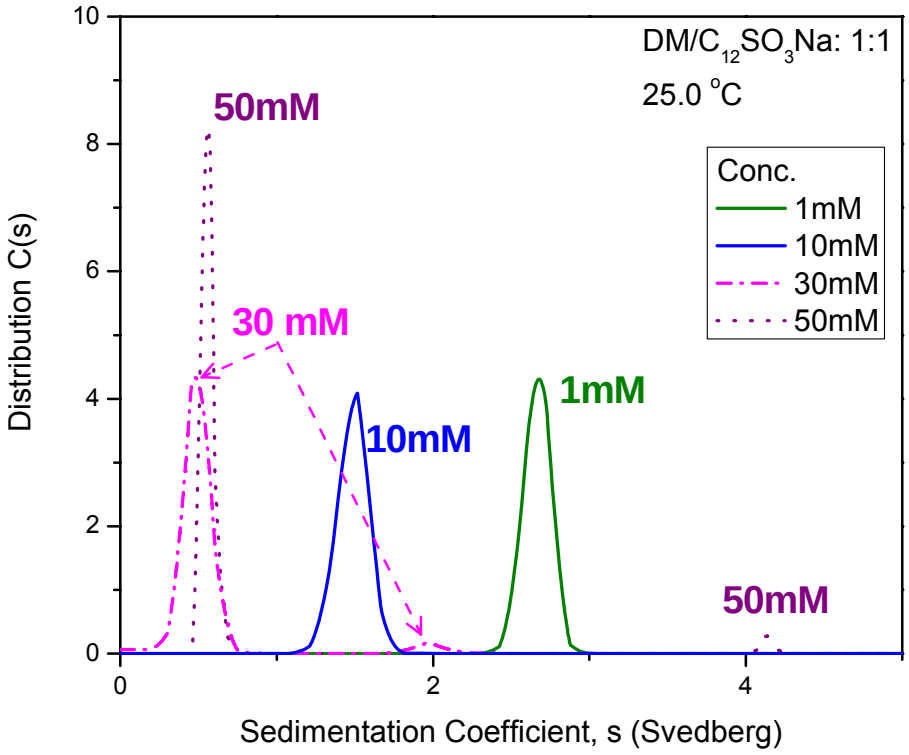

Figure 63 Effects of surfactant concentration on the size distributions over sedimentation coefficient for mixed DM/SDS system.

It is clear that the mixed DM/micelles at 1:1 ratio become smaller with an increase in SDS ratio. Furthermore, only one type of micelle was observed at 1 mM and 10 mM, while the coexistence of two types was identified at 30mM and 50 mM. The micellar evolution with concentration can be attributed to the interactions between DM and SDS molecules. SDS molecules do not form micelles at concentrations lower than its CMC while they can be dissolved in DM micelle and form mixed aggregates. Also the SDS has a higher molar ratio as a monomer at low concentrations, which results in a low ratio in the micellar phase. With increase in concentration, more SDS molecules are incorporated into micellar phase and cause an enhancement in the

electrostatic repulsion, which results in the shrinking of the mixed micelles, while at higher concentrations, DM-rich micelles are proposed to exist as the second micellar species.

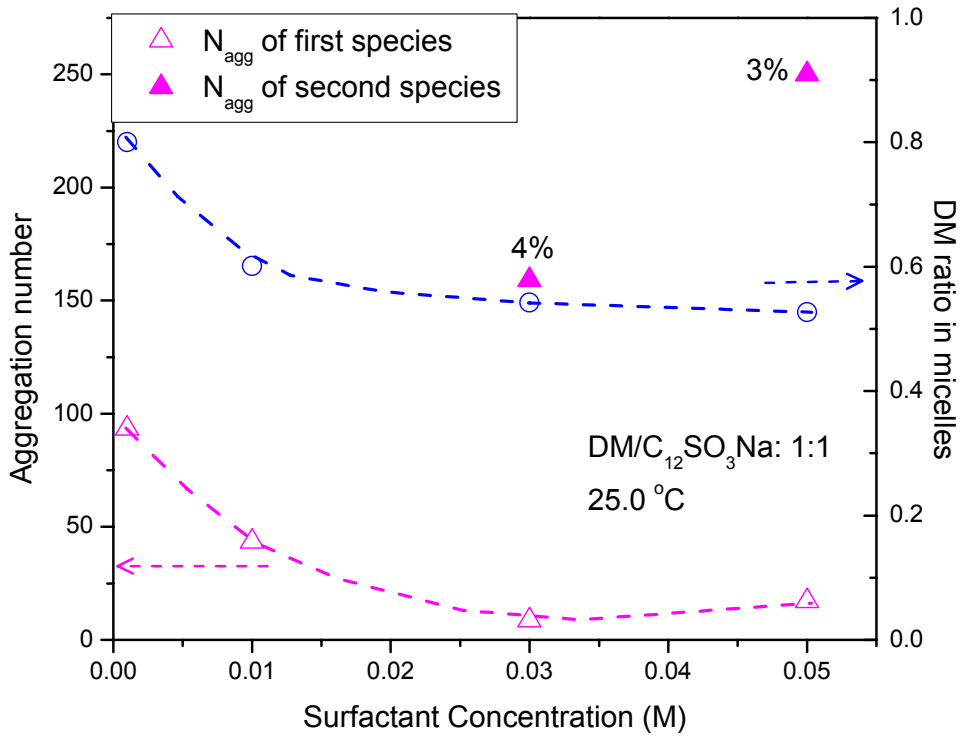

Figure 64 Effects of concentration on aggregation numbers and DM ratio in micellar phase for mixed DM/SDS system.

The aggregation numbers of mixed DM/SDS at 1:1 mixing ratio are plotted in figure 11 along with the DM ratio in the micellar phase. Interestingly, it was found that the aggregation number decreases with an increase in surfactant concentration as well as the DM ratio in the micellar phase. Judging from the data it is apparent that the aggregation number of mixed DM/SDS micelles is correlated to the DM ratio in the micellar phase. At low concentrations, DM molecule is the dominating component in the mixed micelles and the electrostatic repulsion between SDS molecules is screened by the presence of uncharged DM molecules. With an increase in the

concentration, more SDS molecules are incorporated into the mixed micelle. The electrostatic repulsion begins to take place and this causes the disassembly of surfactant micelles. With further increase in surfactant concentration, DM-rich micelles are proposed to appear as the second species.

Micellar size and shape revolution with temperature

Analytical ultracentrifugation technique was employed to elucidate surfactant micellar information in terms of aggregate number, micellar size and shape at different temperatures. The experiments were run at 40000 rpm. The sedimentation velocity curves were scanned for 15 hours. Afterwards, the results were analyzed using sedfit92 software. Based on the sedimentation process of micellar samples, information on the size and shape of the species can be obtained.

To further understand the effect of temperature on the surfactant mixtures at solid/liquid interface, analytical ultracentrifugation technique was employed with the mixed DM/SDS system. The experiments were done at 15 ℃, 25 ℃ and 35 ℃. The results at 25 ℃ have been reported previously. The introduction of the technique and data analysis was also reported previously. The micellar size distributions at these three temperatures are shown in figures 65 to 67.

The micellar size is expressed as a function of sedimentation coefficient, which indicates the terminal velocity of a particle settling under unit centrifugal force: the greater the sedimentation coefficient, the larger is the particle.

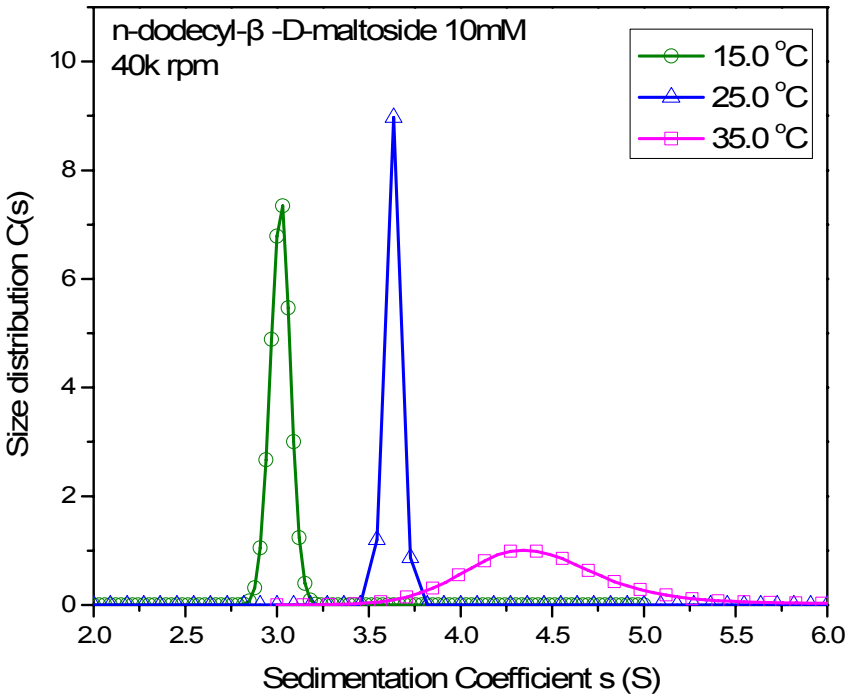

Fig65 Size distributions over sedimentation coefficient of DM at 10 mM at different temperature.

Figure 65 shows the micellar size distribution of DM at different temperatures. Clearly it indicates that the micellar size increases with temperature. The increase in temperature changes the interactions between surfactant molecules as well as the interaction between water molecules and the surfactant molecules, which affects the hydration of the surfactant head groups. When the intermolecular packing in the micellar phase is affected, the micellar shape and size also changes. This result can be used to explain how the adsorption density decreases with temperature. The surfactant molecules in the adsorbed layer become loose due to the intermolecular packing change at high temperature, causing a decrease in adsorption density.

The average aggregation numbers and sedimentation coefficients are summarized in table 4. From 15 ℃ to 25 ℃, the aggregation number increases only from 102 to 106 whereas it almost

doubles from 25℃ to 35 ℃. In addition, only one micellar species was observed for DM alone with a spherical shape.

Table 4 Micellar size for DM at 10 mM at different temperatures

Temperature	Aggregation number	Sedimentation coefficient
15	102	3
25	106	3.7
35	183	4.7

The micellar distribution for mixed DM/SDS with mixing ratio 1:1 at different temperatures is shown in figure 66. Interestingly, for this surfactant mixture only one micellar specie was observed at 15 ℃ and 25 ℃, whereas two micellar species coexist at 35 ℃. The distribution peaks are almost identical at 15 ℃ and 25 ℃. The temperature effects can be attributed to the low Kraft point of SDS. At low temperatures, SDS molecules are dissolved in the DM micellar phase forming mixed micelles, while at high temperatures SDS molecules can form micelles itself. It can be further predicted that the first species at 35 ℃ is SDS-rich while the second one is DM-rich.

The information on the micellization of mixed DM/SDS system is summarized in table 5. The aggregation number is the same at 15 ℃ and 25 ℃. At 35 ℃, the first micellar specie contributes almost 30% to the total micellar species. The formation of two micellar species instead of one mixed micelle may be responsible for the adsorption properties of this mixture at high temperatures. It should be noticed that the total molar ratio for DM/SDS is 1:1 and the micellar species distribution should be different at other mixing ratios.

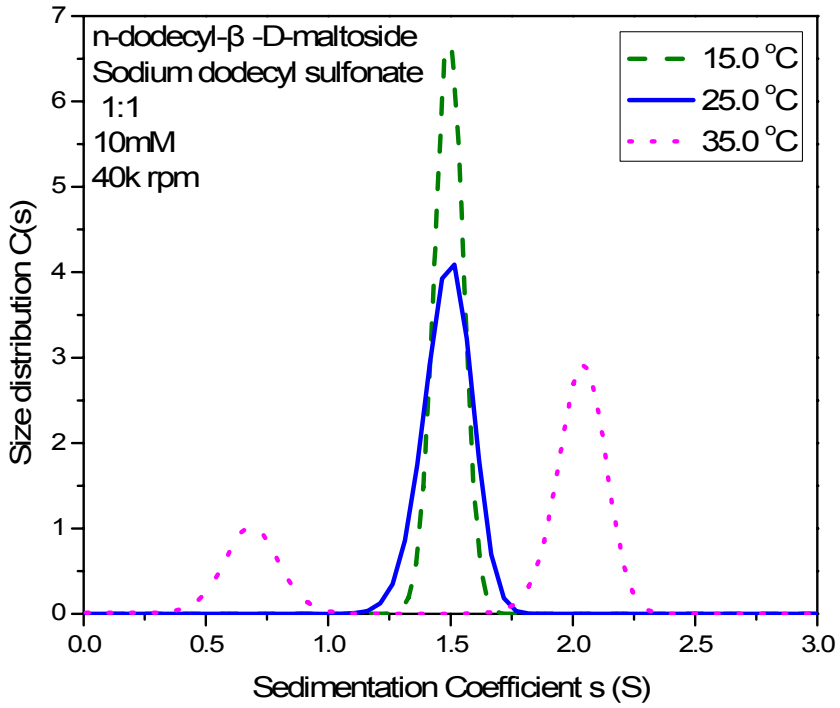

Figure 66 Size distributions over sedimentation coefficient of mixed DM/SDS (1:1 ratio) at 10 mM at different temperature.

Table 5 Micellar size for mixed DM/SDS at 10 mM at different temperatures

Temperature	Peak #/toal	Peak ratio	Aggregation number	Sedimentation coefficient
15	1/1	1	46	1.5
25	1/1	1	46	1.5
35	1/2	0.29	15	0.7
35	2/2	0.71	73	2

The results for mixed DM/SDS at 3:1 ratio are shown in figure 67 and table 6. It can be seen that the micellar distribution is different at this mixing ratio. Due to the high molar ratio of DM, micellar species were observed at a high sedimentation coefficient range. At 15 ℃, only one micellar species was observed, while three species were seen at 25 ℃ and 35 ℃.

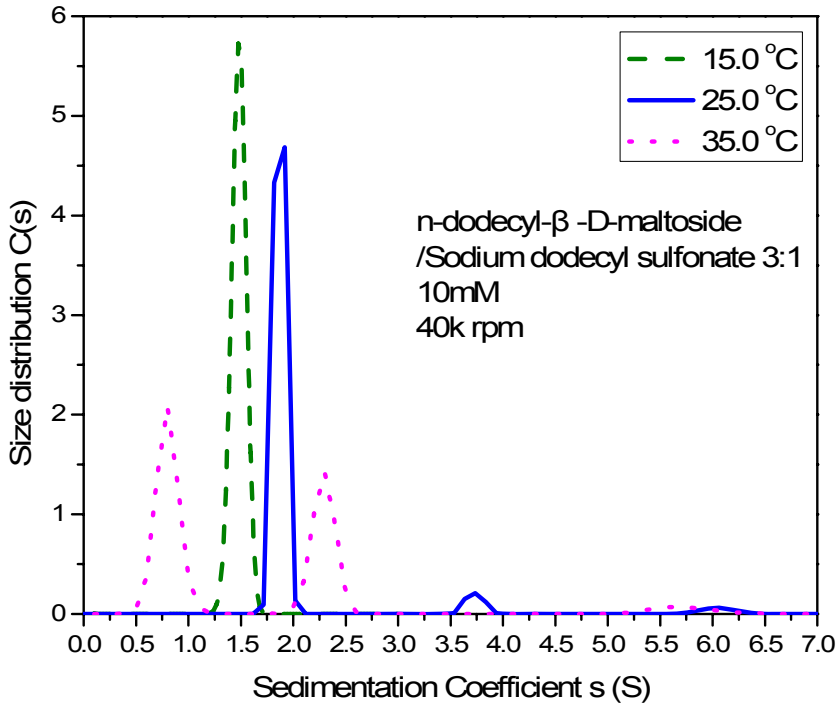

Figure 67 Size distributions over sedimentation coefficient of mixed DM/SDS (3:1 ratio) at 10 mM at different temperature.

Table 6 Micellar size for mixed DM/SDS at 10 mM at different temperatures

Temperature	Peak #/toal	Peak ratio	Aggregation number	Sedimentation coefficient
15	1/1	1	46	1.5
25	1/2	0.93	65	1.9
25	2/2	0.07	250	4.5
35	1/3	0.56	18	0.8
35	2/3	0.4	88	2.3
35	3/3	0.04	348	5.7

Clearly, the micellar distribution evolves with temperature as revealed using analytical ultracentrifugation.

Steady state fluorescence study of adsorption of Dodecyl Maltoside at solid/liquid interface

Steady-state emission spectra were obtained using a Horiba Jobin Yvon Fluorolog FL-1039 spectrophotometer. A portion of the solid slurry sample from adsorption experiments or surfactant solution sample containing pyrene was transferred to quartz cells, and then the samples were excited at 335 nm and their emission between 360 and 500 nm was recorded. For fluorescence measurements at solid/solution interfaces, the same adsorption procedure was followed as for the experiments conducted in the absence of probe. After the adsorption reached equilibration, the solid was separated from residual solution; and both the residual solution and the solid slurry were measured using fluorescence spectroscope.

The emission intensity from the residual solution and solids was plotted as a function of residual concentration in figure 68. The fluorescence intensity from the residual solution decreased sharply with concentration and becomes undetectable at CMC, as most pyrene molecules were extracted into the hemimicelles at solid/liquid interface. Interestingly, the intensity from the solids showed a sharp increase up to CMC and then decreased by almost half. The shape of the peak corresponded with the peak of hydrophobicity as shown in figure 69.

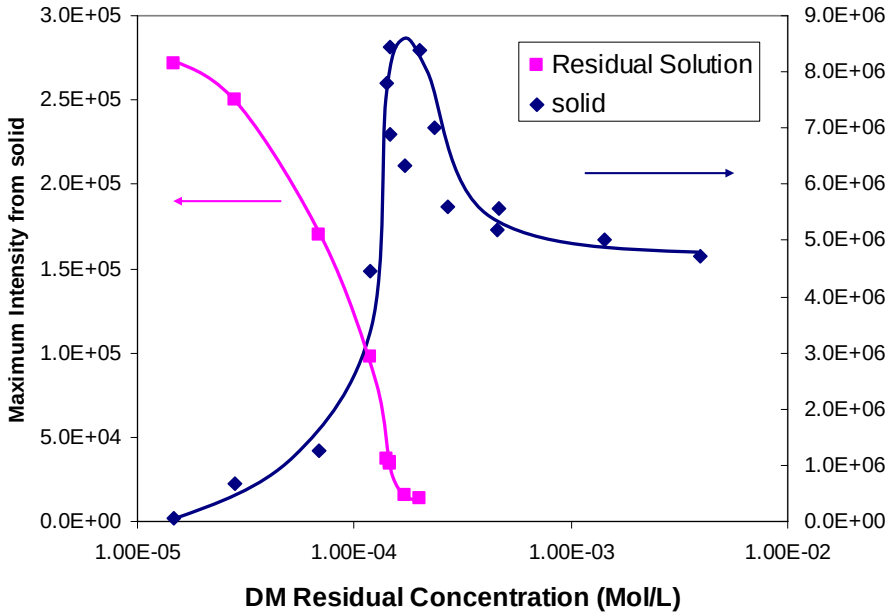

Fig68. Effects of adsorption density on the intensity of pyrene emissions from solid and residual solution

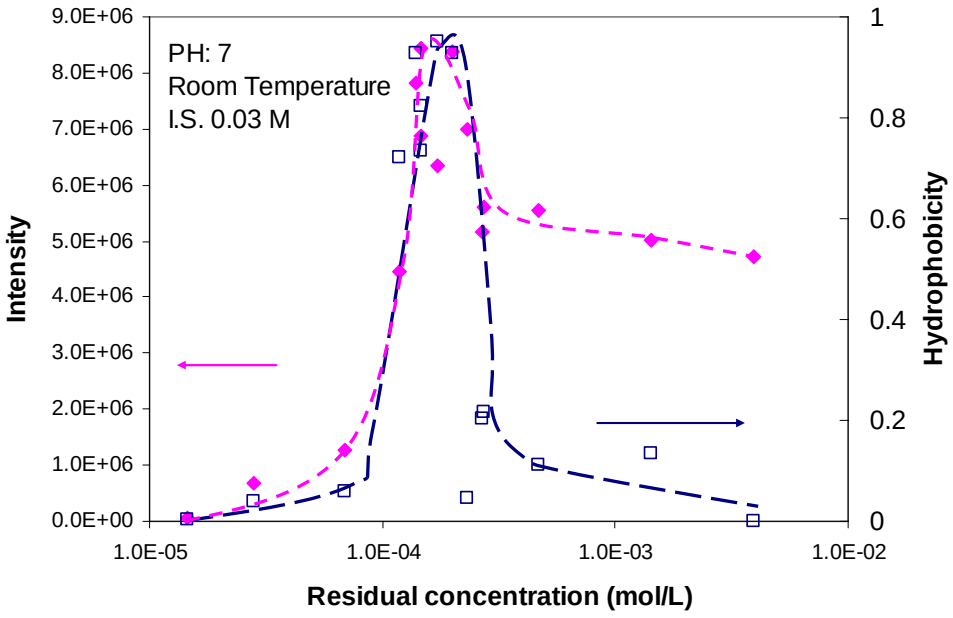

Fig69. Intensity of pyrene emission compared with hydropobicity of alumina surface at same adsorption situation.

Surfactant mixture studied by fluorescence spectroscopy

In the last section, fluorescence spectroscopic technique was successfully employed to obtain basic information on the structure of the micelles of DM. Dodecyl maltoside/$C_{12}SO_3Na$ mixture system was studied to reveal the mechanism of adsorption and performance. In fluorescence spectroscopy, the ratio of relative intensities of the I_1 (373nm) and I_3 (383nm) peaks (I_3/I_1) in a pyrene emission spectrum show the greatest dependency of environment around the probe. This ratio decreases as the polarity increases and can be used to estimate the polarity of the environment and thus detect the presence of surfactant aggregate in solution. The polarity parameter of pyrene is shown in Figure 70 as a function of surfactant concentration. At low concentration for each system, the value of I_3/I_1 ratio corresponds to that of water (0.5~0.6). At certain concentrations, there is a rapid increase in the value of I_3/I_1 ratio indicating the formation of micelles at this concentration. The CMC of the surfactant obtained from fluorescence tests is in good agreement with those obtained from surface tension measurements.

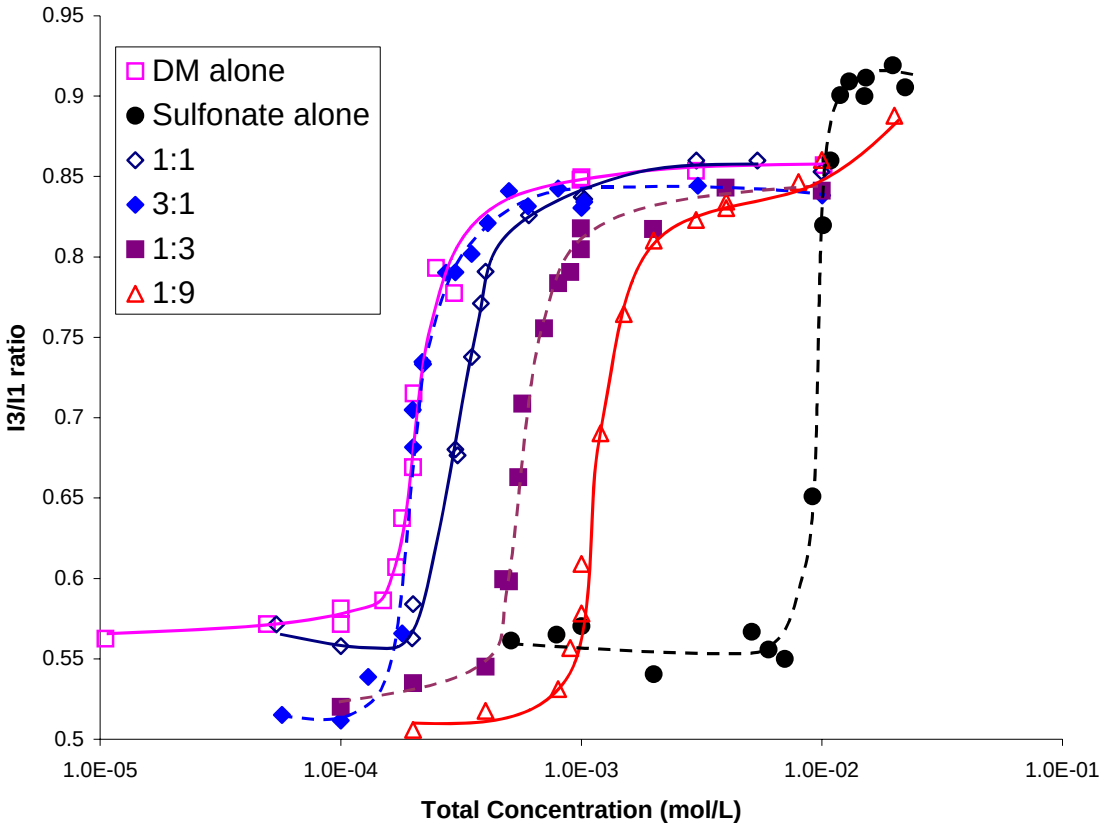

Figure 70 Variation of solution polarity, as indicated by I3/I1 ratio, at different mixing ratios.

The polarity parameter of the pyrene at concentrations higher than cmc provides information on the hydrophobicity and thereby the structure of the micelles. In DM/ C12SO3Na system, I3/I1 ratio for C12SO3Na is higher than that for DM above cmc, suggesting that the core of dodecyl maltoside micelles is more hydrophobic than that of DM micelles, but less hydrophobic than that of pure hydrocarbons. I3/I1 polarity parameter of the micelles decreases with increase in dodecyl sulfonate ratio in the mixtures below a certain concentration. The polarity parameter however increases and gets close to the value of dodecyl sulfonate alone above a certain concentration, at which the transition from dodecyl maltoside rich micelles to dodecyl sulfonate rich micelles happens. Compositional change in the mixed micelles has been predicted and observed for many binary surfactant mixtures at concentrations

above solution cmc, the extent of the compositional change being determined by the strength of surfactant interactions and the difference in surface activity of the components in the mixtures.

Nanostructure of mixed surfactants on minerals

Previous sections have shown that the wettability of minerals particles is determined not only by the adsorption density but also by the orientation of the surfactant molecules in aggregation. An example is given in figure 71. Adsorption tests were conducted with mixtures of sodium dodecyl sulfonate and sugar-based n-dodecyl-β-D-maltoside (DM) on alumina minerals at different surfactant mixing ratios. The total adsorption density is less than 50% of that at other pH levels below a mixing ratio of 0.6, but the mineral surface is surprisingly hydrophilic under this condition, which suggests that the head groups of surfactant molecules are oriented towards the bulk solution. This condition is beneficial for efficient chemical flooding.

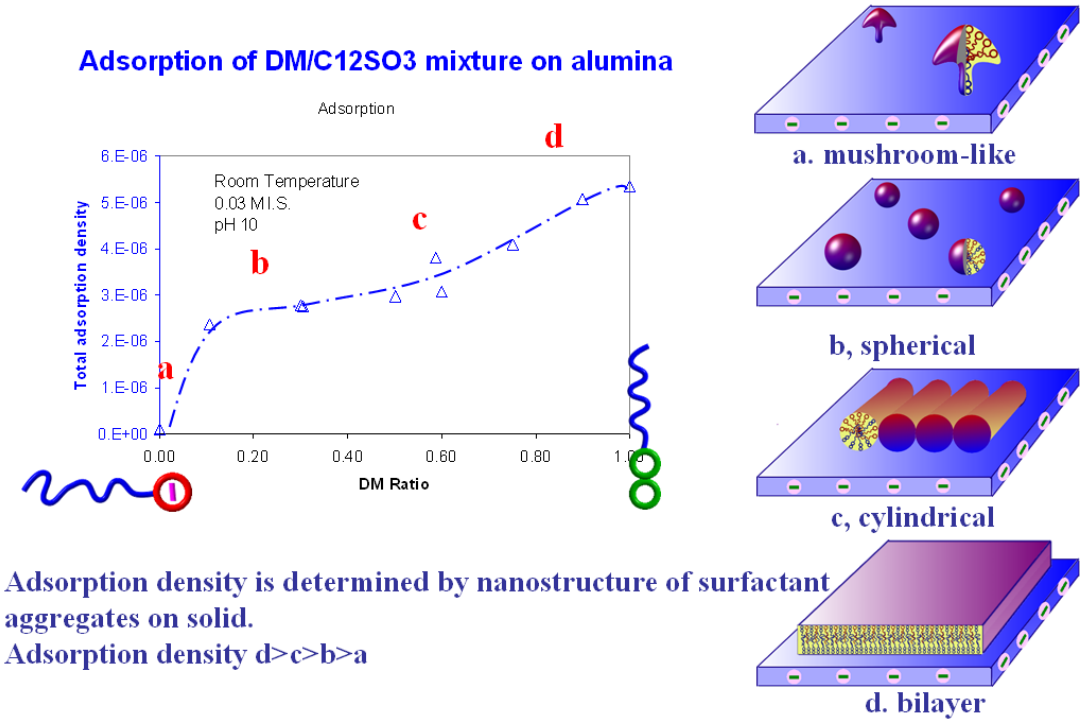

Figure 71: Molecular packing at solid/liquid interface determines the loss of reagents in improved oil recovery

Possible nanostructures formed at different mixing ratio ranges are illustrated on the right of figure 71, which shows that the nanostructure is determined mainly by the mixing ratio. In b and c ranges, the mineral surface is hydrophilic, even though the surface is not fully covered, because of the spherical and cylindrical structures, in which, the surfactant molecules arranged on the top have the head groups oriented towards water.

Monomer concentration changes in mixed DM/SDS system

In surfactant solutions, micellization is in equilibrium with monomer surfactant molecules. Information on the monomer concentrations helps understand the aggregation behavior of mixed DM/SDS system. The monomer molecules were separated from bulk using ultrafiltration technique. The membranes employed were specified to exclude molecules with molecular weight greater than 3000. A small amount of solution was collected for each sample to avoid the concentration increase in the bulk. The permeates were then analyzed to determine the concentration for each component respectively. The experiments were carried at DM ratio 0.75, 0.5 and 0.25. The results are shown in figure 1 in term of DM ratio in the monomers.

Based on the regular solution theory developed by Holland and Roubingh, the monomer concentrations of a binary surfactant mixture can be estimated suing the following equations.

The molar fraction of surfactant 1 in the mixed micelle can be calculated using the equation

$$x_1 = \frac{-(C - \Delta + \sqrt{(C-\Delta)^2 + 4\alpha C\Delta}}{2\Delta} \qquad (1)$$

where $\Delta = f_2 C_2 - f_1 C_1$, f_1 and f_2 are the activity coefficients of surfactant 1 and 2 in the mixed micelle respectively and can be calculated as,

$$f_1 = \exp(\beta(1 - x_1)^2) \qquad (2)$$

$$f_2 = \exp(\beta x_1^{\,2}) \qquad (3)$$

The monomer concentrations can be then calculated,

$$C_1^{\,M} = x f_1 C_1 \qquad (4)$$

$$C_1^{\,M} = (1-x) f_2 C_2 \qquad (5)$$

The calculated results were found to be in good agreement with the experiment data as shown in figure 72. Below CMC, the DM monomer ratios are same as those in bulk, while above CMC, the DM monomer ratios were seen to decrease with the increase in total surfactant concentration, which suggests the formation of mixed micelles and is partially due to its higher surface activity.

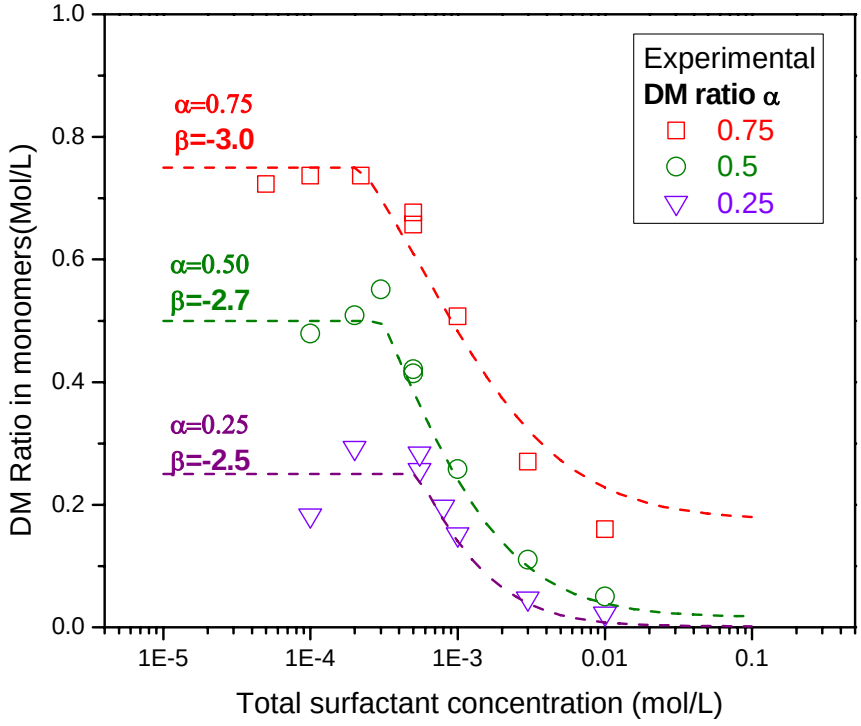

Figure 72: DM ratio in monomers as a function of total surfactant concentration. Symbols represent the experimental data using ultrafiltration and the dashed lines stands the curved predicted using regular solution theory using the interaction parameters obtained from surface tension measurement.

To further test the validity of regular solution theory on mixed DM/SDS system, more tests were done. The DM concentration was fixed at 5×10^{-4} M, while the SDS concentration was varied from 0 to 3×10^{-3} M. The DM monomer concentration was found to decrease sharply with increase in SDS ratio as shown in figure 73. Also the DM monomer concentration was calculated using regular solution theory using different interaction parameters, β, from 0 to -6. Interestingly, it was found that the experimental data cross over the curves from -6.0 to -4.0, suggesting the decrease in interaction parameter with increase in SDS ratio.

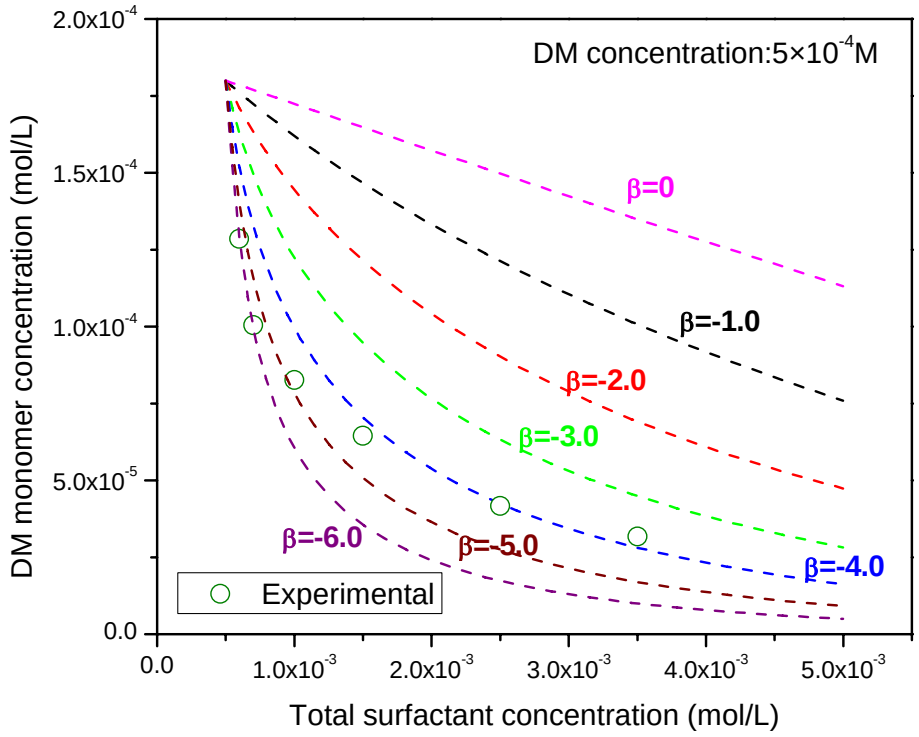

Figure 73 DM monomer concentration as a function of total surfactant concentration. (DM concentration was fixed at 5×10^{-4} M). The symbols represent the experimental data and the dashed lines represent the results predicted using regular solution theory using various interaction parameter.

Micellar shape revealed using Cryo-TEM

Since the size and shape of the surfactant aggregates are important to understand the interaction and molecular packing in surfactant mixture systems, it is critical to get such information. The shape of surfactant micelles can be predicted using the critical packing parameter of the surfactant, $P = v/a_0l_c$ (v is the volume occupied by the tail group, a_0 is the area/head group and l_c the length of the hydrocarbon tail). The packing parameter of DM is around 0.35, which suggests a spherical shape. To understand the micellization behavior, it is necessary to obtain direct information on the micellar size and shape. Cryogenic temperature-TEM technique, the best technique for monitoring micellar shapes, has been employed to study the micellar sample containing 50 mM DM. High curvature spherical micelles have been identified as shown in figure 74. Since SDS has a higher molecular curvature than DM, the overall curvature of mixed DM/SDS is higher than DM alone. It is expected that the mixtures of DM and SDS forms spherical micelles, since SDS has a higher molecular curvature. The information obtained is helpful for understanding the aggregation structure of the adsorbed layer on mineral surfaces.

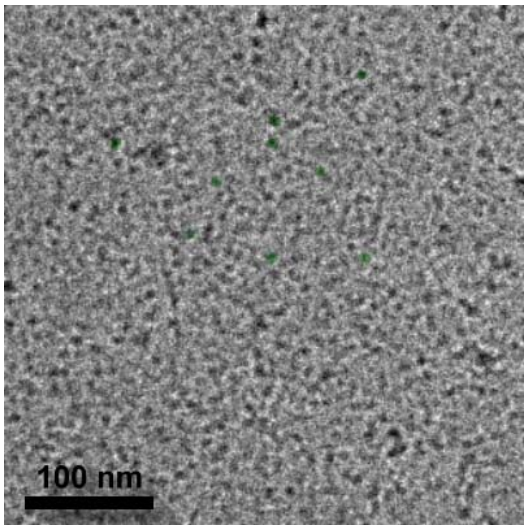

Fig74 Cryo-TEM micrograph of a 50mM dodecyl maltoside solution – spherical micelles

Polymer-surfactant interactions at air/solution interface

In polymer/surfactant flooding system, the interactions between them control their surface activity and performance. During this project, PVCAP/ $C_{12}SO_3$, PVCAP/AOT, PVCAP/SLE3 and hydrophobically modified polymer/SDS systems were studied by surface tension measurement to understand the micellization of surfactants in the presence of polymers.

Surface tension of C12SO3 with and without 1000ppm PVCAP in 0.03M NaCl medium is plotted in Figure 75 as a function of the surfactant concentration. For the C12SO3 surfactant alone, the surface tension curve yields a cmc of 3 ± 0.2mM. The presence of PVCAP lowered the surface activity even below the cmc of C12SO3, suggesting cooperative binding on the polymer PVCAP. Due to the solubility limit of the surfactant, the point of binding saturation above which free surfactant micelles form in the bulk phase could not be reached.

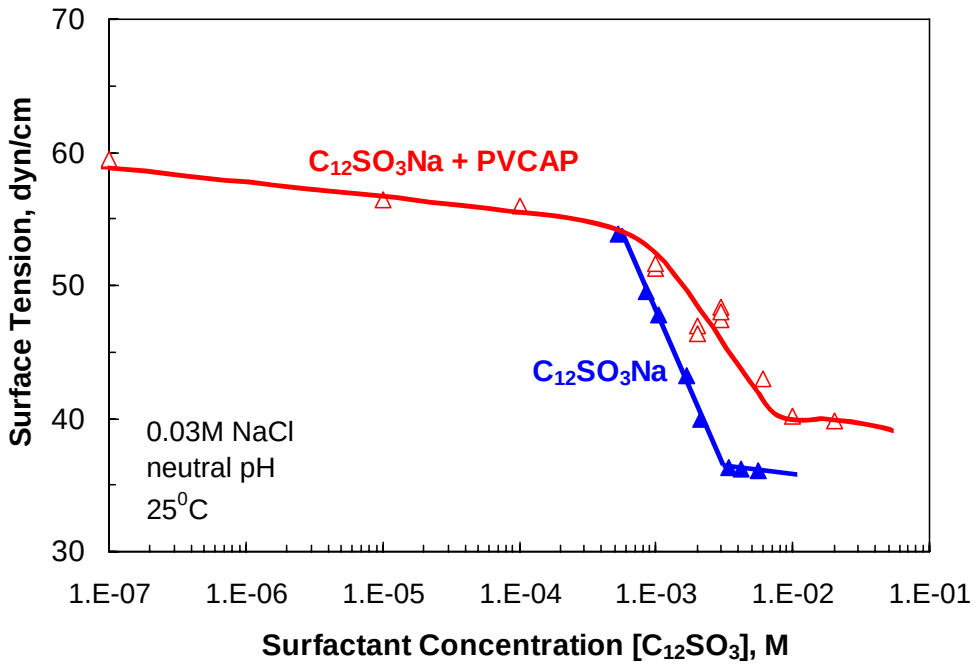

Figure 75: Equilibrium surface tension of C12SO3Na alone(filled triangles) and the corresponding mixtures with 1000ppm PVCAP (open triangles) in 0.03M NaCl.

Similar observations were made for the surface tension of branched, AOT, in the presence of polymer PVCAP. Binding of AOT to the polymer begins at a concentration lower than the surfactant cmc, resulting in a lower surface activity (Figure 76). Unlike the previous mixture, there is no clear point on the surface tension curve indicating critical aggregation concentration (cac) for AOT in the presence of PVCAP. Decrease of surface activity is determined by the binding strength of the surfactant on PVCAP. The more the surfactant binding on PVCAP, the greater is the decrease in the surface activity.

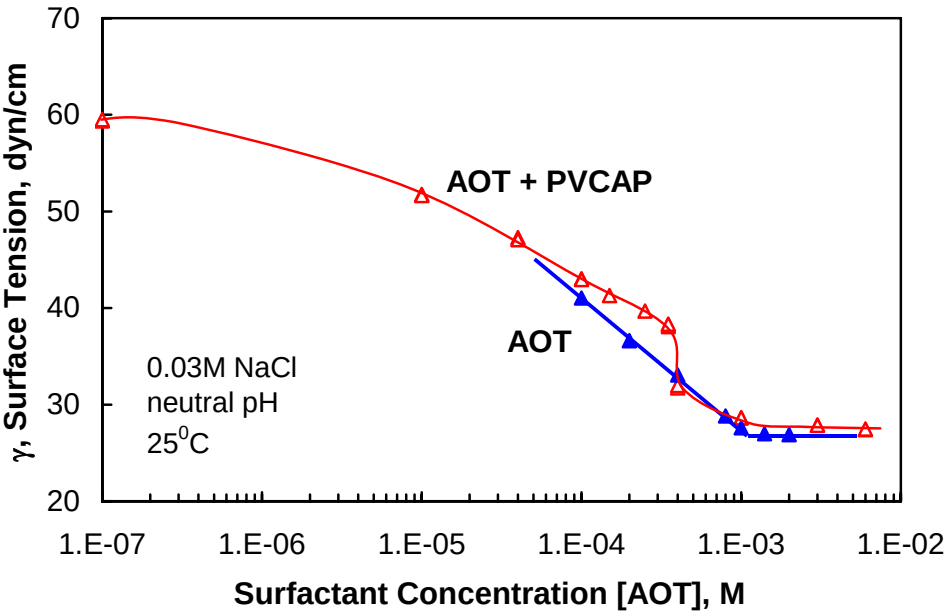

Figure 76: Equilibrium surface tension of AOT alone (filled triangles) and the corresponding mixtures with 1000ppm PVCAP (open triangles) in 0.03M NaCl.

In the case of SLE3 with the insertion of ethylene oxide units and double-charged headgroup, a very different behavior than those of AOT and C12SO3 was observed at concentrations below cmc (Figure 77). The same surface activity was obtained for the mixture and for SLE3 surfactant alone, suggesting absence of any cooperative binding of SLE3 surfactant to PVCAP polymer below cmc. Above the surfactant cmc, a gradual decrease in surface activity

resulted considerable micellar interaction between SLE3 surfactant and PVCAP polymer. Evidently, for the SLE3, the presence of ethylene oxide units and double-charged headgroup makes the formation of surfactant micelles more favorable than those of polymer-surfactant complexes.

Adsorption density was calculated using Gibbs equation. In the cases where binding of surfactant on polymer occurs at a concentration below the surfactant cmc, the cross-sectional area of the surfactant increases in the presence of polymer, indicating that the polymer or polymer-surfactant complexes are surface active and act together with the surfactants at the air/aqueous solution interface.

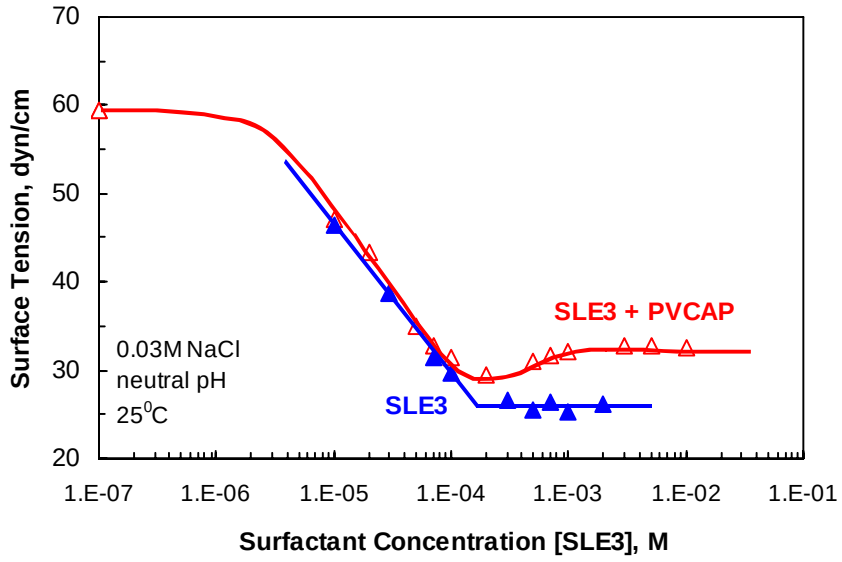

Figure 77: Equilibrium surface tension of SLE3 alone(filled triangles) and the corresponding mixtures with 1000ppm PVCAP (open triangles) in 0.03M NaCl.

Figure 78(b) shows the surface tension of aqueous SDS solutions as a function of SDS concentration. As expected, the surface tension of an aqueous solution of 0.1 % PMAOVE is lower than that of water. Addition of SDS to the PMAOVE solution caused a change of

surface tension in two stages. At 2 mM of SDS, a sharp decrease of surface tension occurred (indicating the formation of mixed micelles of SDS and hydrophobic groups of PMAOVE) followed by a gradual decrease with SDS concentration. Above 2mM, the binding of SDS on polymer caused the decrease in free SDS molecule concentration and thus the increase in surface tension. At approximately 20 mM of SDS the surface tension reached a value similar to that of SDS micelle solutions and remained constant with further increase in SDS concentration, suggesting the coexistence of mixed micelles and pure SDS micelles in the solution at that concentration.

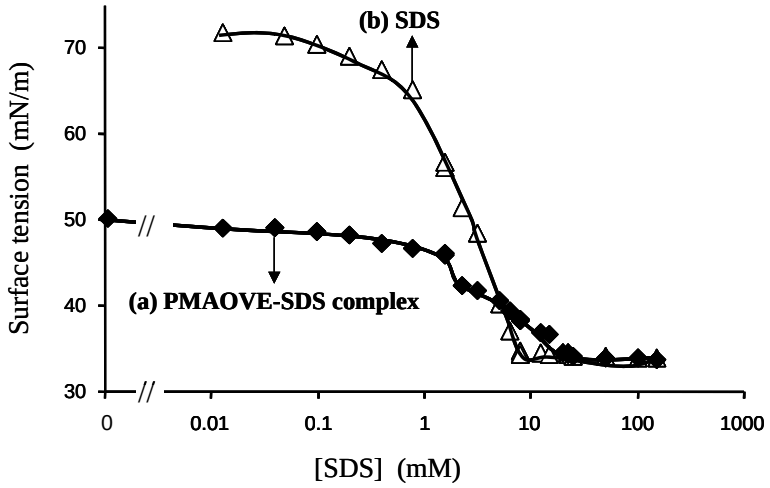

Figure 78 Equilibrium surface tension of SDS solutions alone (b) and in the presence of 0.1% (w/w) PMAOVE(a)

Polymer-surfactant interactions studied by EPR

EPR spectroscopy is commonly used to probe micro-environments of supramolecular structures involving surfactants and macromolecules. 5-doxyl stearic acid (5-DSA) was selected as spin probe, because of its structural similarity with SDS.

In the presence of SDS micelles, a broadened EPR spectrum was observed compared to

the spectrum in water. This is consistent with partial hindered rotational mobility of the probe molecule, because of incorporation of 5-DSA molecules into the SDS micelles. In the presence of PMAOVE, a significantly different EPR spectrum was observed. Addition of SDS to PMAOVE solutions containing the spin probe 5-DSA causes significant changes in the EPR spectra.

The mobility parameter, the rotational correlation time, of the spin probe was determined by spectral simulation of the experimental EPR spectra using the program of Schneider, Freed and Budil. Figure 79 illustrates the changes in rotational correlation time of 5-DSA in 0.1% PMAOVE and different concentrations of SDS. Two inflection points are observed, one at a SDS concentration of 2 mM and the other one at 12 mM. The observations are in good agreement with the results of surface tension measurement, suggesting the beginning and saturation points binding of surfactant on polymer. This SDS concentration (2 mM) was assigned to the critical complexation concentration, where mixed micelles of hydrophobic chains of PMAOVE and SDS molecules are formed. The critical complexation concentration depends on the PMAOVE concentration. The second SDS concentration (12mM) was assigned to the saturation level of PMAOVE with SDS. Upon further addition of SDS the rotational mobility of the spin probe remained constant, implying the coexistence of pure SDS micelles and mixed micelles of PMAOVE with SDS. The saturation level (second inflection point) is expected to depend on the PMAOVE concentration also.

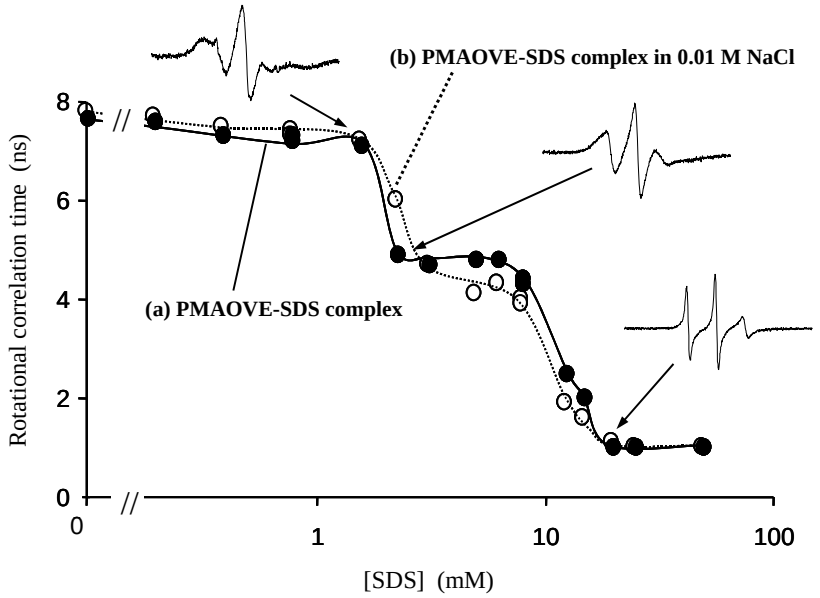

Figure 79 Rotational correlation time of the spin probe (5-DSA; 0.1mM) as a function of the SDS concentration aqueous PMAOVE (0.1% w/w) solutions in the absence (a) and in the presence (b) of NaCl (0.01M)

Summary and general guidelines for the use of surfactants/polymers in enhanced oil recovery.

There is considerable amount of oil trapped, together with water and gas, in reservoirs made up of porous and permeable rocks after the traditional oil production. Surfactant/polymer flooding is one of the promising techniques to recover additional oil from domestic oil reservoirs. In this regard, there is a need for cost-effective reagent schemes to increase the oil recovery and minimize the loss of surfactants and/or polymers on reservoir rocks due to adsorption and precipitation.

The success of any strategy for minimizing the reagent loss and maximizing oil recovery depends on a full understanding of the mechanisms governing minerals/chemicals interactions. Yet this is a complex system given many different interactions involved in a variety of environments. Also adsorption of surfactants, including polymeric ones, on minerals is affected by a large number of system variables arising from chemical and structural properties of the minerals including solubility and interfacial charge, chemical and physical properties of solution such as salinity, hardness, pH, temperature, and the chemical composition and structure of the surfactants.

The studies completed here show that there are three major interactions between reagent compounds and minerals: hydrophobic chain-chain interactions, electrostatic forces and hydrogen bonding. A balance among these three interactions determines the adsorption behavior of surfactant or polymer molecules. Solution conditions (salinity, pH temperature and hardness) affect the magnitude of the three major interactions and thus affect the adsorption behavior.

Our study with dodecyl maltoside clearly shows that sugar based surfactants are promising candidates for EOR process because of its high tolerance to inorganics, particularly multivalent ions. Hydrogen bonding between the sugar rings and the surface hydroxyl groups is the major mechanism that dominates adsorption of DM on mineral surface and is not affected by electrostatic interactions. There is no major depletion or loss of dodecyl maltoside in simulated adsorption process. Besides, its adsorption

Increasing requirements for environmental protection and an escalating demand from consumers has made “going green” an inevitable and inescapable trend for the industries. Sustainability of chemical products in a future environmentally conscious market will favor only products certified to have been made in an environmentally responsible way. Sugar based surfactants are manufactured from renewable starting materials and is readily bio-degradable. Application of this type of novel green surfactants in industry is to be further explored.

Traditional anionic sulfonates have been evaluated in this work under different solution conditions. A novel cationic surfactant of the Gemini type has also been synthesized and evaluated in the study. Results show that the major interaction between the anionic as well as Gemini surfactant and minerals is electrostatic leading to considerable loss of these surfactants, particularly under high salinity conditions. Multivalent ions like calcium or magnesium ions are major deterrents in EOR processes with anionic surfactants. As high multivalent conditions are common in real production, these surfactants cannot be used alone EOR, It must, however, be noted that the cationic Gemini surfactants can be ideal reagents for lime stone reservoirs since the rock surface is positively charged, as we have shown earlier.

In the case of the anionic surfactants, their mixtures with a sugar based nonionic surfactant and ionic surfactants have been evaluated in this work. The studies show antagonistic or synergistic interactions among the surfactants depending on the test conditions. Such antagonism and synergy can be used to control chemical losses.

Mixtures of polymers and ionic surfactants have also been evaluated. The study shows strong interactions between polymer and surfactant species. Hydrophobic moieties of modified polymers tend to from local hydrophobic domains with the carbon chains of the ionic surfactants aggregating around the domains to composite domains. The composite domains can serve as local reservoir of the ionic surfactants, keeping them from adsorbing on minerals. The domains can serve to solubilize and thus mobilize oil. This mechanism can contribute to minimize chemical loss and at the same time it enhances oil extraction efficiency.

Guidelines for Surfactant Selection:

As detailed in earlier sections, a wide range of minerals that are typical reservoir components were chosen for this study. Minerals such as sandstone, kaolinite and silica exhibit negatively charged surface (low iso-electric point of ~ pH 2), whereas minerals such as alumina exhibit net positive surface. Our earlier work has shown minerals like gypsum and limestone to have intermediate or high iso-electric points. Following section contains guidelines for the selection of surfactants for various reservoirs. For negatively charged surfaces such as that of sandstones, silica, and kaolinites, anionic surfactants would be the ideal type. In these cases, cationic surfactants alone or mixed with nonionic surfactant (ex. dodecyl Maltoside, DM) is not advisable, since it may result in higher adsorption due to synergistic effects. Further, non-ionics should be avoided if the presence of cationic surfactant (impurity or otherwise) is suspected.

If the Sandstone mineralogy contains even small quantities of dissolvable polyvalent ions such calcium (Ca^{2+}) then surfactant scheme containing mixtures of anionic (ex. sodium dodecyl sulfonate, SDS) and non-ionic surfactants (ex. DM) are not advisable. Similarly for limestone containing sandstone rocks, anionic (ex. SDS) and non-ionic (ex. DM) surfactant mixture may be avoided. In the case of oxide-rich mineral substrates (ex. Iron oxides, alumina), pH of the surfactant fluids should be kept lower than the iso-electric point of these oxides (especially when non-ionic surfactants are used), since it is found that oxides around IEP form neutral hydroxides which hydrogen bonds with oxygen groups present in the non-ionic surfactants. On the other hand, presence of polyvalent ions such as Ca^{2+} does not seem to increase the adsorption of non-ionic/ionic surfactants (ex. DM/SDS) on oxide minerals. Similarly in the case of non-ionic surfactant adsorption on alumino silicates hydroxides, pH would be a critical parameter

Mixed rocks of Sandstone and pyrite show higher adsorption of cationic surfactants (ex. Gemini), as a result it would be advisable to use anionic (ex. SDS) and/or non-ionic (ex. DM) surfactants.

Limestone has a net positive surface charge; as a result, cationic (ex. Gemini) and non-ionic (ex. DM) or their combinations would be preferable compared to anionic surfactants (ex. SDS)

Following table summarizes these guidelines in terms of the rock mineralogy.

Guidelines in Surfactant selection

Rock Type	Surfactants types	
	Recommended	Not Recommended
Sandstone	Anionic+/non-ionic (ex. SDS, DM)	Cationic (ex. Gemini or alkyl amines)
Sandstone in a Ca-containing reservoir	Anionic (ex. SDS)	Cationic alkyl amines or gemini, Cationic+non-ionic (ex. Gemini+DM)
Sandstone + Limestone rocks	Anionic (ex. SDS)	Cationic alkyl amines, Cationic+non-ionic (ex. Gemini+DM)
Sandstone + Pyrite	Anionic+/non-ionic (ex. SDS, DM)	Cationic alkyl amines
Oxide-rich minerals	Ionics+/Non-ionics (ex. SDS, DM)	Non-ionics – pH not close to oxides' isoelectric point
Limestone	Cationic (Gemini, alkyl amines) +/Non-ionic (DM)	Anionic (SDS)

Summary of tasks completed

The following tasks have been completed under the scope of the project:

1. Mineral characterizations—SEM, BET, size, surface charge, and point zero charge—have been completed.
2. Study of the interactions among typical reservoir minerals (quartz, alumina, calcite, dolomite, kaolinite, gypsum, pyrite, etc.) and surfactants and/or polymers in terms of adsorption properties that include both macroscopic (adsorption density, wettability) and microscopic (orientation conformation of the adsorbed layers), as well as precipitation/abstraction characteristics have been tested and completed.

3. Investigation of the role of dissolved species, especially multivalent ions, on interactions between reservoir minerals and surfactants and/or polymers leading to surfactant precipitation or activated adsorption.
4. Solution behavior tests—surface tension, interaction, ultrafiltration, and other tests—have been completed. Surfactant-mineral interactions relative to adsorption, wettability, and electrophoresis have been tested and completed.
5. Work on the effects of multivalent ions, pH, temp, salinity, mixing ratio on the adsorption is done. Models to explain interactions between surfactants/polymers/minerals are proposed.
6. General guidelines for the use of surfactants polymers in enhanced oil recovery are provided.

Acknowledgment

This project was conducted with the support of the U.S. Department of Energy, under Award No. DOE-DE-FC26-03BC15413. However any opinions, findings conclusions, or recommendations expressed herein are those of the authors and do not necessarily reflect the views of the DOE.

Publications

1. R. Zhang, L. Zhang and P. Somasundaran, “Surface tension and fluorescence study of n-dodecyl--D-maltoside (DM) with anionic, cationic and nonionic surfactant mixtures in aqueous solutions”, Journal of Colloid and Interface Science, Volume 278, Issue 2, 15 October 2004, Pages 453-460
2. P. Somasundaran and Qiong Zhou, “Environmentally Benign Surfactants For Efficient Enhanced Oil Recovery”, Second Joint DOE U.S.-People's Republic of China (PRC) Conference on Clean Energy, Washington DC, November 2003.
3. R. Zhang, P. Somasundaran, “Abnormal micellar growth in sugar-based and ethoxylated nonionic surfactant and their mixtures in dilute regimes using analytical ultracentrifugation”, Langmuir, 20, 8552-8558, 2004.
4. P. Somasundaran and Lei Zhang, “Mineral-Surfactant Interactions and Environmentally Benign Surfactants for Efficient Enhanced Oil Recovery”, 8th International Symposium on Reservoir Wettability, Houston, TX, May 2004.
5. R. Zhang, P. Somasundaran, X.Y. Hua and K.P. Ananthapadmanabhan, “Study of Mixed Micellar Growth of Nonionic Surfactants using Analytical Ultracentrifuge”, 78th ACS Colloid and Surface Science Symposium, New Haven, CT, June, 2004
6. Somasundaran, P.; Chakraborty, Soma; Qiu, Qiang; Deo, P.; Wang, Jing; Zhang, Rui. “Surfactants, polymers and their nanoparticles for personal care applications”, JCS, (2004), 55(Suppl.), S1-S17.
7. Zhang, Rui; Liu, Chi; Somasundaran, P. “Cooperative adsorption of nonionic surfactant mixtures on hydrophilic surfaces: A simple model”, 229th American Chemical Society National Meeting, San Diego, CA, United States, March 13-17, 2005.
8. Shaohua Lu and P Somasundaran, Controllable synergistic or antagonistic adsorption of surfactant mixture on solids, The 230th ACS National Meeting, in Washington, DC, Aug 28-Sept 1, 2005.
9. Shaohua Lu and P Somasundaran, Mineral wettability control by optimizing adsorption of mixed surfactants, the Fifteenth SPE Improved Oil Recovery Symposium.
10. Rui Zhang and P Somasundaran Nano-structure of Mixed Surfactant Aggregates in Solution and on Minerals (for poster), the Fifteenth SPE Improved Oil Recovery Symposium.
11. Puspendu Deo; P. Somasundaran, Interactions of hydrophobically modified polyelectrolytes with nonionic surfactants, Langmuir (2005), 21(9), 3950-6.
12. Puspendu Deo; P. Somasundaran, Conformational Behavior of Hydrophobically Modified Polymers and its effect on the Stability of Emulsions and mineral wettability, the Fifteenth SPE Improved Oil Recovery Symposium.
13. Shaohua Lu and P. Somasundaran, Analytical ultracentrifuge study of micellization of surfactant mixtures, Oral Presentation The 231st ACS National Meeting, Atlanta, GA, March 26-30, 2006

14. Shaohua Lu and P. Somasundaran, Synergy among Surfactants in Solution and on Particles in Suspensions. Industrial Advisory Board meeting in University of Florida, Feb 21 2006, (Received Best Poster Reward).
15. Shaohua Lu and P. Somasundaran, Rock Wettability Control and Chemical Loss Reduction, 2006 AAPG Rocky Mountain Section Annual Meeting (June 11-13, 2006) .
16. Shaohua Lu and P. Somasundaran, Solution behavior of nonionic/anionic surfactant mixtures, The 16th International Symposium on Surfactants in Solution KOREA, June 2006
17. Shaohua Lu and P. Somasundaran, Synergy among Surfactants in Solutions and on Particles in Suspensions. 12th IACIS.
18. Shaohua Lu, Yu Bian, Lei Zhang and P. Somasundaran, "pH dependence of adsorption of n-dodecyl-β-D-maltoside on solids", Journal of colloid and interface science, 316 (2007) 310–316
19. Qiong Zhou and P. Somasundaran, "Synergistic Adsorption of Cationic Gemini and Sugar-Based Nonionic Surfactant Mixtures on Silica", submitted to Langmuir.
20. Shaohua Lu and P. Somasundaran, "Tunable synergism/antagonism in mixed nonionic/anionic surfactant layers at solid/liquid interface", Langmuir. 2008 Apr 15;24(8):3874-9
21. Shaohua Lu and P. Somasundaran, Characterization of nanostructures of mixed surfactant aggregation using Analytical Ultracentrifugation. The 81st ACS Colloid & Surface Science Symposium (June 24-27, 2007).
22. Lu, S. and P. Somasundaran, "Synergy among Surfactants in Solution and on Particles in Suspensions," poster, industrial advisory board meeting, University of Florida, February 2006.
23. Lu, Shaohua, Somasundaran, P., and Zhang, R., "Prediction of the Aggregate Nanostructures of Binary Surfactant Mixtures on Hydrophilic Solids," at the 230th American Chemical Society National Meeting, Washington, D.C., August 28-September 1, 2005.
24. Lu, Shaohua and Somasundaran, P., "Controllable synergistic or antagonistic adsorption of surfactant mixture on solids," 230th American Chemical Society National Meeting, Washington, D.C., August 29, 2005.
25. Columbia alumni association s distinguished achievement award, 2007

National Energy Technology Laboratory

626 Cochrans Mill Road
P.O. Box 10940
Pittsburgh, PA 15236-0940

3610 Collins Ferry Road
P.O. Box 880
Morgantown, WV 26507-0880

One West Third Street, Suite 1400
Tulsa, OK 74103-3519

1450 Queen Avenue SW
Albany, OR 97321-2198

539 Duckering Bldg./UAF Campus
P.O. Box 750172
Fairbanks, AK 99775-0172

Visit the NETL website at:
www.netl.doe.gov

Customer Service:
1-800-553-7681